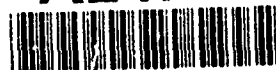


PL-TR-91-2212(III)

AD-A247 548



TGAL-91-07

2

**A STUDY OF SPECTRAL NULLS AND SCALING OF
P-WAVE SPECTRA OF SHAGAN RIVER AND
NOVAYA ZEMLYA (USSR) EXPLOSIONS**

I. N. Gupta
R. A. Wagner

Teledyne Geotech Alexandria Laboratories
314 Montgomery Street
Alexandria, VA 22314-1581

13 NOVEMBER 1991

DTIC
ELECTE
FEB 10 1992
S D D

FINAL REPORT (VOLUME III)
16 APRIL 1989 - 15 JULY 1991

APPROVED FOR PUBLIC RELEASE
DISTRIBUTION UNLIMITED



PHILLIPS LABORATORY
AIR FORCE SYSTEMS COMMAND
HANSCom AIR FORCE BASE, MASSACHUSETTS 01731-5000

02 2 00 029

92-03183

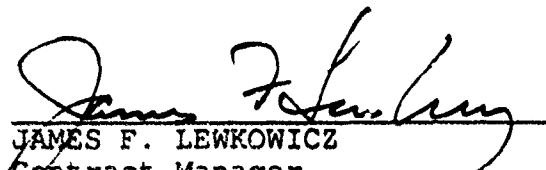


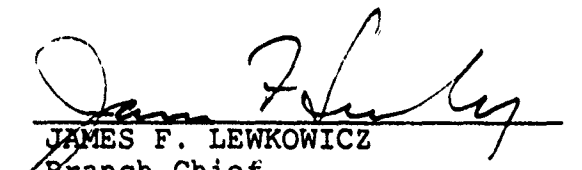
SPONSORED BY
Defense Advanced Research Projects Agency
Nuclear Monitoring Research Office
ARPA ORDER NO. 5307

MONITORED BY
Phillips Laboratory
Contract F19628-89-C-0063

The views and conclusions contained in this document are those of the authors and should not be interpreted as representing the official policies, either expressed or implied, of the Defense Advanced Research Projects Agency or the U.S. Government.

This technical report has been reviewed and is approved for publication.


JAMES F. LEWKOWICZ
Contract Manager
Solid Earth Geophysics Branch
Earth Sciences Division


JAMES F. LEWKOWICZ
Branch Chief
Solid Earth Geophysics Branch
Earth Sciences Division


DONALD H. ECKHARDT, Director
Earth Sciences Division

This report has been reviewed by the ESD Public Affairs Office (PA) and is releasable to the National Technical Information Service (NTIS).

Qualified requestors may obtain additional copies from the Defense Technical Information Center. All others should apply to the National Technical Information Service.

If your address has changed, or if you wish to be removed from the mailing list, or if the addressee is no longer employed by your organization, please notify PL/IMA, Hanscom AFB, MA 01731-5000. This will assist us in maintaining a current mailing list.

Do not return copies of this report unless contractual obligations or notices on a specific document requires that it be returned.

REPORT DOCUMENTATION PAGE			Form Approved OMB No. 0704-0188	
<small>Public reporting burden for this collection of information is estimated to average 1 hour per response, including the time for reviewing instructions, searching existing data sources, gathering and maintaining the data needed, and completing and reviewing the collection of information. Send comments regarding this burden estimate or any other aspect of this collection of information, including suggestions for reducing this burden, to Washington Headquarters Services, Directorate for Information Operations and Reports, 1215 Jefferson Davis Highway, Suite 1204, Arlington, VA 22202-4302, and to the Office of Management and Budget, Paperwork Reduction Project (0704-0188), Washington, DC 20503.</small>				
1. AGENCY USE ONLY (Leave blank)	2. REPORT DATE 13 November 1991	3. REPORT TYPE AND DATES COVERED Final Report, 16 April 1989 - 15 July 1991		
4. TITLE AND SUBTITLE A Study of Spectral Nulls and Scaling of P-Wave Spectra of Shagan River and Novaya Zemlya (USSR) Explosions		5. FUNDING NUMBERS Contract F19628-89-C-0063 PE 62714E PR 9A10 TA DA WU AZ		
6. AUTHOR(S) Indra N. Gupta and Robert A. Wagner				
7. PERFORMING ORGANIZATION NAME(S) AND ADDRESS(ES) Teledyne Geotech 314 Montgomery Street Alexandria, VA 22314-1581		8. PERFORMING ORGANIZATION REPORT NUMBER TGAL-91-07		
9. SPONSORING/MONITORING AGENCY NAME(S) AND ADDRESS(ES) DARPA/NMRO (Attn: Dr. A. Ryall) 3701 North Fairfax Drive Arlington, VA 22203-1714		10. SPONSORING/MONITORING AGENCY REPORT NUMBER PL-TR-91-2212(III)		
Phillips Laboratory Hanscom AFB, MA 01731-5000 Contract Manager: J. Lewkowicz/GEH				
11. SUPPLEMENTARY NOTES				
12a. DISTRIBUTION/AVAILABILITY STATEMENT Approved for Public Release; Distribution Unlimited			12b. DISTRIBUTION CODE	
13. ABSTRACT (Maximum 200 words) Spectral ratios P/P-coda, Pn/Lg, inter-shot ratios of P and Pn, and multichannel deconvolution are used to study spectral nulls on data from nearly 100 Shagan River and Novaya Zemlya explosions recorded at EKA, GBA, YKA, NORESS, MAJO, NORSAR, and WMQ. Spectra of P waves from Shagan River explosions show well-defined nulls due to cancellation by pP at the expected frequency of about 4 Hz for large ($m_b \approx 6$) shots, low-frequency nulls in teleseismic data related to both local geology and depth of burial, and distinct nulls at about 3 Hz in teleseismic data for large and small shots. Low-frequency P-coda appears to be due to the scattering of explosion-generated Rg. Comparison of observed data with synthetics suggests that observed P spectra vary more slowly with m_b than predicted by commonly used scaling relationships. Analysis of data from 19 Novaya Zemlya explosions suggests that P-wave spectra of large shots have distinct spectral nulls at about 2.5-3.0 Hz, probably due to pP. P/P-coda and inter-shot ratios at common receivers provide reliable methods for estimating spectral nulls. A comparison of synthetics with the observed data suggests the amplitude ratio pP/P to be about 0.5 for large shots.				
14. SUBJECT TERMS Scaling, pP nulls, Shagan River explosions, Novaya Zemlya explosions, P and P-coda, scattering, pP/P amplitude, EKA array			15. NUMBER OF PAGES 90	
			16. PRICE CODE	
17. SECURITY CLASSIFICATION OF REPORT Unclassified	18. SECURITY CLASSIFICATION OF THIS PAGE Unclassified	19. SECURITY CLASSIFICATION OF ABSTRACT Unclassified	20. LIMITATION OF ABSTRACT UL	

SUMMARY

Teleseismic and regional data from nearly 100 explosions from the Shagan River and Novaya Zemlya (USSR) test sites are examined to determine and understand the spectral nulls due to cancellation by pP and other secondary arrivals and the scaling of P-wave spectra. The U.K. arrays (EKA, GBA, and YKA), the short-aperture array NORESS and stations MAJO and NORSAR (center element) provided the teleseismic data, whereas the regional data came from the CDSN station, WMQ. Results from the array data, derived by a least squares inversion that isolates the source and receiver terms for each frequency, should be relatively free from frequency-dependent station effects. A combination of several techniques, including spectral ratios P/P-coda, Pn/Lg, inter-shot ratios of P and Pn, and multichannel deconvolution, provide effective means for determination and interpretation of spectral nulls. Analysis of data from nearly 80 Shagan River explosions suggests that, in general, the spectra of P waves have three different types of spectral nulls: (1) well-defined nulls due to cancellation by pP at the expected frequency of about 4 Hz in both teleseismic and regional data for large ($m_b \approx 6$) shots, (2) low-frequency (less than about 2 Hz) nulls in teleseismic data that appear to be related to both local geology and depth of burial, and (3) distinct nulls at about 3 Hz in teleseismic data for large and small shots, probably due to teleseismic path effect such as a multiple arrival. A comparison of P and P-coda shows that the low-frequency P-coda is mainly due to the scattering of explosion-generated Lg and the spectral ratio P/P-coda may be used to estimate shot depths. Scaling of P-wave spectra is investigated over the frequency range of 0.5 to 10 Hz by comparison of observed data from WMQ and NORSAR with synthetics assuming several t^* and pP reflection coefficient values. In qualitative agreement with Stewart's (1988) analysis of Shagan River explosions, the observed P spectra vary more

slowly with m_b than predicted by either Mueller and Murphy (1971) or von Seggern and Blandford (1972) scaling relationships and the differences are more pronounced at lower frequencies than at the higher frequencies.

Teleseismic data from 19 Novaya Zemlya explosions recorded at the EKA, GBA, and YKA arrays are analyzed to understand the characteristics of the pP arrival. Large ($m_b \approx 6$) shots indicate distinct spectral nulls at about 2.5-3.0 Hz, as expected for nulls due to pP. Spectral ratio of P/P-coda, averaged over all available sensors at all arrays, and inter-shot spectral ratios of large and small shots at common receivers, provide reliable methods for estimating spectral nulls. A comparison of synthetics with the observed data suggests the amplitude ratio pP/P to be about 0.5 for large shots. These results obtained by using new frequency-domain techniques are helpful in resolving the controversy over the pP arrival time and amplitude.

TABLE OF CONTENTS

	Page
1. SUMMARY	iii
2. INTRODUCTION	1
3. STUDY OF SHAGAN RIVER EXPLOSIONS	5
3.1. ANALYSIS OF EKA ARRAY DATA	5
3.1.1. Spectral Nulls in Source Spectra	5
3.1.2. Low-Frequency Nulls and Near-Source Geology	9
3.1.3. Comparison of P and P Coda and Origin of Secondary Arrivals	16
3.2. ANALYSIS OF NORESS ARRAY DATA	22
3.3. ANALYSIS OF MULTI-STATION DATA FOR USSR JVE SHOT	23
3.4. ANALYSIS OF REGIONAL DATA AT WMQ	26
3.5. SCALING OF P-WAVE SPECTRA	34
3.5.1. Comparison of Theory and Observed Regional Data	34
3.5.2. Comparison of Theory and Observed Teleseismic Data	37
3.6. DISCUSSION	45
4. STUDY OF NOVAYA ZEMLYA EXPLOSIONS	51
4.1. P-WAVE SOURCE SPECTRA FROM U.K. ARRAY DATA	51
4.2. INTER-SHOT RATIOS AND ESTIMATES OF NULL FREQUENCY	58
4.3. ESTIMATES OF pP/P BY COMPARISON WITH SYNTHETICS	66
5. CONCLUSIONS	71
6. ACKNOWLEDGMENTS	73
7. REFERENCES	74

Accession For	
NTIS CRA&I	<input checked="" type="checkbox"/>
DTIC TAB	<input type="checkbox"/>
Unannounced	<input type="checkbox"/>
Justification	
By _____	
Distribution /	
Availability Codes	
Dist	Avail. and/or Special
A-1	



2. INTRODUCTION

An understanding of the spectral nulls in the P-wave spectra of underground nuclear explosions is essential for constraining the source depth and for determining the bias in the body wave magnitude resulting from the constructive or destructive interference with pP and later arrivals. Determination of the correct spectral nulls due to pP for Shagan River explosions is especially important because of the complete lack of agreement among various workers. The multichannel deconvolution of array data by Der *et al.* (1987a) provided pP-P or delay time values of 0.55 sec for Kazakh events recorded at NORSAR and 0.4 sec for those at EKA. Using network-averaged P-wave spectra, Murphy *et al.* (1991) obtained delay time of 0.82 sec for an explosion with yield of 119 kt at Shagan River test site. Stewart (1988) examined 62 Shagan River explosions recorded at the four U.K. arrays (EKA, GBA, WRA, and YKA), and the deconvolved waveforms suggest that pP delay times for large ($m_b \approx 6$) explosions vary between about 0.4 to 0.9 sec. All these values of delay times are inconsistent with what is known about the site conditions and testing practices which would suggest a delay time for large explosions to be no larger than about 0.25 sec. An examination of the pulse durations and rise times of Shagan River explosions by Stewart (1988) indicated that the source corner frequency scales, at most, as $Y^{-1/10}$, which is much smaller than the $Y^{-1/3}$ predicted by most source models and observed by Lyman *et al.* (1986) in the rise times of NTS explosions. The main objectives of this study are to (1) determine and understand spectral nulls due to cancellation by pP and other secondary arrivals in P-wave spectra of Shagan River (USSR) explosions, and (2) compare the observed variation of P-wave spectra as a function of m_b with von Seggern and Blandford (1972) and Mueller and Murphy (1971) scaling relationships. We examined teleseismic and regional data from 79 underground nuclear

explosions at the Shagan River test site (Table 1). The list includes 40 events (28 from SW and 12 from NE region) recorded at the EKA array, 33 shots at MAJO, 25 at NORSAR (single channel), 20 at the NORESS array, and 17 at WMQ. Most events are recorded at more than one array or station.

A study of characteristics of the P-wave spectra of Novaya Zemlya explosions is important because of the possibility of all future USSR shots taking place in this region. Moreover, there is significant discrepancy between the results of alternate approaches to understanding the character of the pP reflection from these shots. As pointed out by Burdick (1990), the arrival time of "effective pP" is substantially later than one would predict for a point source within an elastic medium and estimates of its amplitude differ by as much as a factor of 5. Our analysis of digital data for 19 Novaya Zemlya explosions recorded at the U.K. arrays provides information regarding pP that appears to be consistent with local geology of the test site.

TABLE 1

79 SHAGAN RIVER EXPLOSIONS USED IN STUDY

No.	DATE	LAT*	LON*	m _b *	EKA	MAJO	NAO	NRSS	WMQ
1	15 Jan 1965	49.940	79.010	5.87	X	-	-	-	-
2	19 Jun 1968	49.982	79.003	5.28	X	-	-	-	-
3	30 Nov 1969	49.913	78.961	6.02	X	-	-	-	-
4	30 Jun 1971	49.949	78.986	4.94	X	-	X	-	-
5	31 May 1974	49.950	78.852	5.81	X	-	-	-	-
6	16 Oct 1974	49.979	78.898	5.41	X	-	-	-	-
7	27 Dec 1974	49.943	79.011	5.50	X	-	X	-	-
8	27 Apr 1975	49.949	78.926	5.51	X	-	-	-	-
9	30 Jun 1975	50.004	78.957	4.52	X	-	X	-	-
10	29 Oct 1975	49.946	78.878	5.61	X	-	-	-	-
11	25 Dec 1975	50.044	78.814	5.69	X	-	-	-	-
12	21 Apr 1976	49.890	78.827	5.12	-	-	X	-	-
13	09 Jun 1976	49.989	79.022	5.07	-	-	X	-	-
14	04 Jul 1976	49.909	78.911	5.85	X	-	-	-	-
15	28 Aug 1976	49.969	78.930	5.74	X	-	-	-	-
16	07 Dec 1976	49.922	78.816	5.80	X	-	X	-	-
17	29 May 1977	49.937	78.710	5.75	X	-	X	-	-
18	29 Jun 1977	50.006	78.819	5.20	X	-	X	-	-
19	05 Sep 1977	50.035	78.911	5.73	X	-	X	-	-
20	30 Nov 1977	49.958	78.815	5.89	X	-	-	-	-
21	11 Jun 1978	49.898	78.717	5.83	X	X	X	-	-
22	05 Jul 1978	49.887	78.811	5.77	X	X	X	-	-
23	15 Sep 1978	49.916	78.819	5.89	X	X	X	-	-
24	04 Nov 1978	50.034	78.943	5.56	X	X	X	-	-
25	23 Jun 1979	49.903	78.855	6.16	X	X	X	-	-
26	07 Jul 1979	50.026	78.991	5.84	X	X	X	-	-
27	04 Aug 1979	49.894	78.904	6.13	X	X	X	-	-
28	18 Aug 1979	49.913	78.938	6.13	X	X	-	-	-
29	28 Oct 1979	49.913	78.997	5.98	X	X	X	-	-
30	02 Dec 1979	49.891	78.796	5.99	X	X	X	-	-
31	23 Dec 1979	49.916	78.755	6.13	X	X	-	-	-
32	12 Jun 1980	49.981	79.001	5.52	-	X	-	-	-
33	29 Jun 1980	49.931	78.815	5.69	X	X	-	-	-
34	14 Sep 1980	49.921	78.802	6.21	-	X	X	-	-
35	12 Oct 1980	49.961	79.028	5.88	X	X	X	-	-
36	14 Dec 1980	49.899	78.918	5.93	X	X	X	-	-
37	27 Dec 1980	50.057	78.911	5.87	X	X	X	-	-
38	29 Mar 1981	50.007	78.982	5.49	X	X	X	-	-
39	22 Apr 1981	49.885	78.811	5.94	X	X	X	-	-
40	27 May 1981	49.985	78.981	5.30	-	-	X	-	-
41	13 Sep 1981	49.910	78.915	6.06	X	X	-	-	-

42	18 Oct 1981	49.923	78.859	6.00	X	X	.	.	.
43	29 Nov 1981	49.887	78.860	5.62	X
44	27 Dec 1981	49.923	78.795	6.16	.	X	.	.	.
45	25 Apr 1982	49.903	78.913	6.03	.	X	.	.	.
46	31 Aug 1982	49.924	78.761	5.20	X
47	26 Dec 1982	50.071	78.988	5.58	X
48	12 Jun 1983	49.913	78.916	6.02	.	X	.	.	.
49	26 Oct 1983	49.901	78.828	6.04	.	X	.	.	.
50	25 Apr 1984	49.929	78.870	5.90	.	X	.	.	.
51	26 May 1984	49.969	79.006	6.01	.	X	.	.	.
52	14 Jul 1984	49.893	78.884	6.10	.	X	.	.	.
53	27 Oct 1984	49.920	78.777	6.19	.	X	.	.	.
54	02 Dec 1984	49.989	79.011	5.77	.	X	.	X	.
55	16 Dec 1984	49.926	78.820	6.12	.	X	.	X	.
56	28 Dec 1984	49.866	78.703	6.00	.	X	.	X	.
57	10 Feb 1985	49.888	78.781	5.83	.	X	.	X	.
58	25 Apr 1985	49.914	78.902	5.84	.	.	.	X	.
59	15 Jun 1985	49.898	78.845	6.05	.	.	.	X	.
60	30 Jun 1985	49.848	78.658	5.92	.	.	.	X	.
61	20 Jul 1985	49.936	78.785	5.89	.	.	.	X	.
62	12 Mar 1987	49.939	78.823	5.31	.	.	.	X	X
63	03 Apr 1987	49.928	78.829	6.12	X
64	17 Apr 1987	49.886	78.691	5.92	.	.	.	X	.
65	20 Jun 1987	49.913	78.735	6.03	.	.	.	X	X
66	02 Aug 1987	49.880	78.917	5.83	.	.	.	X	X
67	15 Nov 1987	49.871	78.791	5.98	.	.	.	X	X
68	13 Dec 1987	49.989	78.844	6.06	.	.	.	X	X
69	27 Dec 1987	49.864	78.758	6.00	X
70	13 Feb 1988	49.954	78.910	5.97	.	.	.	X	X
71	03 Apr 1988	49.917	78.945	5.99	.	.	.	X	X
72	04 May 1988	49.928	78.769	6.09	X
73	14 Jun 1988	50.045	79.005	4.80	.	.	.	X	X
74	14 Sep 1988	49.870	78.820	6.03	.	.	.	X	X
75	12 Nov 1988	50.056	78.991	5.20	.	.	.	X	X
76	17 Dec 1988	49.818	78.910	5.80	.	.	.	X	X
77	12 Feb 1989	49.930	78.740	5.90	X
78	08 Jul 1989	49.870	78.820	5.60	X
79	02 Sep 1989	50.020	79.050	5.00	X

* from Ringdal and Marshall (1989), Norsar Rept. 2-88/89

3. STUDY OF SHAGAN RIVER EXPLOSIONS

3.1. ANALYSIS OF EKA ARRAY DATA

We examined the short-period, vertical-component data from 40 Shagan River explosions well recorded at the Eskdalemuir (EKA) array, which has 20 elements arranged in an "L" configuration with element spacing of 0.9 km and maximum spacing of 9.8 km (Bache *et al.*, 1985). The epicentral distance of Shagan explosions to the array is about 47° along the azimuth of about 310° or $N50^\circ W$. As compared to results from a single receiver, use of multichannel data has the advantage that frequency-dependent receiver effects, which can drastically influence the observed signals (*e. g.*, Murphy *et al.*, 1989), can be eliminated or at least suppressed.

3.1.1. Spectral Nulls in Source Spectra

Using a window length of 6.4 sec, starting 2 sec before the onset of direct P and with Parzen taper, Fourier spectra were obtained for all data except a few channels with spikes or clipping. These P windows are effectively only a few sec long and are kept short so as to minimize the effects of later secondary arrivals. The spectra were corrected for instrument response and for noise by taking Fourier spectra of a sample of noise preceding the P arrival. A least squares inversion method that isolates the source and receiver terms for each frequency was applied to all spectral amplitudes with the signal/noise (or S/N) power ratio greater than 1. The derived source terms, arranged in order of decreasing m_b for 28 shots from the southwest Shagan test site region, are shown in Figures 1a, b whereas the remaining 12 from the northeast Shagan region are shown in Figure 1c. All (40) source spectra, arranged in the same order as in Figure 1 but with incremental shifts along both axes, are

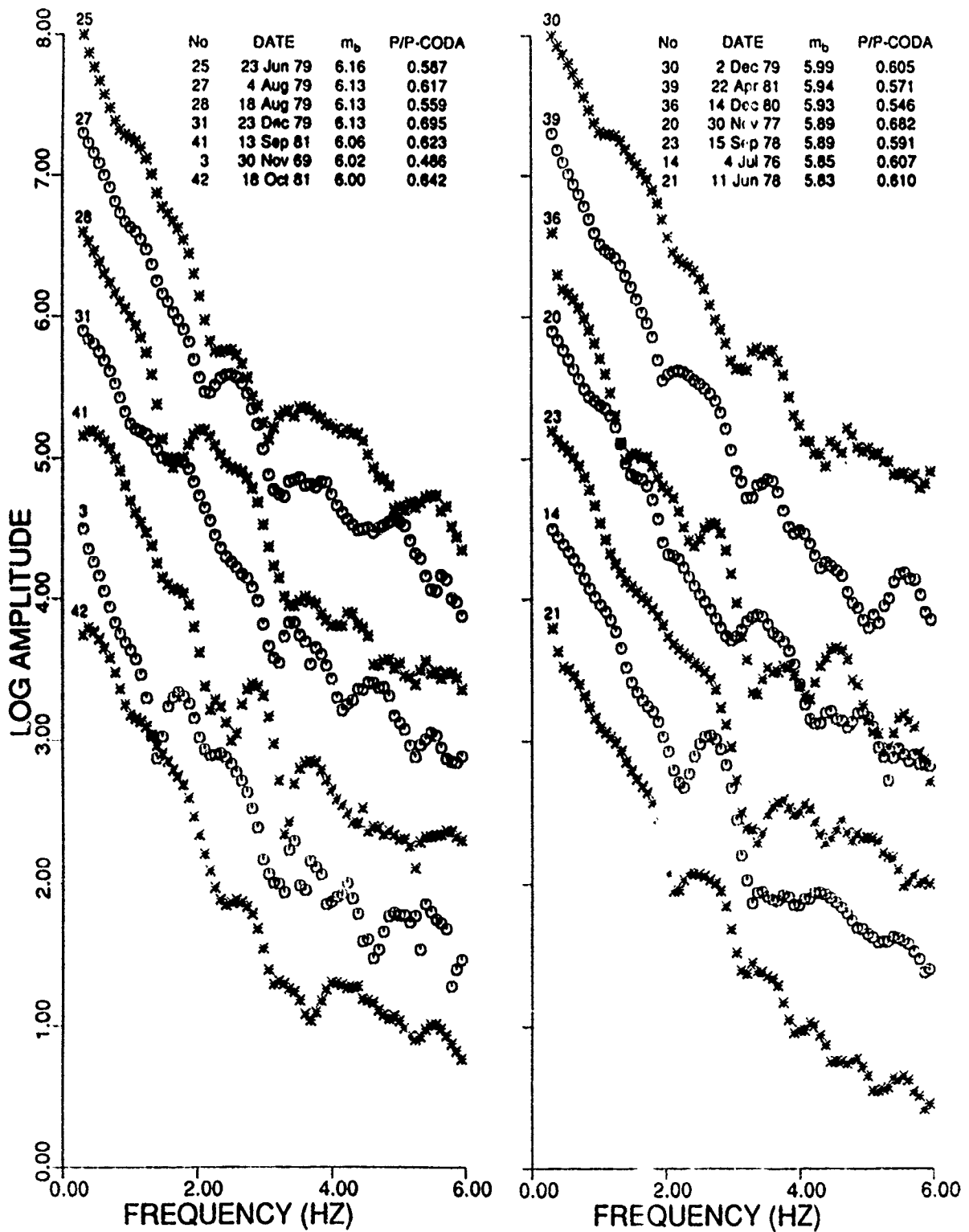


Figure 1a. Source spectra, based on the P(6.4 sec) window, corrected for instrument response, of the 14 largest SW Shagan shots recorded at EKA, arranged in order of decreasing m_b . Mean values of the amplitude ratio P/P-coda (0.5-2.0 Hz) are also indicated. Prominent low-frequency nulls are generally associated with smaller values of P/P-coda.

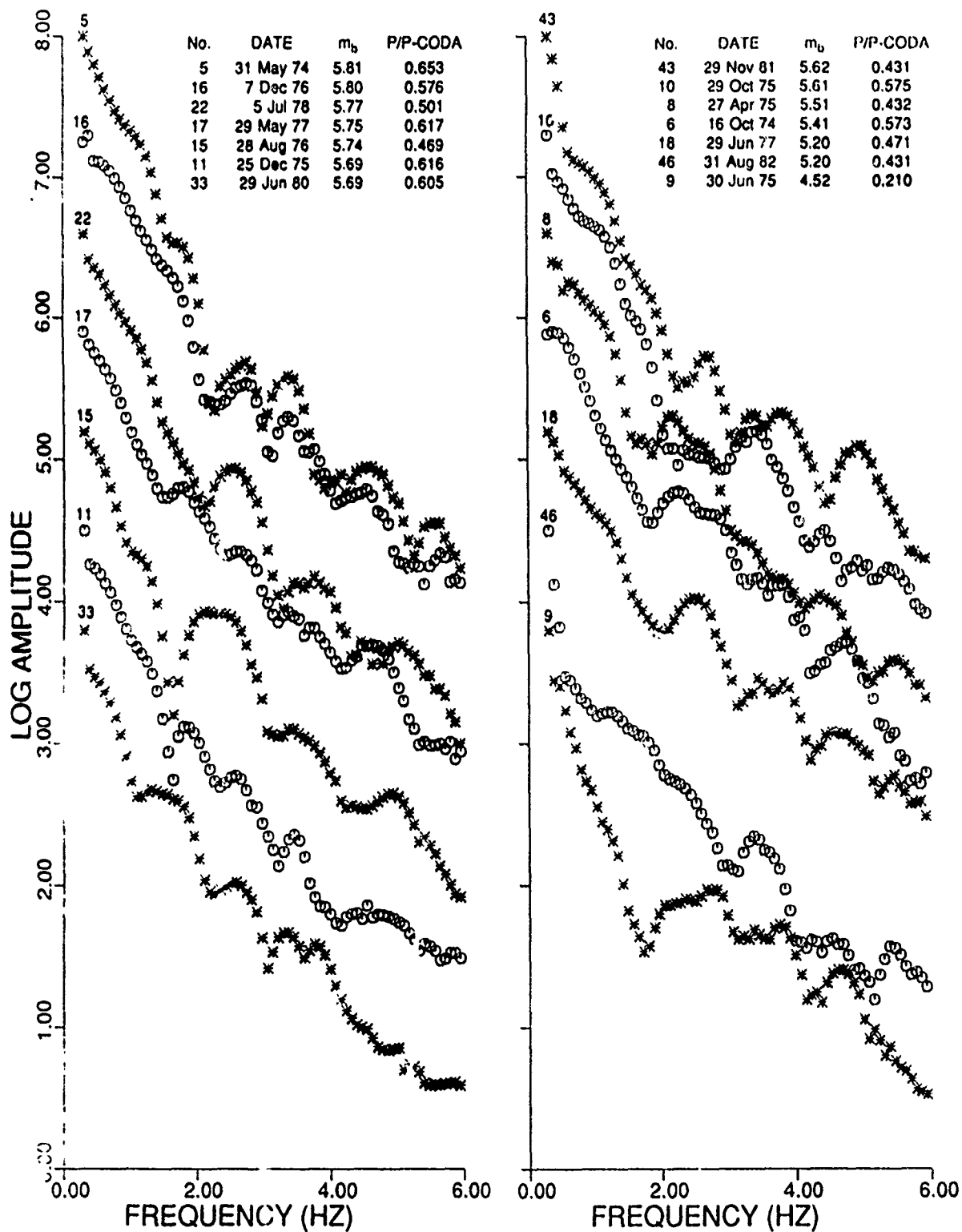


Figure 1b. Similar to Figure 1a for the next 14 SW Shagan shots, arranged in order of decreasing m_b . The low-frequency n. lls, more distinct for smaller explosions, are generally associated with smaller values of P/P-coda.

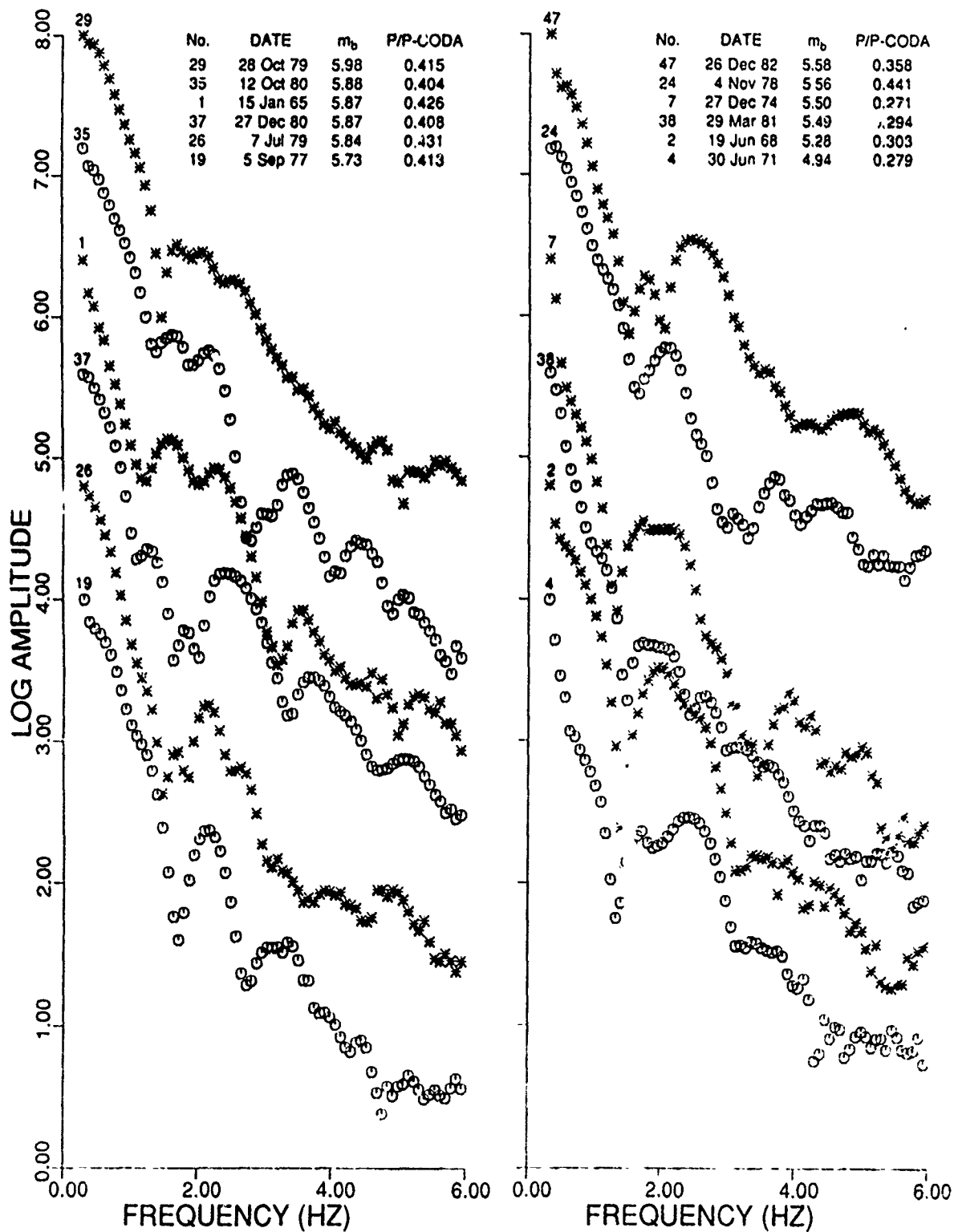


Figure 1c. Similar to Figure 1a for 12 NE Shagan shots, arranged in order of decreasing m_b . The low-frequency nulls, generally more distinct for smaller explosions and for shots in the NE Shagan region, are generally associated with smaller values of P/P-coda.

shown in Figure 2. An examination of the spectra in Figures 1 and 2 suggests three general trends: (1) a majority of shots, including the cratering shot of 15 January 1965, have spectral nulls at about 3 Hz, (2) several explosions have spectral nulls at about 4 Hz, and (3) a majority of shots have low-frequency (less than about 2 Hz) nulls which are generally more distinct for smaller explosions and for shots in the northeast Shagan region. These three types of spectral nulls are also evident in the average power spectrum for all 40 shots (Figure 3) which indicates the most pronounced null to be at about 3 Hz and less distinct nulls at about 4 Hz and 1.5 Hz.

3.1.2. Low-Frequency Nulls and Near-Source Geology

The Shagan River test site is believed to be underlain by about 100 m of unconsolidated sediments with the thickness decreasing gradually towards southwest (Bonham *et al.*, 1980). The P(6.4 sec) source spectra of 10 explosions (a subset of the 40 source spectra in Figure 1 but without correction for instrument response) with shot points lying approximately along a SW-NE profile across the test site (Figure 4a) suggests a gradual build-up of the low-frequency nulls as the thickness of sediments increases. Moreover, the peak-amplitude and the null frequencies appear to be decreasing with increasing thickness of sediments. A null at about 3 Hz is also observed in most spectra. Figures 1a and 1b indicate that these low-frequency nulls are also associated with smaller m_b and therefore shallower shots in the SW Shagan region. Source spectra derived from the P(3.2 sec) windows for the same 10 explosions, shown in Figure 4b, indicate almost total absence of the low-frequency nulls and some evidence of nulls at about 4 and 3 Hz. Moreover, for most large shots, the 4 Hz null is relatively more prominent in spectra of the shorter window (Figure 4b) than in spectra of the

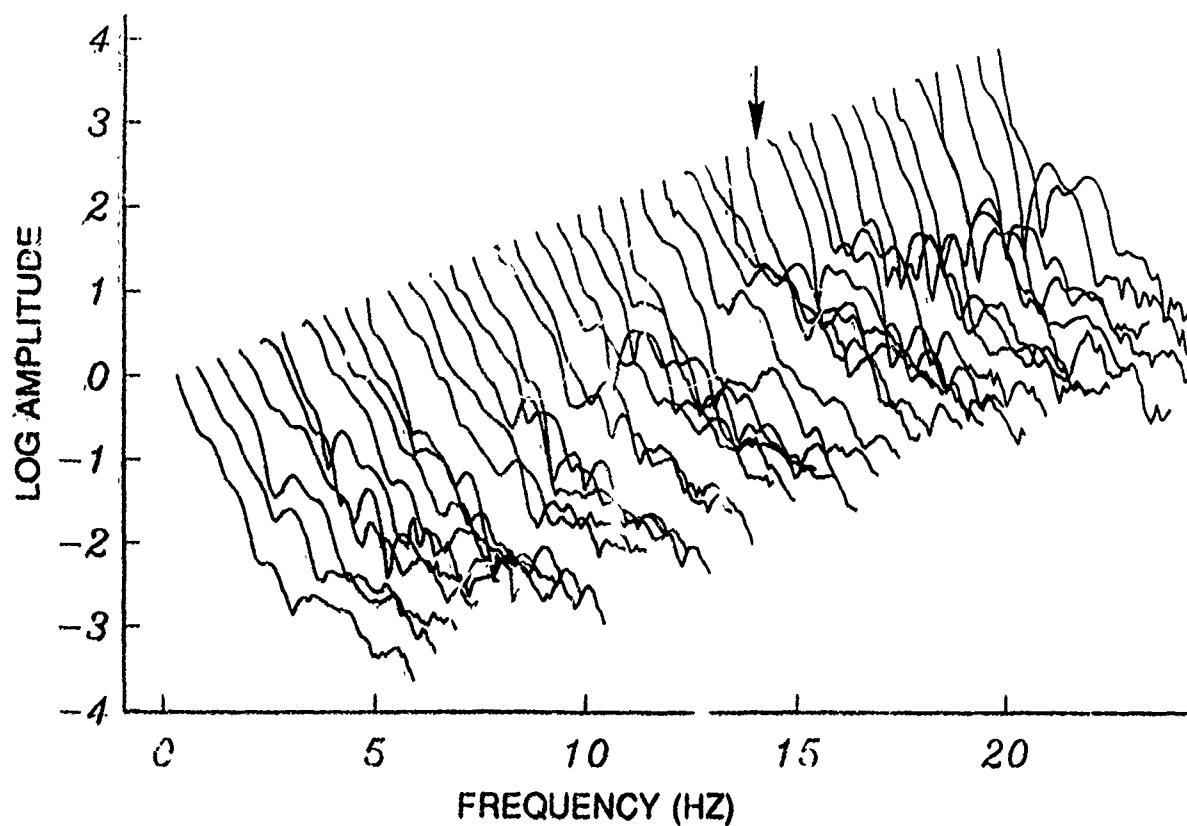


Figure 2. Source spectra of 40 explosions, same as in Figures 1a, b, c and arranged in the same order but with incremental shifts along both axes. The log amplitude values are normalized to the first frequency and the arrow divides the SW and NE Shagan populations.

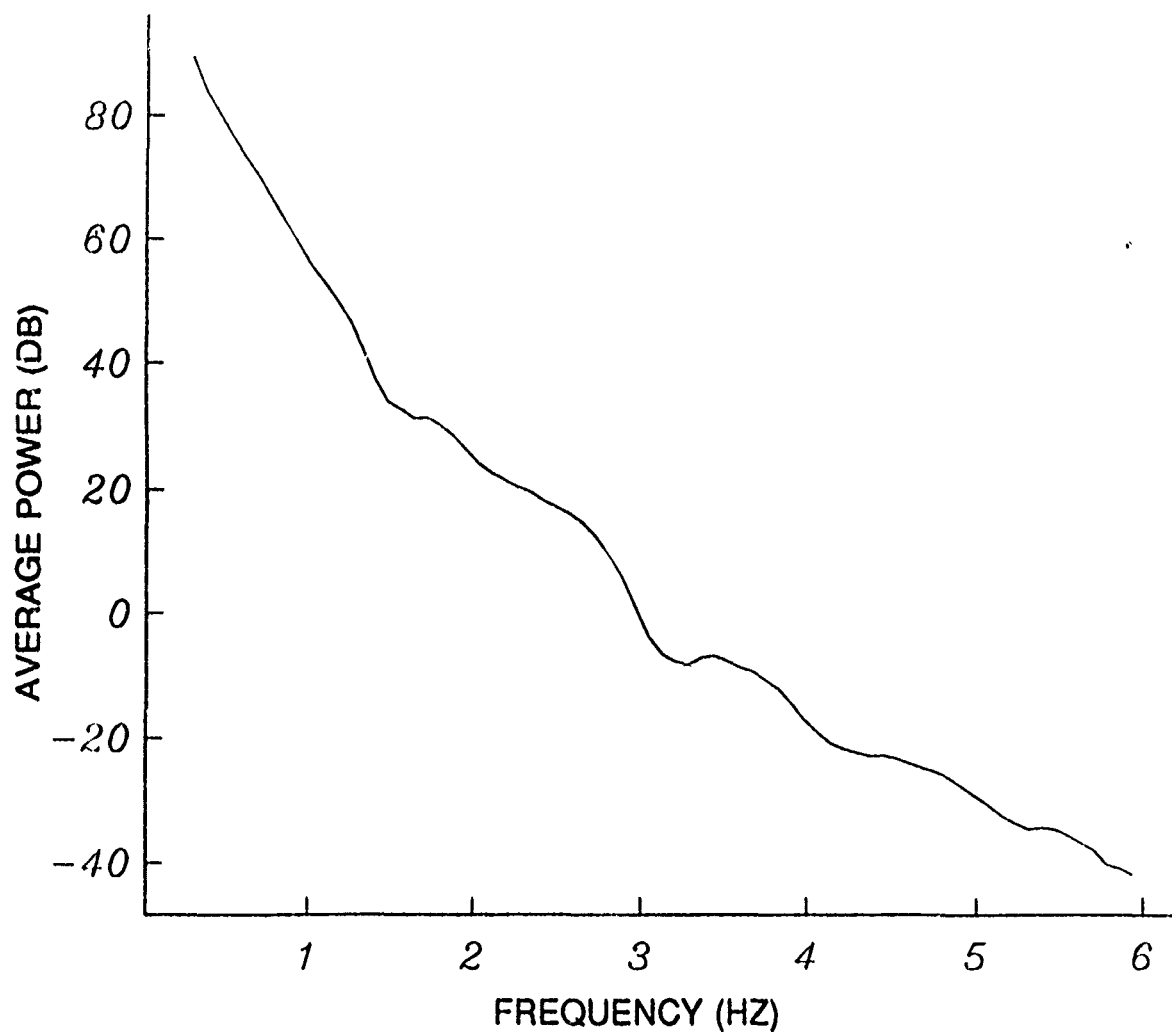


Figure 3. Average power spectrum (log units) of all 40 shots recorded at EKA indicating a distinct null at about 3 Hz and weaker nulls at about 4 Hz and 1.5 Hz.

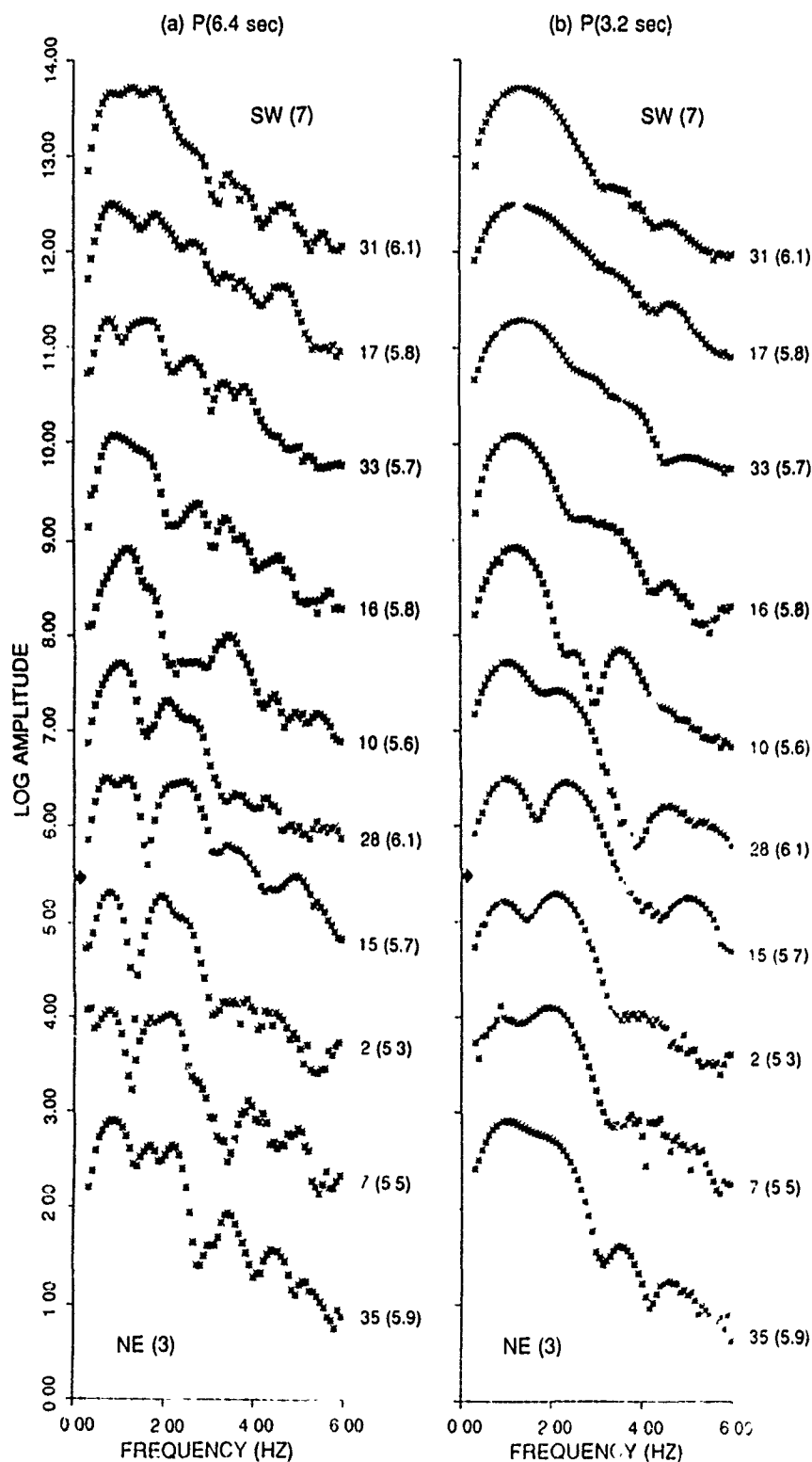


Figure 4. Source spectra derived from EKA array data, not corrected for instrument response, of 10 explosions with shot points lying approximately along a SW-NE profile across the test site, for (a) P(6.4 sec) and (b) P(3.2 sec) windows. Note the gradual build-up of the low-frequency nulls which are more dominant in (a) than in (b). Numbers (in parentheses) next to the spectra indicate m_b .

longer window (Figure 4a). Even the 3 Hz null is relatively less prominent in Figure 4b than in Figure 4a, suggesting the possibility that its origin is also due to a somewhat later arrival. It is therefore clear that the low-frequency nulls are due to secondary (later) arrivals. Furthermore, a probable reason for their existence is greater near-source scattering for explosions under thicker low velocity sediments or shallower shot depths because the near-source environment in both cases is likely to be associated with greater near-source heterogeneity. Thin low velocity sediments may not be "seen" by seismic waves of low frequency or long wavelengths and therefore not make significant contribution to the scattered waves.

Figure 5 shows source deconvolutions for a set of Shagan River explosions recorded at EKA as derived by Der *et al.* (1987b). The first three shots are from the SW and the remaining three from the NE region of the test site. The corresponding source spectra, a subset of those in Figure 1 but without the correction for instrument response (similar to Figure 4a), are shown in Figure 6. Similar to the results in Figure 4, a comparison of Figures 5 and 6 also suggests that the low-frequency nulls are associated with prominent secondary arrivals within a few sec of the first P. The deconvolutions have distinct low-frequency secondary arrivals within a few sec of the first P for the last 4 shots in Figure 5 and spectra of the same 4 shots show distinct low-frequency nulls (Figure 6). The three SW shots in Figure 5 have fairly distinct pP phases and the spectra of the first two show the expected nulls due to cancellation by pP at about 4 Hz (Figure 6). The third (29 June 80) shot indicates a strong secondary arrival with its positive peak arriving about 1.3 sec after the positive peak in the first P. These two same-polarity arrivals should give rise to spectral peaks at about 0.8 Hz, 1.6 Hz, 2.4 Hz, . . . , in good agreement with the observed source spectra in Figure 6. Similar interpretations appear to be valid for the strong low-frequency peaks and nulls in the spectra of the three NE

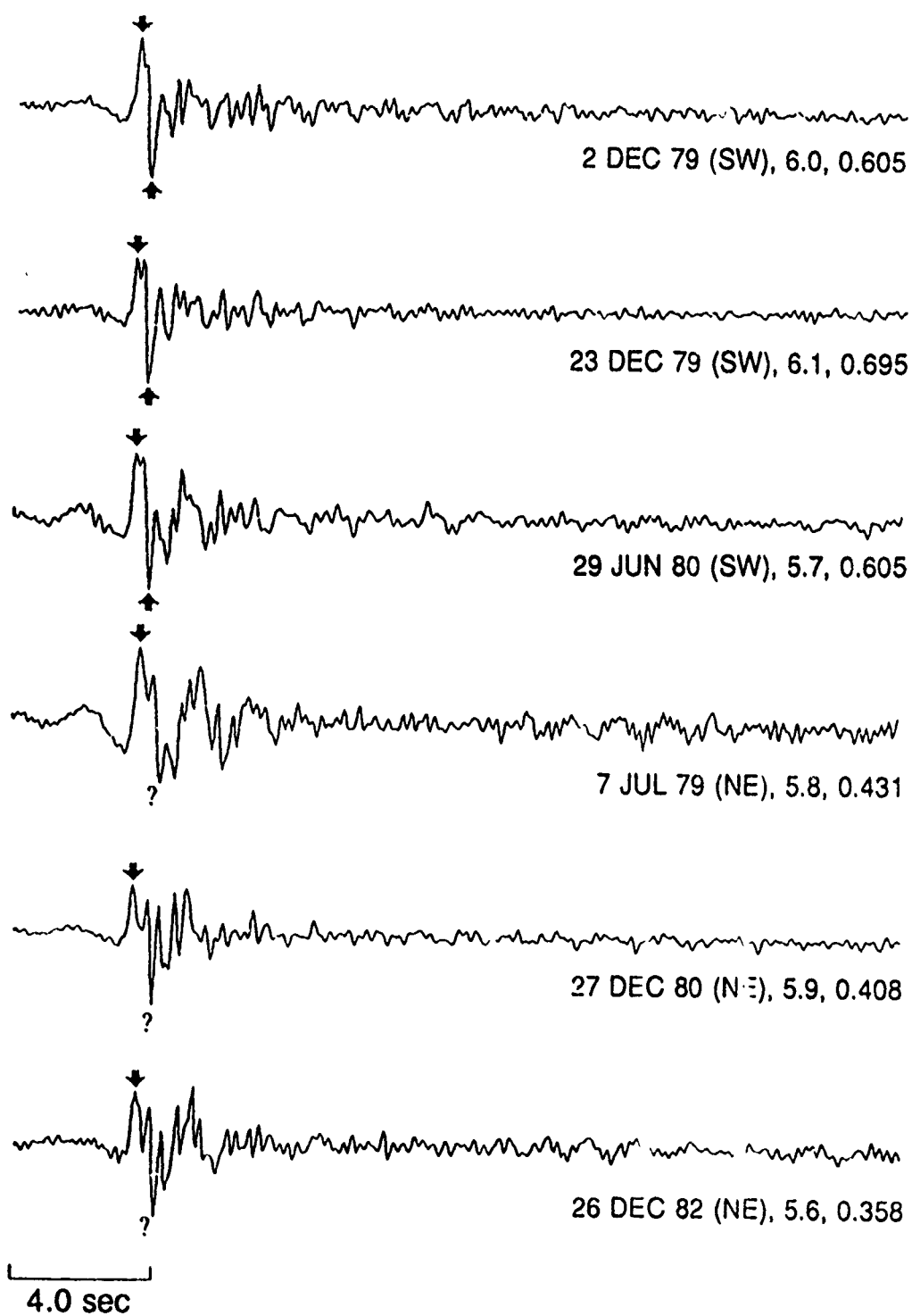


Figure 5. Deconvolved source functions of 6 Shagan River explosions derived from EKA array data. The P and pP arrivals, if present, are denoted by arrows. m_b and mean values of the amplitude ratio P/P-coda (0.5-2.0 Hz) are also indicated.

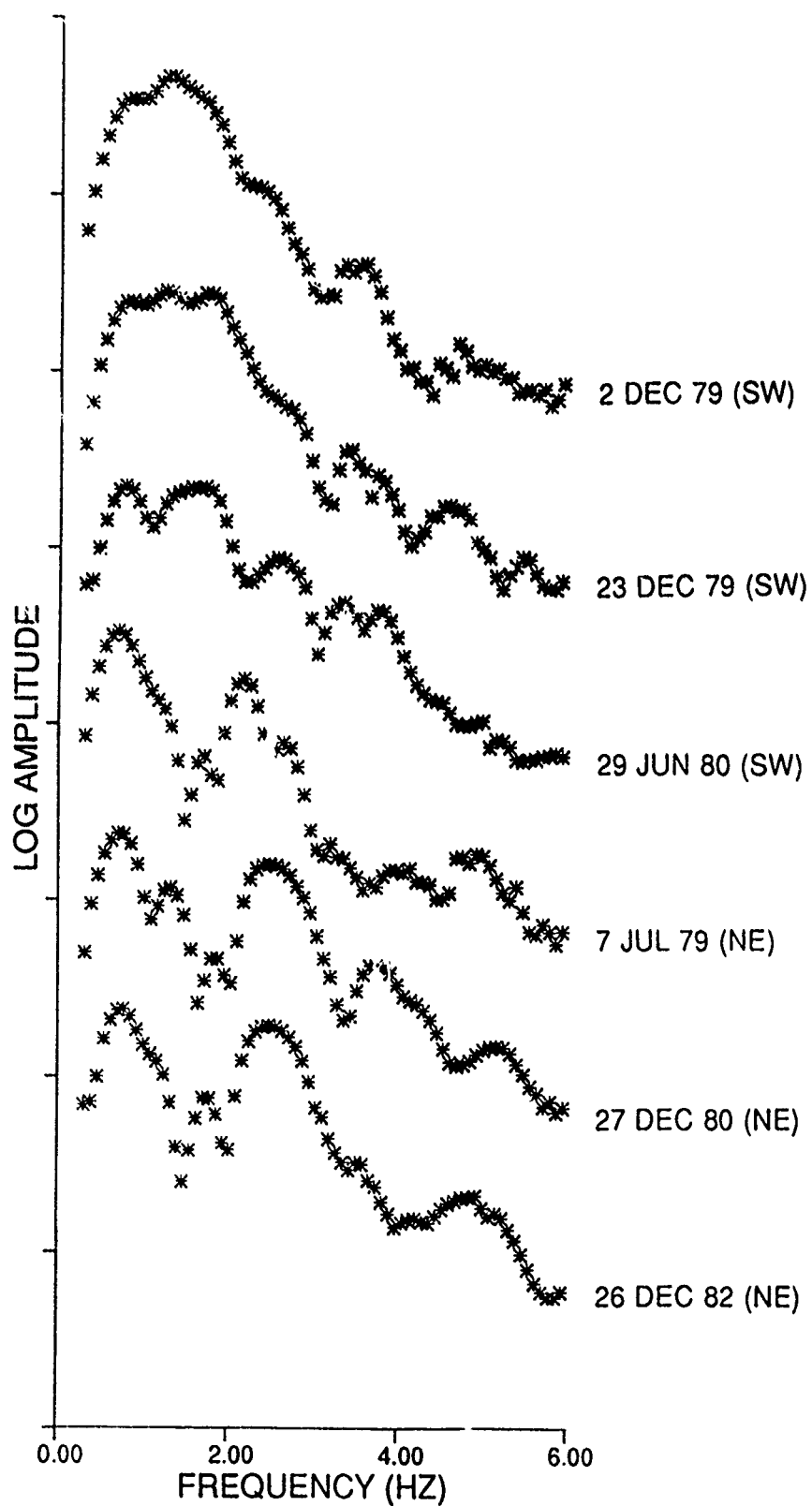


Figure 6. Source spectra, not corrected for instrument response, of the same 6 Shagan River explosions as in Figure 5.

shots which do not show distinct pP arrivals. Each set of 3 shots is closely spaced (within about 5 km), and the codas from each set seem to have several common arrivals.

3.1.3. Comparison of P and P Coda and Origin of Secondary Arrivals

In order to understand the origin of secondary arrivals and the associated spectral nulls, we made a comparison of the spectral characteristics of P and P coda. It is known that the null due to cancellation by pP in the P-wave spectra is significantly reduced in the spectra of P coda (Gupta and Blandford, 1987). Furthermore, the amplitude ratio P/P-coda may provide an indication of near-source scattering, such as scattering of the explosion-generated Rg into teleseismic P arrivals (Gupta *et al.*, 1991).

For an explosion source with source function $S(f)$ within a homogeneous half space, the fundamental-mode Rayleigh wave amplitude $R_g(f)$ is given by the expression (Hudson and Douglas, 1975):

$$R_g(f) = \frac{A \bar{\phi}(\omega)}{r^{0.5} \rho \alpha^{3.5}} f^{1.5} 10^{-4.4 \frac{h}{\alpha} f} \quad (1)$$

where $\bar{\phi}(\omega)$ is the Fourier transform of the source RDP $\phi(t)$, h is the shot depth, $\omega = 2\pi f$, α is the compressional-wave velocity of the shot medium, ρ is the density, r is the epicentral distance, A is a numerical constant, and a Poisson's ratio of 0.25 is assumed. The far-field P-wave displacement, in the frequency domain, may be written as (Hudson and Douglas, 1975):

$$P(f) = \frac{1}{4 \pi \rho \alpha^3 R} \omega \bar{\phi}(\omega) \quad (2)$$

where R is the teleseismic source-receiver distance. If the source-receiver path and the medium velocity do not change, equations (1) and (2) yield

$$\frac{Rg \rightarrow P}{P}(f) = k C(f) f^{0.5} 10^{-4.4 \frac{h}{\alpha} f} \quad (3)$$

where k is a constant and $C(f)$ denotes the scattering function $Rg \rightarrow P$. Assuming that the low-frequency P-coda in teleseismic data is mainly due to the scattering of $Rg \rightarrow P$, we replace $Rg \rightarrow P$ and P in equation (3) by P-coda and P , respectively, and obtain

$$\log \frac{P}{P\text{-coda}}(f) = 4.4 \frac{h}{\alpha} f - \log k - \log C(f) - 0.5 \log f \quad (4)$$

This shows that if we consider explosions for which the $Rg \rightarrow P$ -coda scattering function may be assumed to be the same (such as closely spaced explosions) and the frequency is kept fixed (i.e. for a narrow frequency band), a plot of $\log P/P\text{-coda}$ versus shot depth, h should have a slope of about $4.4 f/\alpha$. Observations of the spectra of Rg signals from both explosions and very shallow-focus earthquakes indicate the dominant energy in Rg to be confined to frequencies less than about 2 Hz and the most important parameter for the generation of Rg to be source depth (e.g. Kafka, 1990).

Excluding a few channels with spikes or clipped data, spectra and spectral ratios $P/P\text{-coda}$ were obtained for each record by selecting a window length of 12.8 sec (beginning 4 sec before the onset of P) as the P -window and the following 25.6 sec signal as the $P\text{-coda}$, and applying Parzen taper to each (see Figure 1 of Gupta and Blandford, 1987 for examples). A correction for noise was made by selecting a sample of noise before the onset of P and obtaining its spectra. The average amplitude ratio of $P/P\text{-coda}$ over the frequency range of 0.5-2.0 Hz, was obtained by using only those data points for which the S/N power ratio was at least 2 for each of P and $P\text{-coda}$. All available amplitude ratios $P/P\text{-coda}$ were used as input to a least squares inversion that separated the source and receiver terms. A plot of the source-term amplitude ratio $P/P\text{-coda}$ versus m_b (Figure 7a) suggests generally larger $P/P\text{-coda}$

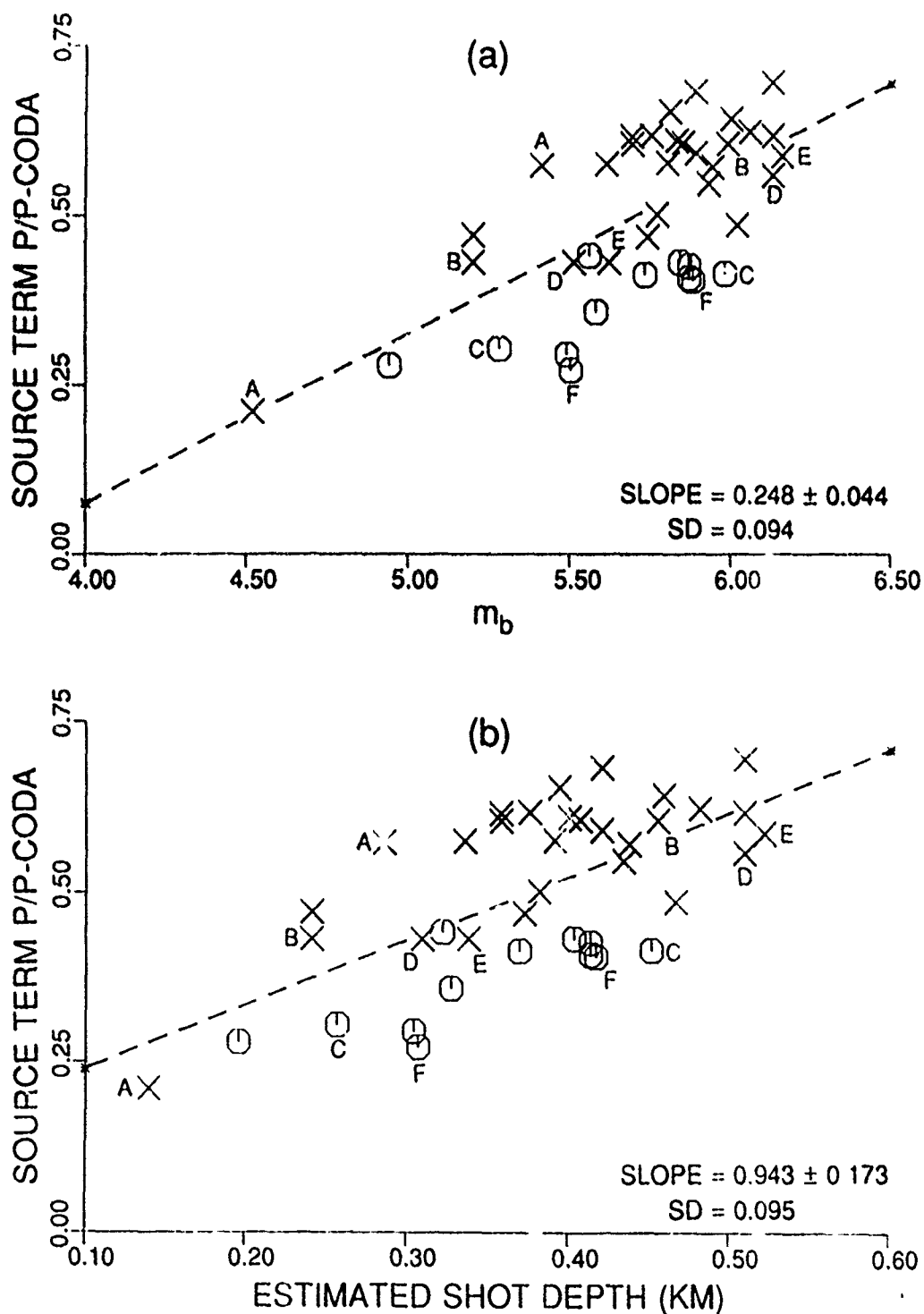


Figure 7. Source term amplitude ratio $P/P\text{-CODA}$ (log units), averaged over the frequency range of 0.5-2.0 Hz, for 40 Shagan River explosions recorded at the EKA array plotted versus (a) m_b and (b) estimated shot depth. The least squares linear regression (dashed line), mean slope (with associated standard deviation), and one standard deviation of residuals (SD) are indicated on each plot. Six pairs of closely spaced explosions are identified by the letters A through F and the SW and NE explosion populations are denoted by X and O, respectively.

for larger explosions. Figure 7a also shows that the NE Shagan shots generally have smaller values of P/P-coda than the SW shots. This will be consistent with generally larger P-coda and greater complexity observed for the NE shots than for the SW shots by Bache *et al.* (1984) and Marshall *et al.* (1985).

A relationship between the average ratio P/P-coda and shot depth was obtained by converting the known m_b into shot depth by using empirical relationships based on the information on shot depths and yields recently released by Bocharov *et al.* (1989). These relationships, derived from the Shagan River and Konystan (Murzhik) explosions are (R. S. Jih, written communications, 1990):

$$m_b = 0.690 \log Y + 4.605 \quad (5)$$

where Y is the yield in kt, and

$$\log h = 0.241 \log Y + 2.174 \quad (6)$$

where h is shot depth in meters. These two equations would indicate an explosion of $m_b = 6$ to have a yield of about 105 kt and a depth of 458 m. Using equations (5) and (6), one obtains

$$\log h = 0.349 m_b + 0.567 \quad (7)$$

which can be used to estimate shot depth for an explosion with known m_b . A plot of the observed amplitude ratio P/P-coda versus estimated shot depth in km (Figure 7b) indicates a mean slope of 0.943 with one standard deviation of residuals of only 0.095.

Assuming the P-wave velocity for the uppermost 0.5 km of the crust in the Shagan test site region to be 5 km/sec, $4.4 f/\alpha = 1.1$, if f is taken to be the average of 0.5 and 2.0 or 1.25 Hz. Good agreement between the mean slope expected from simple theory and observation (Figure 7b) suggests that the low-frequency P-coda is mainly due to the scattering of

explosion-generated Rg.

Figure 7 includes results from six (including two from NE Shagan) pairs of explosions within less than 2 km of each other (identified by the letters A through F). It is known that propagation paths can exert significant influence on seismic recordings (e.g. Blandford, 1981) so that results from closely spaced explosions recorded at a common station should be considered more reliable than others. It is important to note that the slope from each of the six pairs of shots in Figure 7b is nearly the same as derived from the average of all (40) shots and is in good agreement with the theoretically expected value.

Results similar to those in Figure 7 but for the frequency range of 3.0-5.0 Hz are shown in Figure 8 which shows good separation between explosions from the SW and NE regions of the Shagan River test site. The lack of any systematic variation with shot depth is consistent with the suggestion of explosion-generated Rg contributing to P-coda because Rg is important only for frequencies less than about 2 Hz. Following Levander and Hill (1985), the relatively larger high-frequency P coda for shots in the NE Shagan region could be due to the presence of an irregular low-velocity surface layer in that region.

If the scattering of explosion-generated Rg contributes mainly to P coda, what is the origin of the secondary arrivals appearing within a few sec of the first P and causing distinct low-frequency nulls in the spectra of the initial P window? The answer appears to be that these secondary arrivals are due to near-source or local scattering because our observations suggest the low-frequency nulls to be stronger for shots associated with greater near-source heterogeneity. The scattering may include body-wave (P-to-P and S-to-P) scattering and the near-source S may be generated by mechanisms such as source anisotropy or strain release. Local scattering, expected to be larger for both shallower shots and for those in NE Shagan,

40 SR SHOTS, EKA ARRAY (3.0-5.0 Hz)

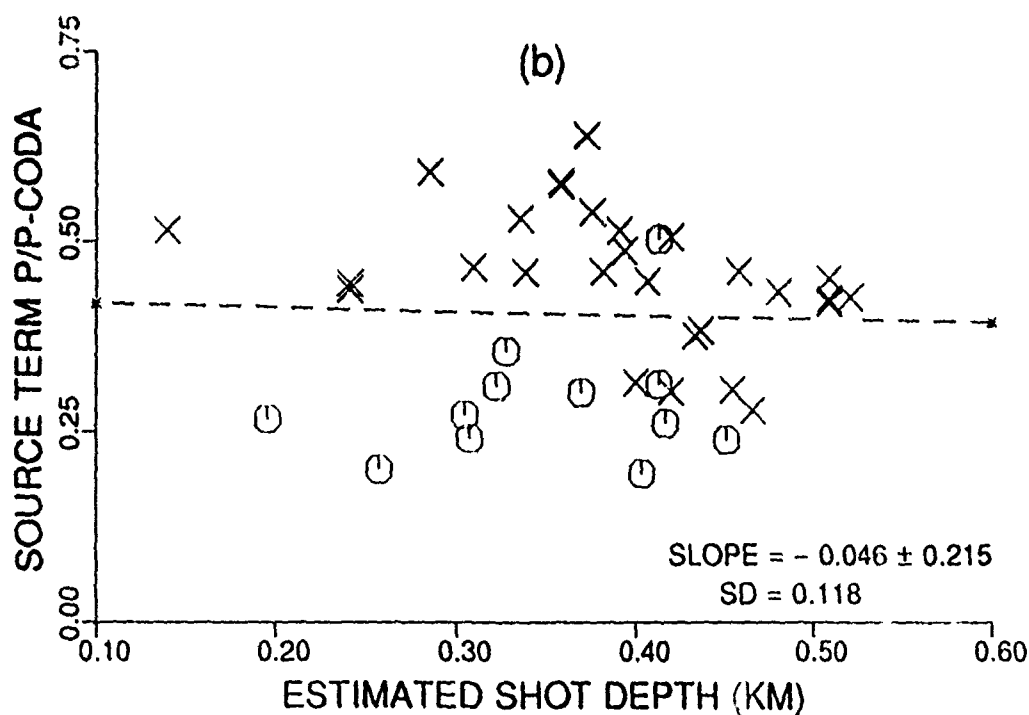
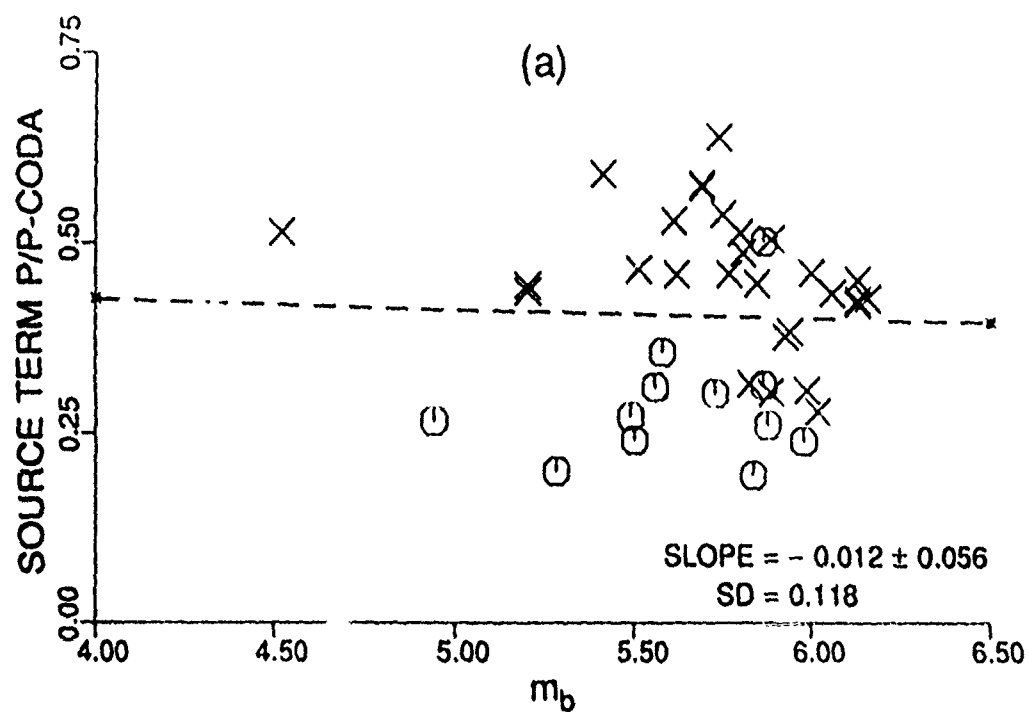


Figure 8. Similar to Figure 7 but for the frequency range of 3.0-5.0 Hz. There is no significant dependence of P/P -coda on m_b or estimated shot depth but the SW and NE explosion populations appear well separated.

may therefore be responsible for the low-frequency nulls.

P coda is known to be an excellent measure of yields of underground nuclear explosions at both NTS and USSR test sites (Gupta *et al.*, 1985). The observed stability of P coda appears to imply that the Rg-to-P scattering must be occurring over a fairly large region of the shallow crust. Our observations and analysis suggest that the most important parameter controlling Rg-to-P scattering within a given region is the shot depth. Thus local body-wave scattering may be responsible for the low-frequency nulls whereas the scattering of Rg-to-P occurs on a regional basis and appears in P coda. A prominent low-frequency spectral null and relatively large value of P/P-coda observed for the nuclear shot of 29 June 1980 (Figures 5 and 6) may therefore be explained by large local scattering but small regional Rg-to-P scattering because of the explosion being fairly deep and in the SW Shagan region. The 40 values of source term P/P-coda, indicated for each explosion in Figure 1, suggest that the low-frequency nulls on the spectra of most shots are associated with relatively low values of P/P-coda (see especially spectra of shot nos. 3 and 16 in Figure 1a, 15 and 9 in Figure 1b, and 7, 38, 2, and 4 in Figure 1c). The probable explanation is that, in most cases, factors such as shallower shot depth and lower medium velocity that enhance local scattering (which is responsible for the low-frequency nulls) also enhance the generation of Rg and its contribution by scattering to P coda.

3.2. ANALYSIS OF NORESS ARRAY DATA

Analysis similar to that for the EKA array data was carried out for the short-period, vertical-component data from 20 Shagan River explosions (Table 1) well recorded at the NORESS array which has 25 vertical component sensors located within a 3 km diameter

aperture. The epicentral distance of Shagan River explosions to NORESS is about 38° along the azimuth of about 313° or $N47^\circ W$. Again, the use of multichannel data and a least squares inversion method isolated the source and receiver terms for each frequency. The derived source terms appeared to show characteristics similar to those observed for the EKA data. By using P and contiguous P-coda windows of 6.4 and 12.8 sec, respectively and applying Parzen taper, spectral ratios P/P-coda were obtained for data from each sensor of the NORESS array. These ratios were also used in a least squares inversion procedure to obtain the source terms. Results for two large ($m_b = 6.0$) explosions are shown in Figure 9. Both figures indicate spectral nulls at the expected frequency of about 4 Hz in addition to prominent nulls at frequency of about 3 Hz. The remarkable similarity of spectral nulls between spectra of P(6.4 sec) and P(6.4 sec)/P-coda (12.8 sec) for frequency greater than about 2 Hz shows that the spectral nulls in P are almost completely filled in P coda and P/P-coda may provide an alternate effective method for detecting spectral nulls due to cancellation by pP.

3.3. ANALYSIS OF MULTI-STATION DATA FOR USSR JVE SHOT

The USSR Joint Verification Experiment (JVE) shot of 14 September 1988 in SW Shagan test region was well recorded at many stations. Data from 11 teleseismic ($\Delta > 30^\circ$) stations (Table 2) was used to derive the average spectra of P(6.4 sec) and average spectral ratio P(6.4 sec)/P-coda (12.8 sec). The average spectra (not corrected for instrument response), scaled to the average amplitudes in the frequency range of 0.5 to 3.0 Hz, and the 11-station average ratio of P/P-coda, with no scaling, are shown in Figures 10 a and b, respectively. Note that the average spectra of both P and P/P-coda indicate nulls at the expected frequency of about 4 Hz and there is not much evidence for a spectral null at about 3 Hz.

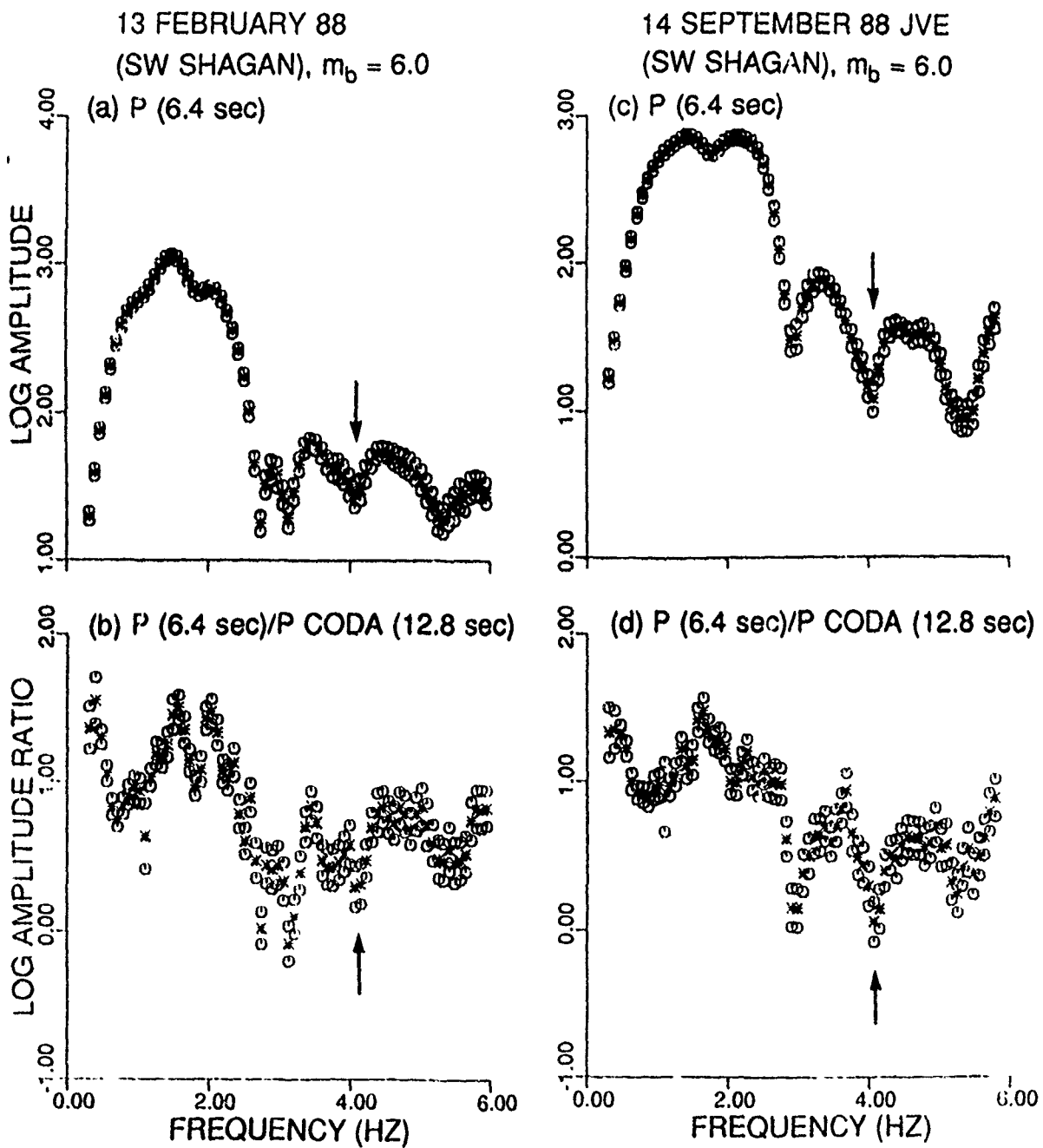


Figure 9. Source terms for (a,c) P and (b,d) P/P-coda for two shots derived by least squares inversion of NORESS array data for 20 Shagan River shots. Note prominent spectral nulls at about 4 Hz (denoted by arrows) and 3 Hz in both P and P/P-coda spectra of both shots.

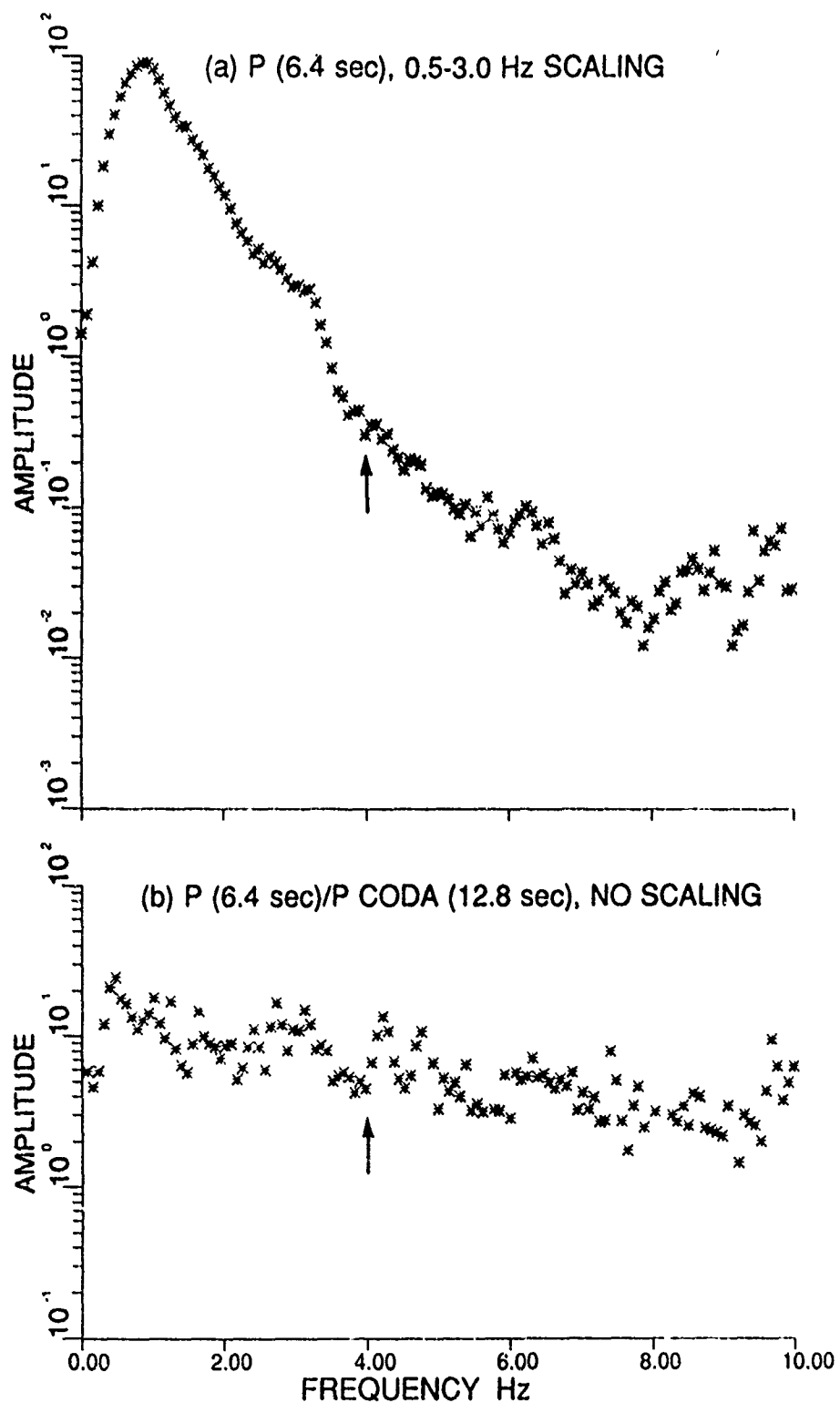


Figure 10. Spectra of (a) P and (b) P/P-coda for the Shagan River shot of 14 September 1988 derived from teleseismic data from 13 stations. Null at the expected frequency of about 4 Hz is not distinct in the spectra of P but is somewhat better seen in the spectra of P/P-coda.

observed in the spectral data from many stations such as the EKA array and NORESS.

TABLE 2
STATIONS RECORDING USSR JVE SHOT OF 14 SEPTEMBER 1988

No.	STATION	LAT	LON	DISTANCE (DEG)	AZIMUTH (DEG)
1	ANTO	39.900 N	32.783 E	33.6	271
2	CHTO	18.790 N	98.977 E	35.0	145
3	KONO	59.649 N	9.598 E	39.3	311
4	GRFO	49.692 N	11.205 E	42.3	297
5	TOL	39.881 N	4.049 W	56.7	294
6	LEM	6.833 S	107.617 E	61.8	147
7	LON	46.750 N	121.810 W	82.1	14
8	SCP	40.795 N	77.865 W	87.4	342
9	NWAO	32.927 S	117.237 E	89.2	148
10	CMB	38.035 N	120.385 W	90.8	15
11	ANMO	34.946 N	106.457 W	95.4	4

3.4. ANALYSIS OF REGIONAL DATA AT WMQ

We examined the spectra of regional phases from 17 Shagan River underground nuclear explosions recorded on the broadband instrument at the Chinese network station Uru nchi (WMQ), located about 8.6° or 950 km southeast of the test site. The explosions are listed in Table 1, which includes data from Ringdal and Marshall (1989) for 14 Shagan River explosions prior to the year 1989. Examples of seismograms are shown in Gupta *et al.* (1990a). The first arrival Pn was distinct on all records, and the beginning of Lg was assumed to be at a group velocity of 3.5 km/sec, in agreement with the observed data. Spectra of Pn were obtained for both P(6.4 sec) and P(12.8 sec) windows and by applying both Parzen and a 10% cosine taper. The resulting spectra, without any smoothing, are shown in Figures 11 and 12 for explosions of 13 February 1988 and 14 September 1988 (JVE), respectively. An

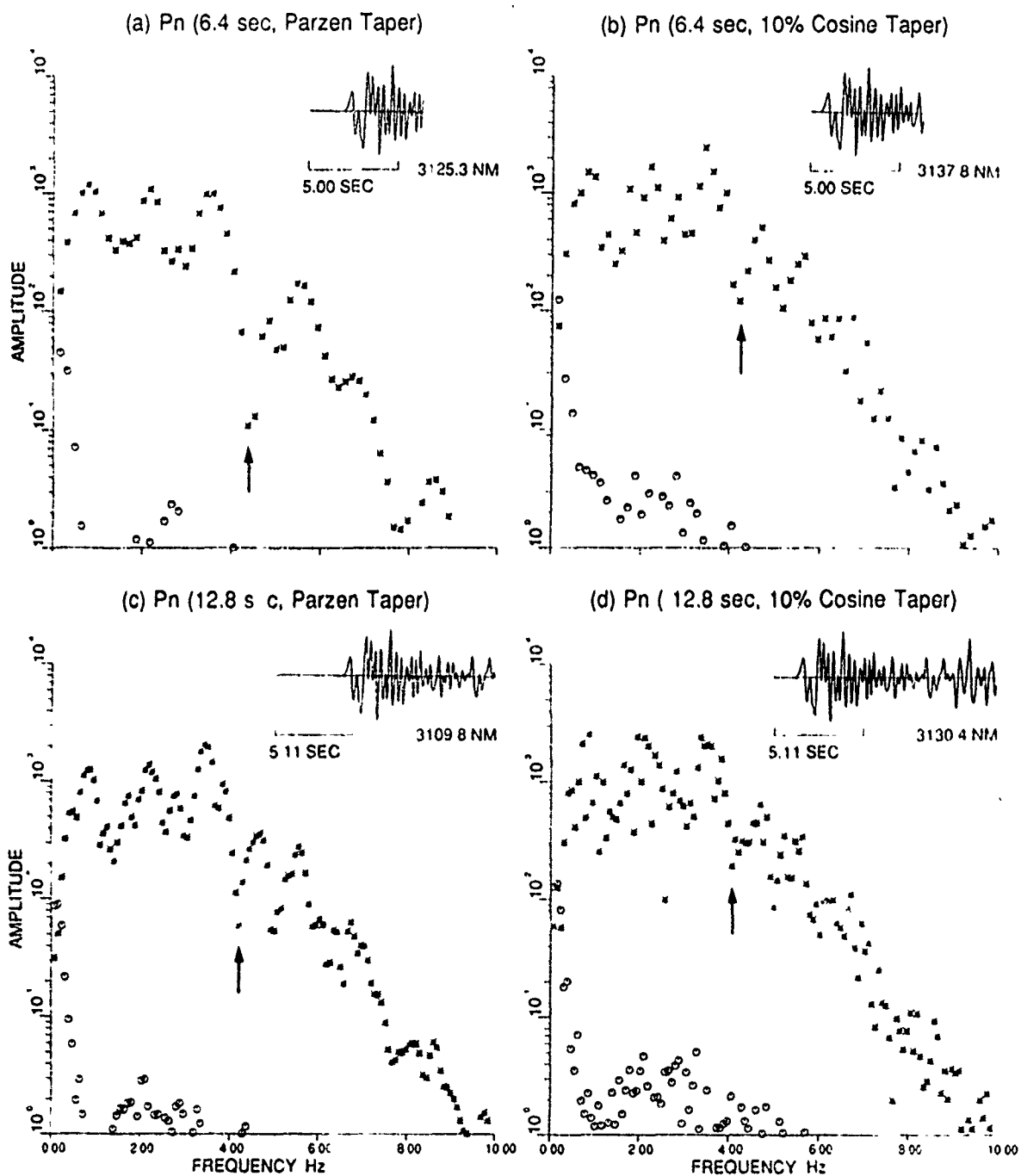


Figure 11. Spectra and waveforms of Pn for two different window lengths and two tapers for the SW Shagan explosion of 13 February 1988 ($m_b = 6.0$) recorded at WMQ. Prominent nulls in spectra at about 4 Hz are denoted by arrows.

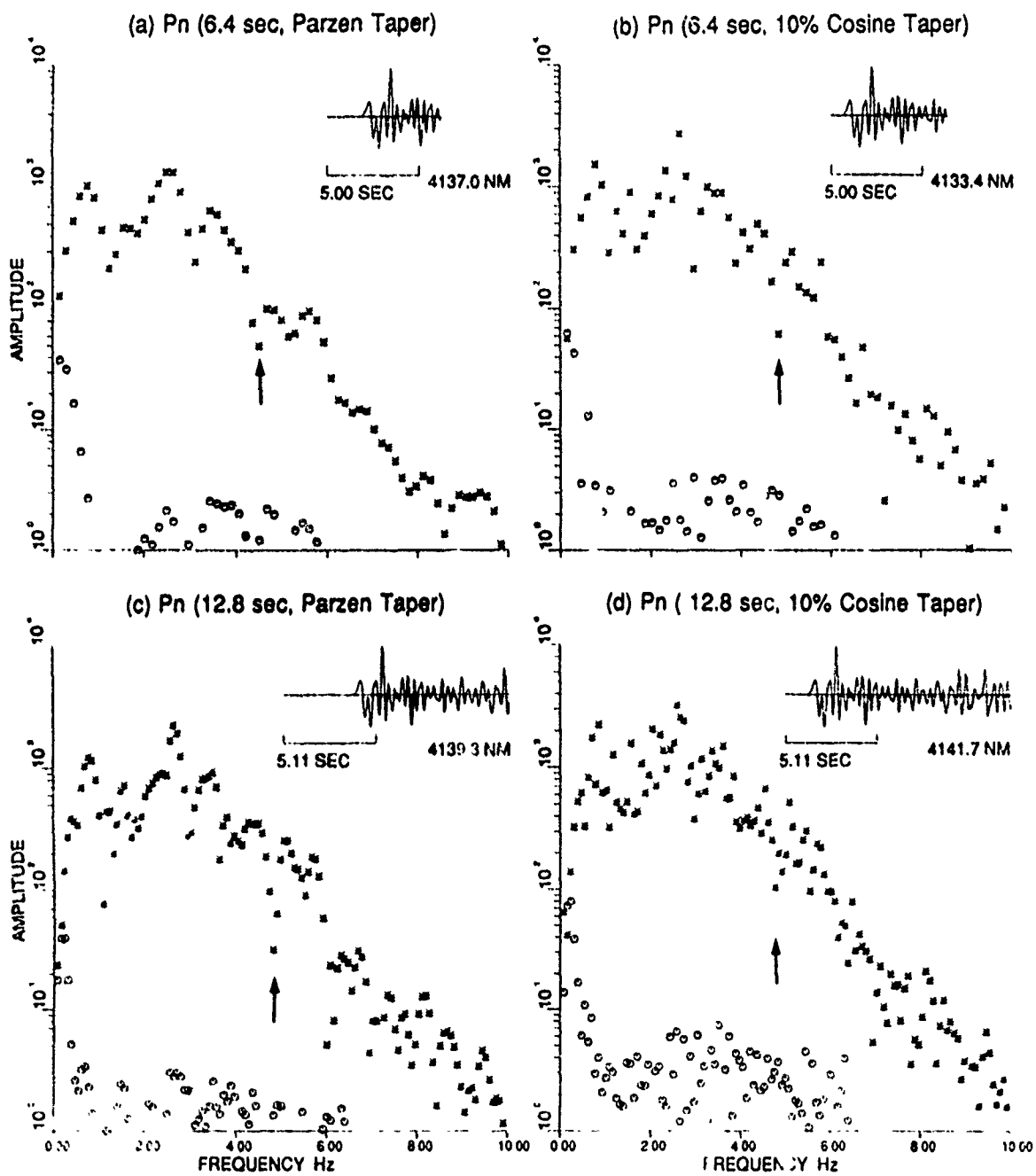


Figure 12. Similar to Figure 11 for the explosion of 14 September 1988 ($m_b = 6.0$).

examination of the eight spectra of the two large explosions confirms the presence of spectral nulls at about 4 Hz, in agreement with the expected value. Note that Parzen taper provides better resolution of the spectral nulls than the cosine taper. The same is true of shorter versus longer windows, perhaps because of less contamination by later (secondary) arrivals which will tend to fill in the spectral holes.

Using a window length of 51.2 sec for Lg, the spectra of Lg and the spectral ratios Pn/Lg for explosions of 13 February 1988 and 14 September 1988 are shown in Figures 13 and 14, respectively. The spectral ratios are corrected for noise by using a sample of noise before the onset of Pn. In order to accentuate the spectral nulls in Pn, the spectral ratios Pn/Lg were derived by using only those data points for which the power ratio of $S/N > 1.0$ for Pn and > 1.5 for Lg. As expected, the shorter Pn window and the use of Parzen taper (Figures 13b and 14b), provided the most credible evidence for nulls due to cancellation by pP at the expected frequency of about 4 Hz.

Several Shagan River explosions were recorded at both NORESS and WMQ. The spectra of teleseismic P and regional Pn for two closely-spaced explosions are shown in Figures 15 and 16. For each station, the spectral shapes including peaks and nulls of the two explosions appear similar for frequencies lower than about 3 Hz. A possible reason is that the lower frequency nulls are caused mainly by near-source scattering which should be similar for closely-spaced shots. The NORESS spectra for the sensor NRA0 show a prominent null at about 4 Hz for the larger explosion of 20 June 1987 of $m_b = 6.0$ and nulls at about 3 Hz for both shots. The spectra of Pn at WMQ also indicate a distinct null at about 4 Hz for the larger explosion but there is not much evidence for nulls at about 3 Hz. The Pn spectra of the shots of 13 February 1988 and 14 September 1988 recorded at WMQ (Figures 11 and 12)

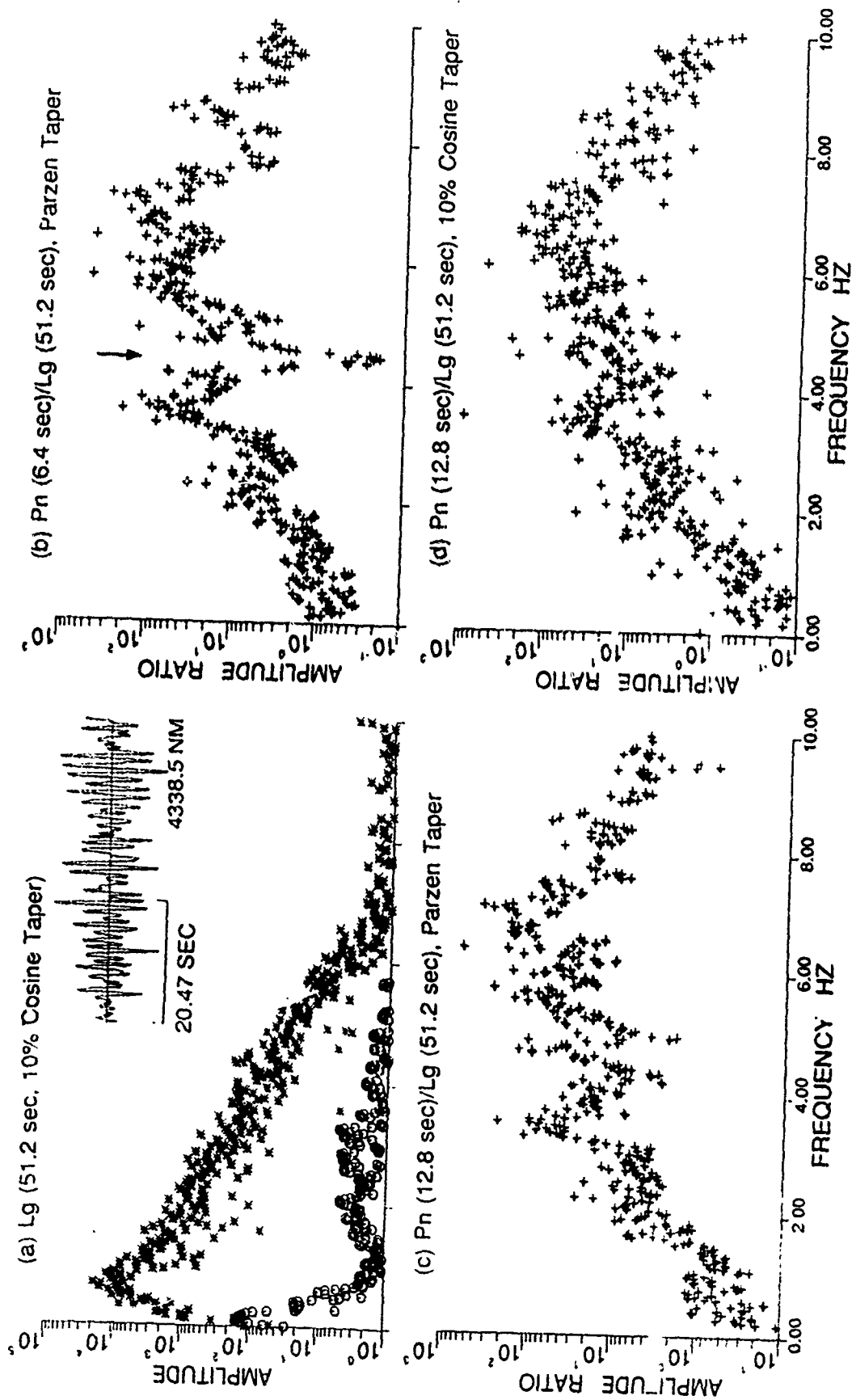


Figure 13. Spectra and waveform of Lg and spectral ratios Pn/Lg for the SW Shagan explosion of 13 February 1988 recorded at WMQ. The three spectral ratios are corrected for noise and are based on the use of points for which power ratio of $S/N > 1.0$ for Pn and > 1.5 for Lg. Prominent null at about 4 Hz is denoted by an arrow.

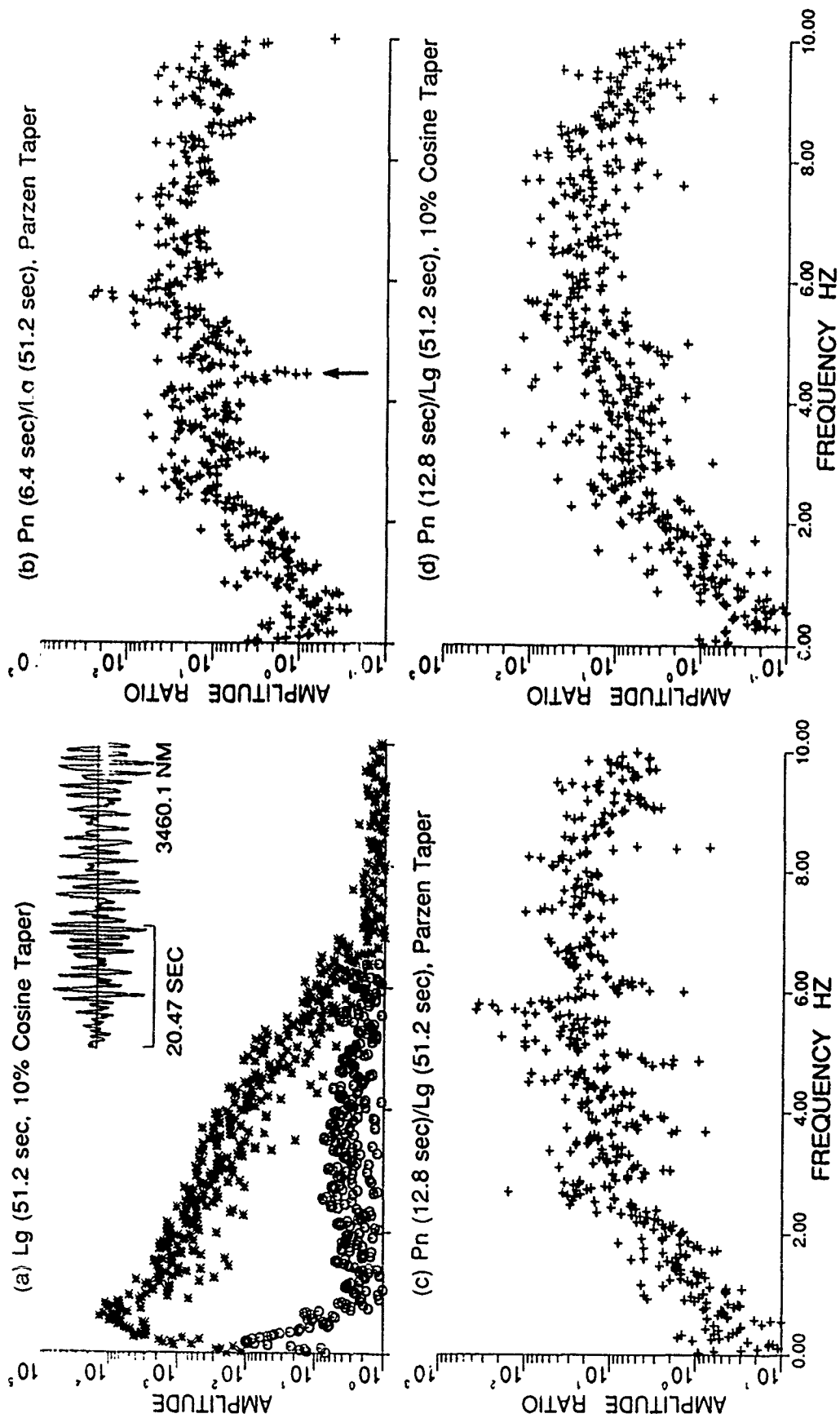


Figure 14. Similar to Figure 13 for the SW Shagan explosion of 14 September 1988.

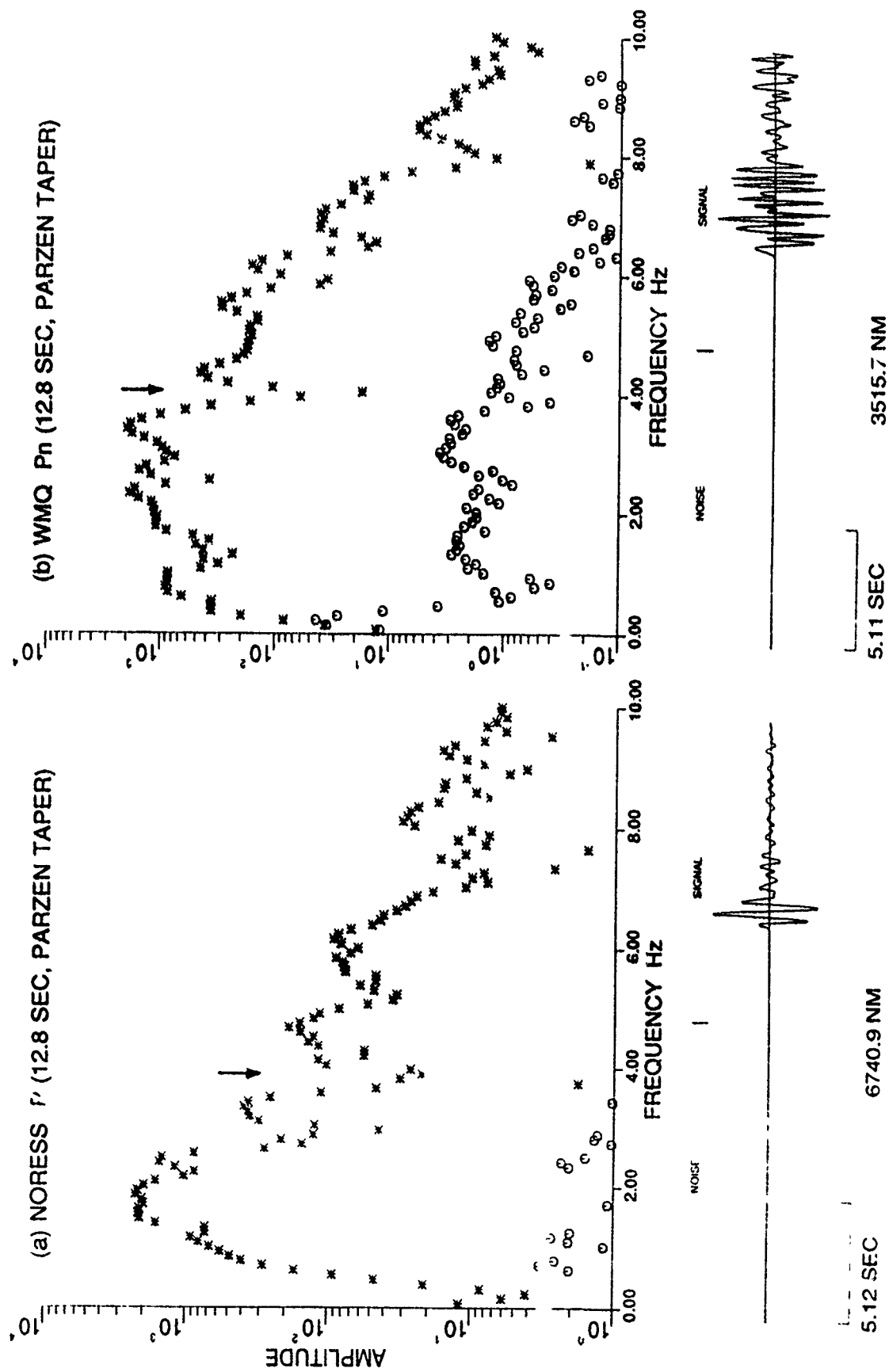


Figure 15. Spectra and waveforms of P at NORESS and Pn at WMQ for the SW Shagan explosion of 20 June 1987 ($m_b = 6.0$). Prominent nulls in spectra at about 4 Hz are denoted by arrows.

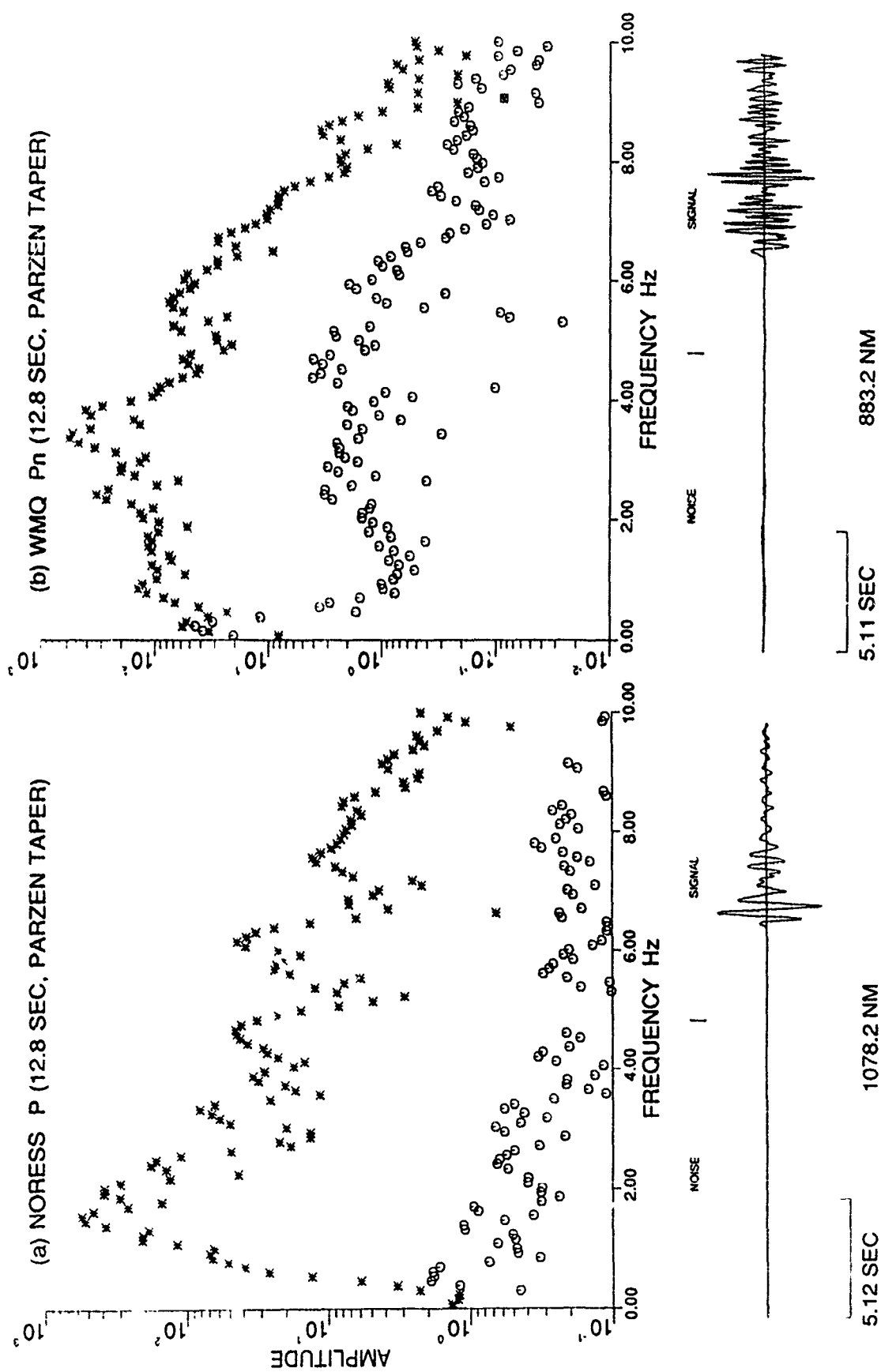


Figure 16. Spectra and waveforms of P at NORESS and Pn at WMQ for the SW Shagan explosion of 12 March 1987 ($m_b = 5.3$). The spectra do not show prominent nulls at about 4 Hz.

also did not indicate distinct nulls at about 3 Hz. On the other hand, most shots recorded at EKA (Figure 1) showed prominent nulls at about 3 Hz. It seems therefore that the 3 Hz null is due to teleseismic path effect, such as a multiple arrival. Additional support for this is provided by the two inter-shot spectral ratios in Figure 17. The common 3 Hz null in the NORESS spectra of both shots has disappeared whereas the 4 Hz null due to cancellation by pP in the spectra of the explosion of 20 June 1987 is prominent because the pP null for the smaller explosions occurs at a frequency significantly different than 4 Hz. The inter-shot spectral ratio from WMQ (Figure 17b) also provides clear evidence of a null at about 4 Hz for the larger explosion. Note that the null observed at WMQ occurs at a frequency slightly higher than that of the null observed at NORESS. This agrees with what is theoretically expected because of the somewhat different take-off angles for Pn and teleseismic P.

3.5. SCALING OF P-WAVE SPECTRA

It is important to study how the P-wave spectra of Shagan River explosions vary with explosive yield or m_b and to determine if their scaling differs significantly from the scaling relationships of nuclear explosions proposed by Mueller and Murphy (1971) and von Seggern and Blandford (1972). A detailed study of a large number of Shagan River explosions by Stewart (1988) found that the observed P spectra varied more slowly with m_b than predicted by either of these two scaling relationships and the differences are more pronounced at lower frequencies than at the higher frequencies.

3.5.1. Comparison of Theory and Observed Regional Data

In order to compare the observed dependence of P-wave spectra on yield or m_b with that predicted by von Seggern and Blandford (1972) and Mueller and Murphy (1971) scaling

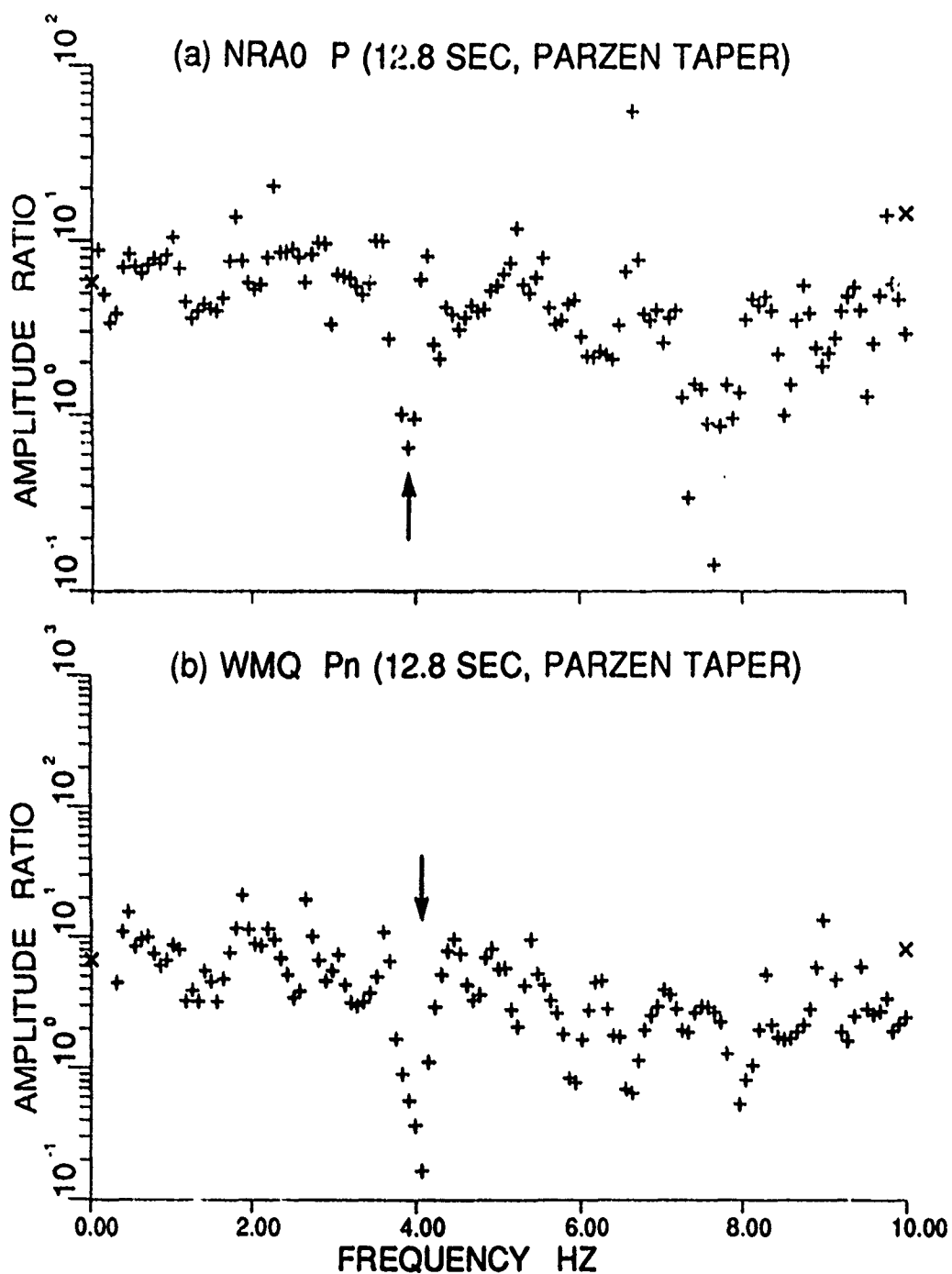


Figure 17. Inter-shot spectral ratio (20 June 1987)/(12 March 1987) for (a) P at NORESS, and (b) Pn at WMQ derived from the spectra in Figures 15 and 16. Prominent nulls at about 4 Hz are denoted by arrows.

relationships, synthetic seismograms were made for several assumed t^* and pP reflection coefficient values. As discussed by Shumway and Blandford (1978), a realistic approach is to consider the pP reflection coefficient, r , to be frequency-dependent and given by

$$r(f) = -0.5 (1 + e^{-f^2}) \quad (8)$$

This relationship implies $r(f) = -1$ and -0.684 at frequencies of 0 and 1 Hz, respectively and $r(f)$ approaches -0.5 for high frequencies. The Mueller and Murphy (1971) scaling relationship depends on both shot depth and shot medium whereas the von Seggern and Blandford (1972) relationship is independent of the shot depth. Shot depths for a given value of m_b were estimated by using equation (7). Assuming the P-wave velocity for the uppermost 0.5 km of the crust in the Shagan River region to be 5 km/sec, pP and P are separated in time by

$$t_d = 2 \frac{h}{5000} \text{ sec} \quad (9)$$

Synthetic seismograms were constructed for $m_b = 4.5, 5.0, 5.5, 6.0,$ and 6.5 and assuming the explosion source medium to be granite. Three combinations of t^* and $t(\text{pP} - \text{P})$ used were:

- (1) $t^* = 0.1, t(\text{pP} - \text{P}) = t_d,$
- (2) $t^* = 0.1, t(\text{pP} - \text{P}) = 2 t_d,$ and
- (3) $t^* = 0.2, t(\text{pP} - \text{P}) = 2 t_d.$

The use of $t^* = 0.1$ for WMQ may be a good approximation on the basis of Sereno's (1990) study suggesting a frequency-independent Q value of 1175. The instrument response was that of the broadband short-period instrument at WMQ.

Synthetic seismograms based on the use of both von Seggern and Blandford (1972) and Mueller and Murphy (1971) scaling relationship and the observed data were bandpassed for the frequency bands of 0.5-1.0 Hz, 4.0-6.0 Hz, and 7.0-9.0 Hz by using a three-pole phaseless

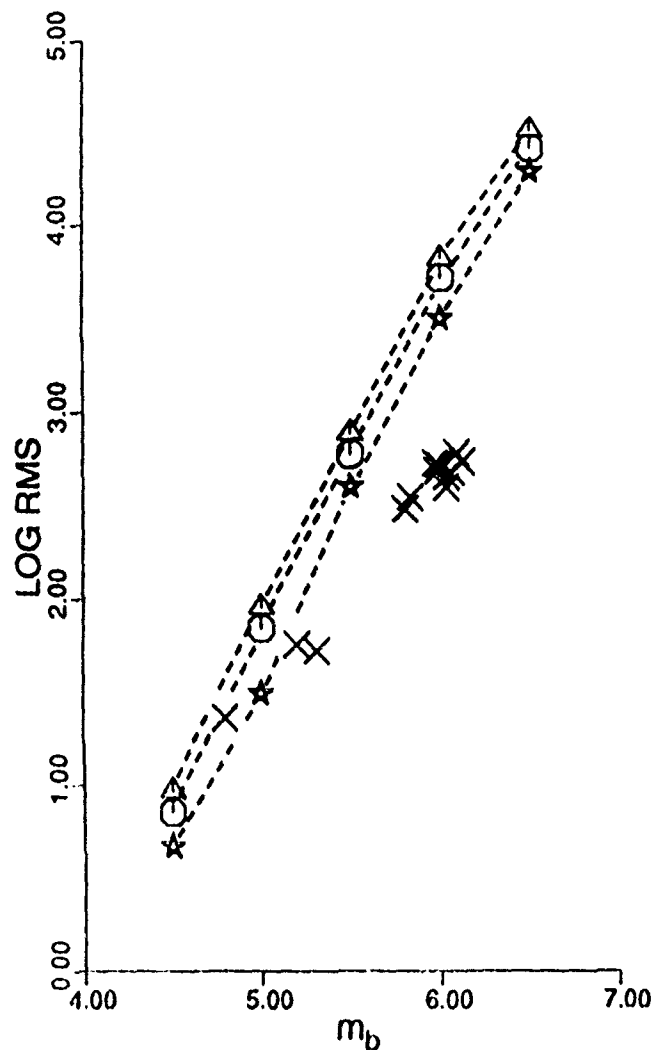
Butterworth filter. For the observed data, only 14 Shagan River explosions prior to the year 1989 for which precise m_b values were available from Ringdal and Marshall (1989) were used. Log RMS values were computed for the P(12.8 sec) windows with 10% cosine taper and correction for instrument response. For the observed data, a correction for noise was made by using a sample of noise prior to the onset of P and subtracting the power in noise from that in signal. Plots of log RMS values versus m_b for the synthetic and the observed data for frequency bands of 0.5-1.0 Hz, 4.0-6.0, and 7.0-9.0 are shown in Figures 18, 19, and 20, respectively. The amplitude scale is arbitrary. The three sets of synthetics provide results that are not much different whether von Seggern and Blandford or Mueller and Murphy model is used. There is, however, a large discrepancy between the observed and synthetic data with the observations indicating much slower variation with m_b for the lowest frequency band of 0.5-1.0 Hz (Figure 18). The discrepancy is considerably reduced for the frequency band of 4.0-6.0 Hz (Figure 19) and appears further reduced for the frequency band of 7.0-9.0 Hz (Figure 20).

The results for spectral ratios (0.5-1.0 Hz)/(4.0-6.0 Hz) and (0.5-1.0 Hz)/(7.0-9.0 Hz) for the two theoretical models and the observed data are shown in Figures 21, 22, 23, and 24 in which the amplitude scale is *not* arbitrary. A comparison of the observed and the theoretical results again indicates the low-frequency spectra to vary more slowly with m_b than expected from either of the two theoretical models.

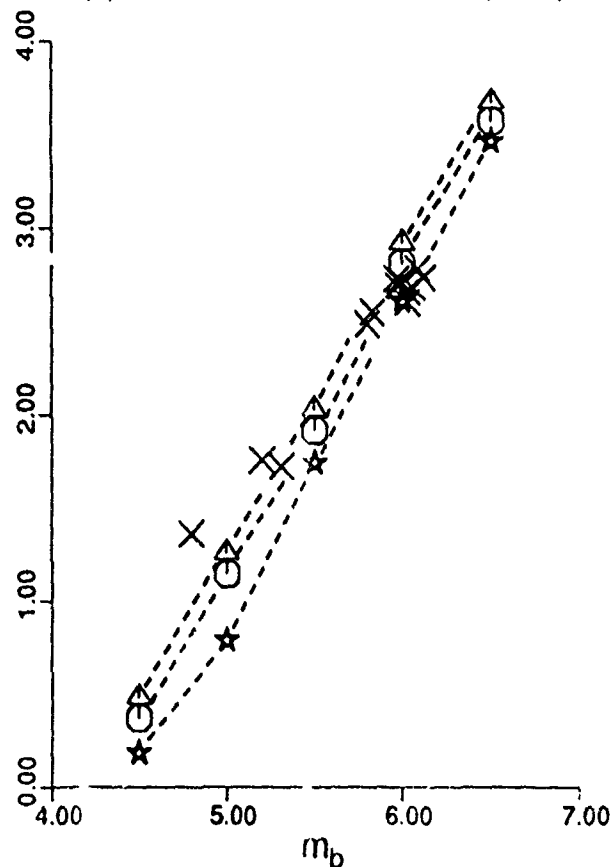
3.5.2. Comparison of Theory and Observed Teleseismic Data

A comparison of the scaling of spectra with m_b between the theoretical results based on von Seggern and Blandford (1972) and Mueller and Murphy (1971) and observation was

(a) VON SEGGERN AND BLANDFORD (1972)



(b) MUELLER AND MURPHY (1971)



- ★ $t^* = 0.1, t(pP - P) = t_d$
- △ $t^* = 0.1, t(pP - P) = 2 t_d$
- $t^* = 0.2, t(pP - P) = 2 t_d$

Figure 18. Log RMS versus m_b for frequency band of 0.5-1.0 Hz for observed data at WMQ and three synthetics with t^* and $t(pP-P)$ values as indicated. The amplitude scale is arbitrary.

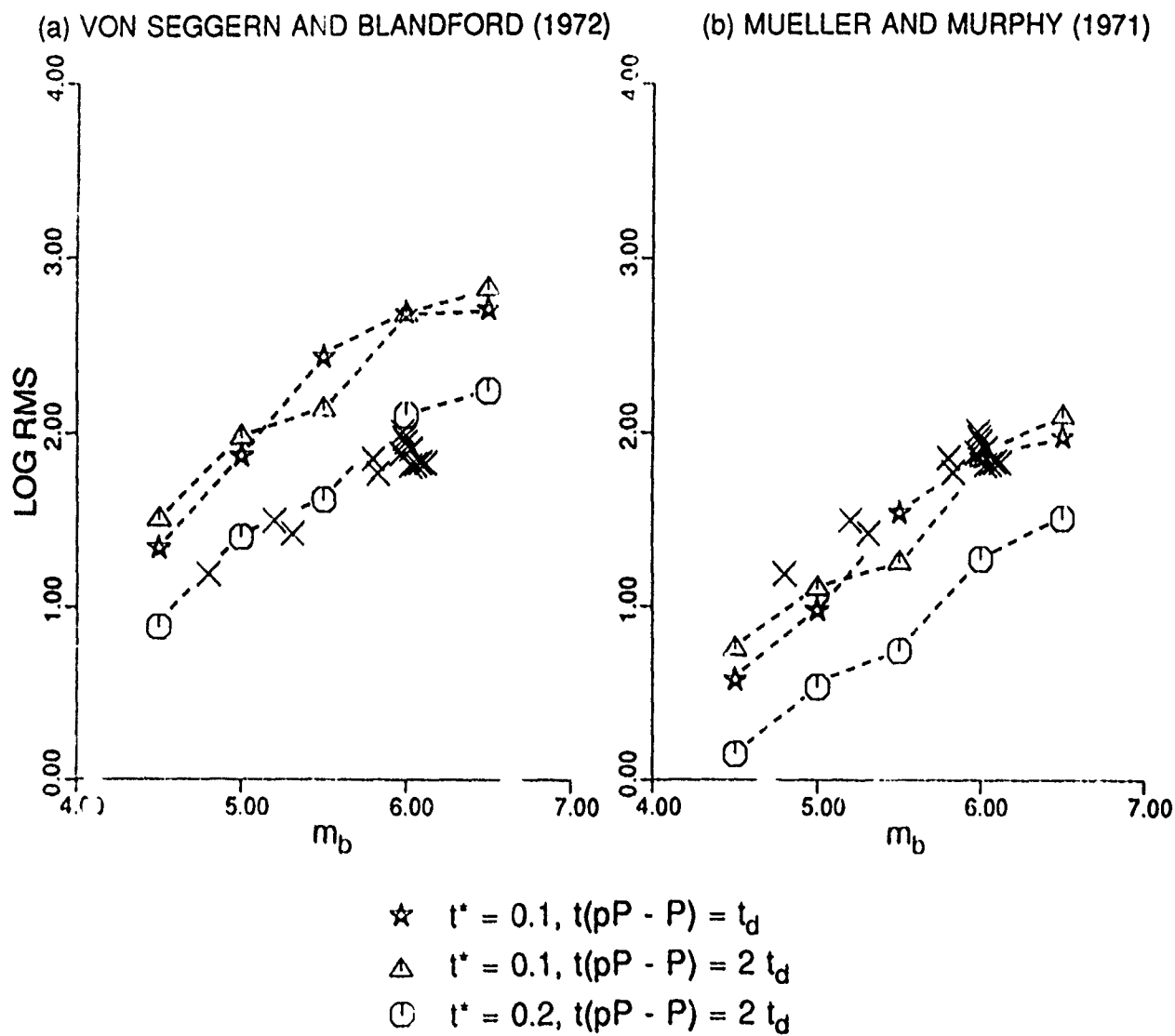


Figure 19 Log RMS versus m_b for frequency band of 4.0-6.0 Hz for observed data at WMQ and three synthetics with t^* and $t(pP - P)$ values as indicated. The amplitude scale is arbitrary.

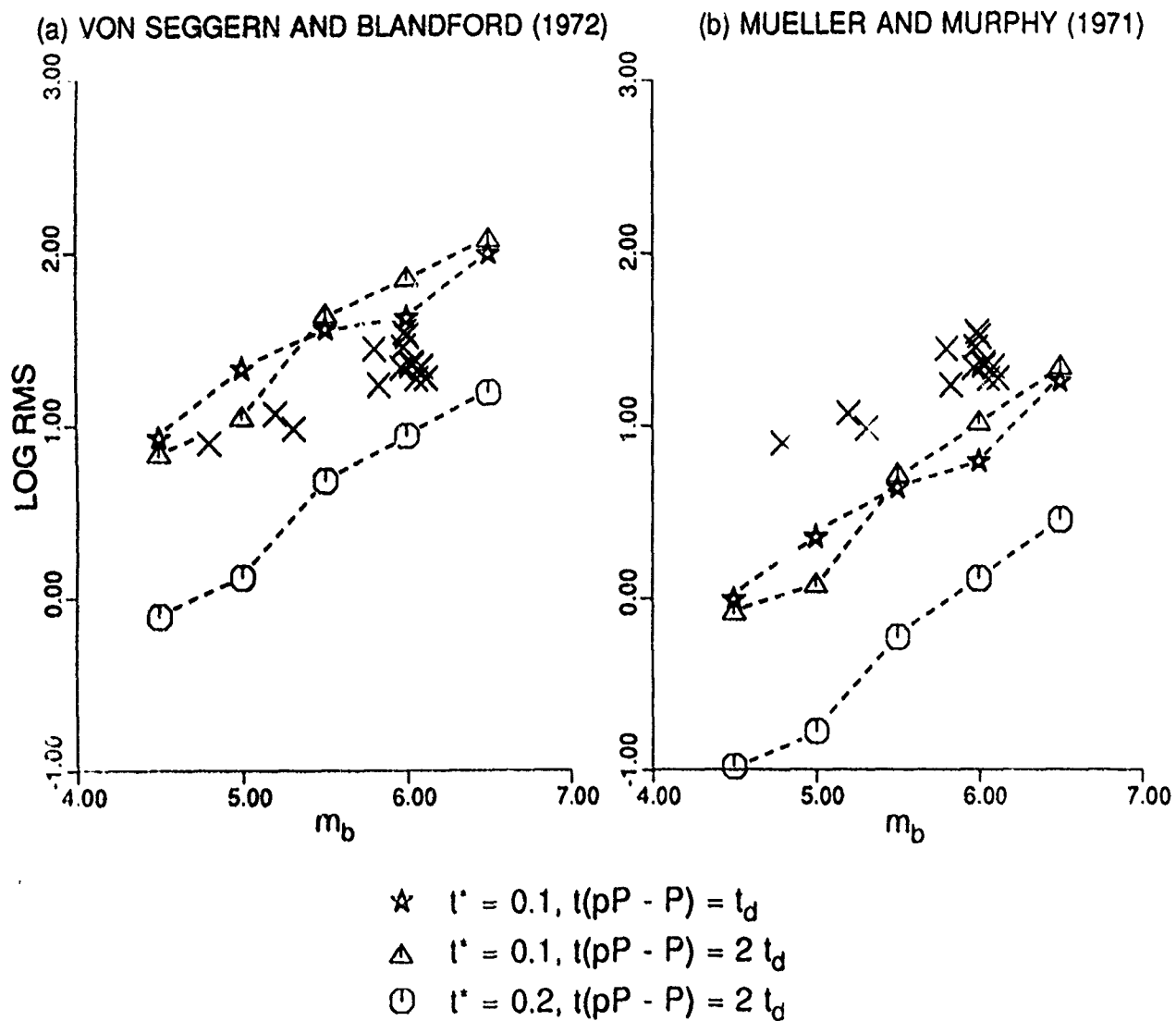


Figure 20. Log RMS versus m_b for frequency band of 7.0-9.0 Hz for observed data at WMQ and three synthetics with t^* and $t(pP-P)$ values as indicated. The amplitude scale is arbitrary.

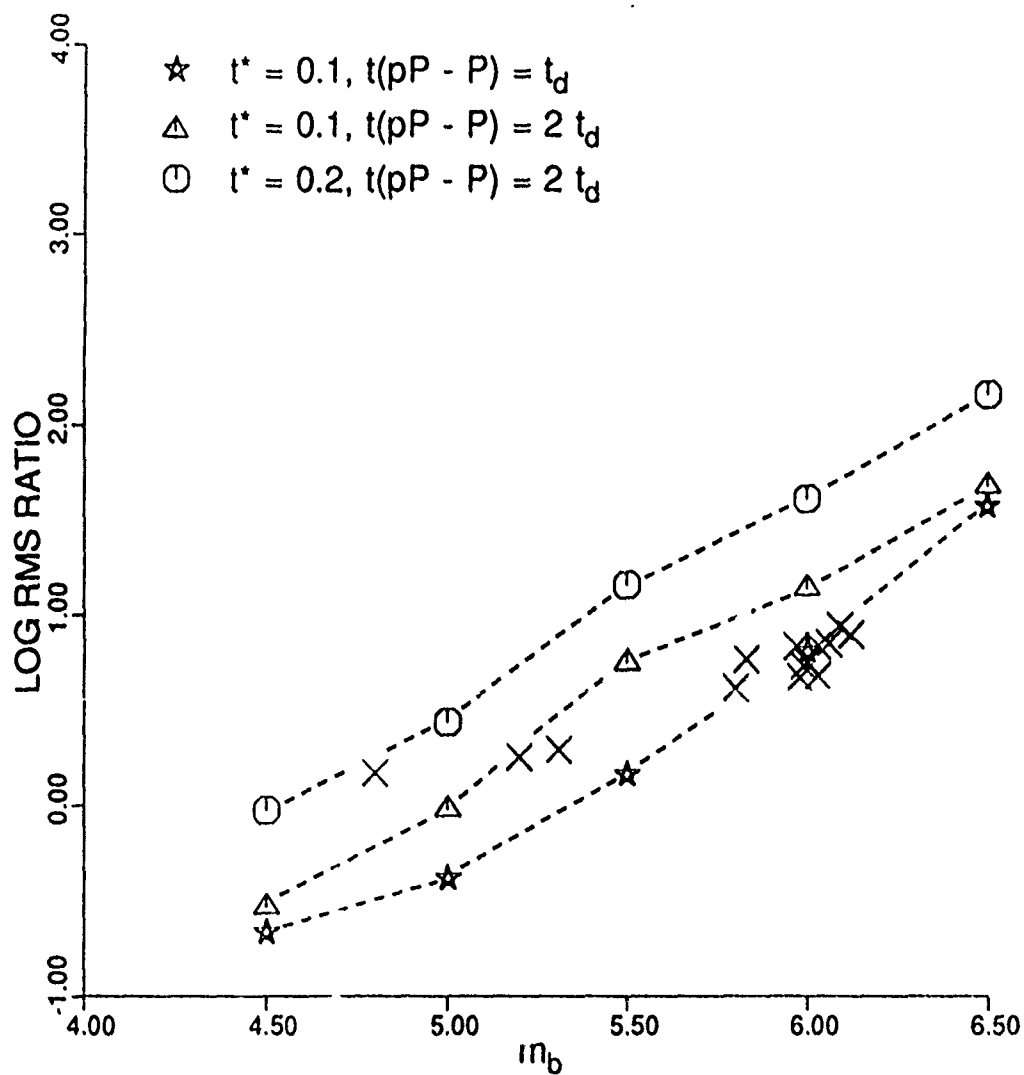


Figure 21. Log RMS ratio (0.5-1.0)/(4.0-6.0) versus m_b for observed data at WMQ and three synthetics based on von Seggern and Blandford (1972) scaling and t^* and $t(pP-P)$ values as indicated.

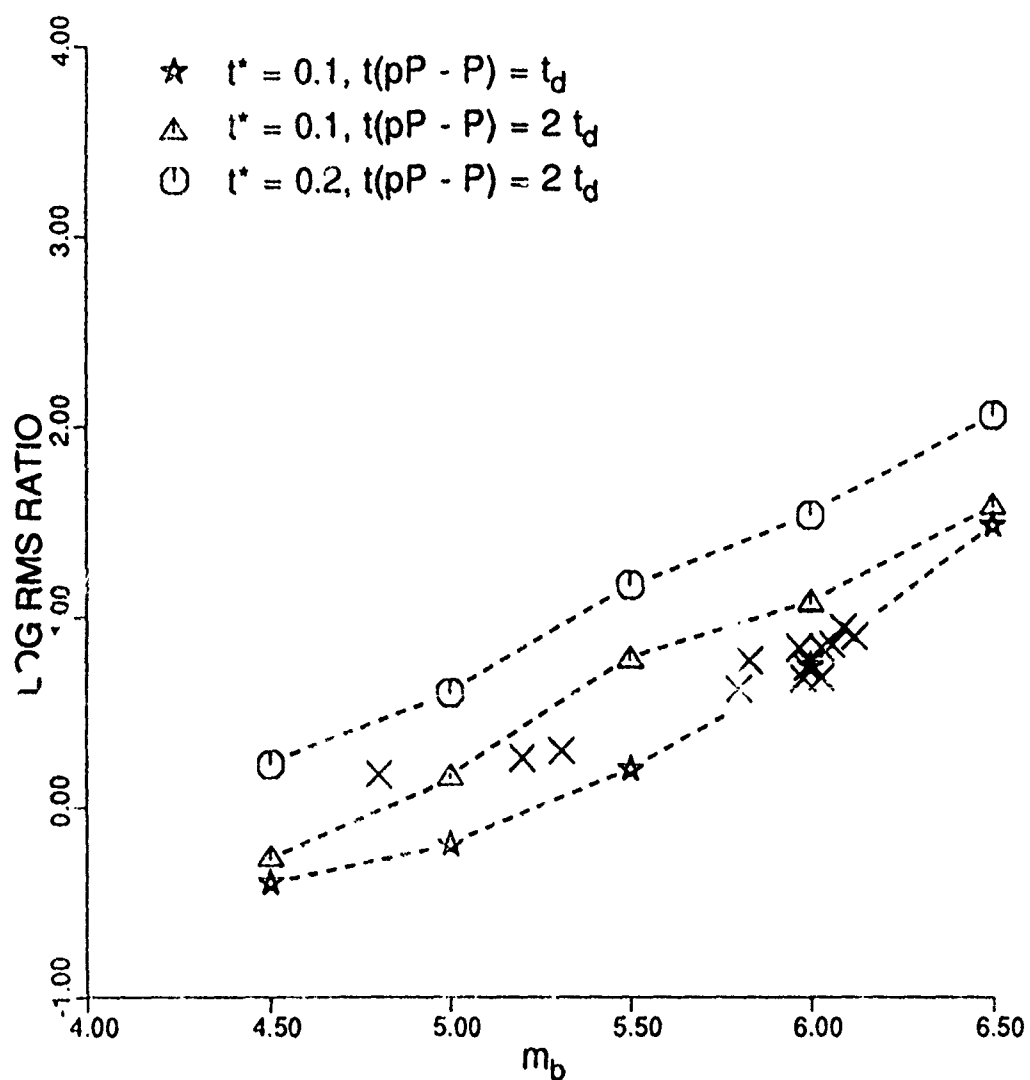


Figure 22. Log RMS ratio (0.5-1.0)/(4.0-6.0) versus m_b for observed data at WMQ and three synthetics based on Mueller and Murphy (1971) scaling and t^* and $t(pP-P)$ values as indicated.

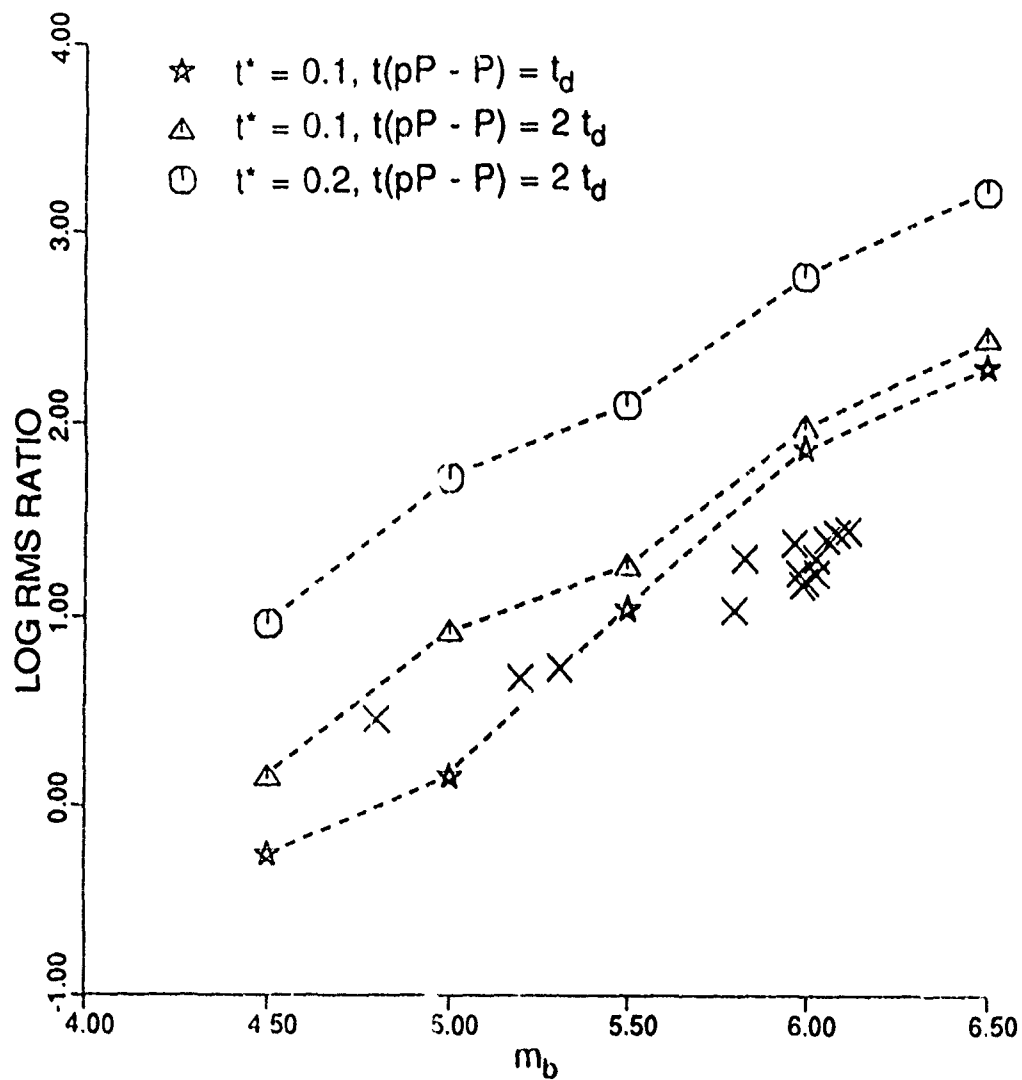


Figure 23. Log RMS ratio (0.5-1.0)/(7.1-9.0) versus m_b for observed data at WMQ and three synthetics based on von Seggern and I landford (1972) scaling and t^* and $t(pP - P)$ values as indicated.

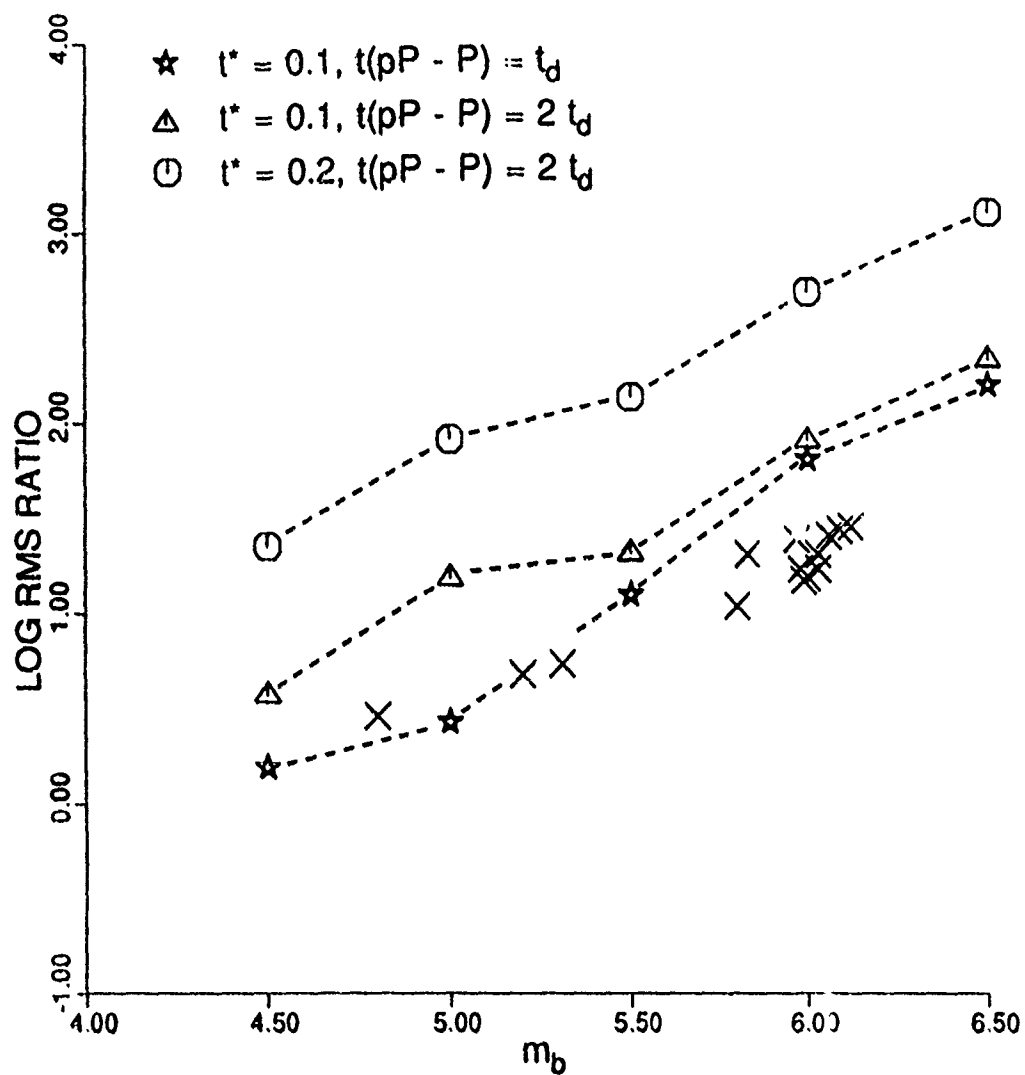


Figure 24. Log RMS ratio (0.5-1.0)/(7.0-9.0) versus m_b for observed data at WMQ and three synthetics based on Mueller and Murphy (1971) scaling and t^* and $t(pP-P)$ values as indicated.

made by using teleseismic data from 25 Shagan River explosions recorded at the center element of NORSAR subarray 1A. Most of these data had good S/N up to about 3 Hz. Synthetic seismograms were again made for the same two assumed values of t^* and the same two values of $t(pP - P)$. In fact, all parameters were selected to be the same except that a Parzen taper was used on 6.4 sec long P-windows and, of course, NAO instrument response was used. Note that Der *et al.* (1985) suggested $t^* = 0.14$ for Shagan River explosions recorded at NORSAR. The results for spectral ratios $(0.5-2.0 \text{ Hz})/(3.0-5.0 \text{ Hz})$ and $(0.5-2.0 \text{ Hz})/(7.0-9.0 \text{ Hz})$ for the two theoretical models and the observed data are shown in Figures 25, 26, 27, and 28. A comparison of the observed and the theoretical results shows large discrepancy, especially for the smaller m_b shots. The discrepancy is of the same type as for the regional data (Figures 21 through 24) but somewhat larger in magnitude. These results also suggest that the observed low-frequency spectra vary more slowly with m_b than expected from either of the two theoretical models.

3.6. DISCUSSION

A three-dimensional geological model of the Shagan River test site by Leith and Unger (1989) shows a distinct difference between the NE and SW portions of the test site, with the granites closer to the surface and the alluvium thinner in the southwest. Finite difference simulations of scattering due to near-source geology for the Yucca Flats explosions by McLaughlin *et al.* (1987) and Stead and Helmberger (1988) indicate large amplitude arrivals within a few sec of the first P. P-wave spectra of the Pahute Mesa explosion, MAST, shows a spectral null at the frequency expected for interference by pP for short time windows and at considerably lower frequency for longer windows (Gupta *et al.*, 1991). F-k analysis of

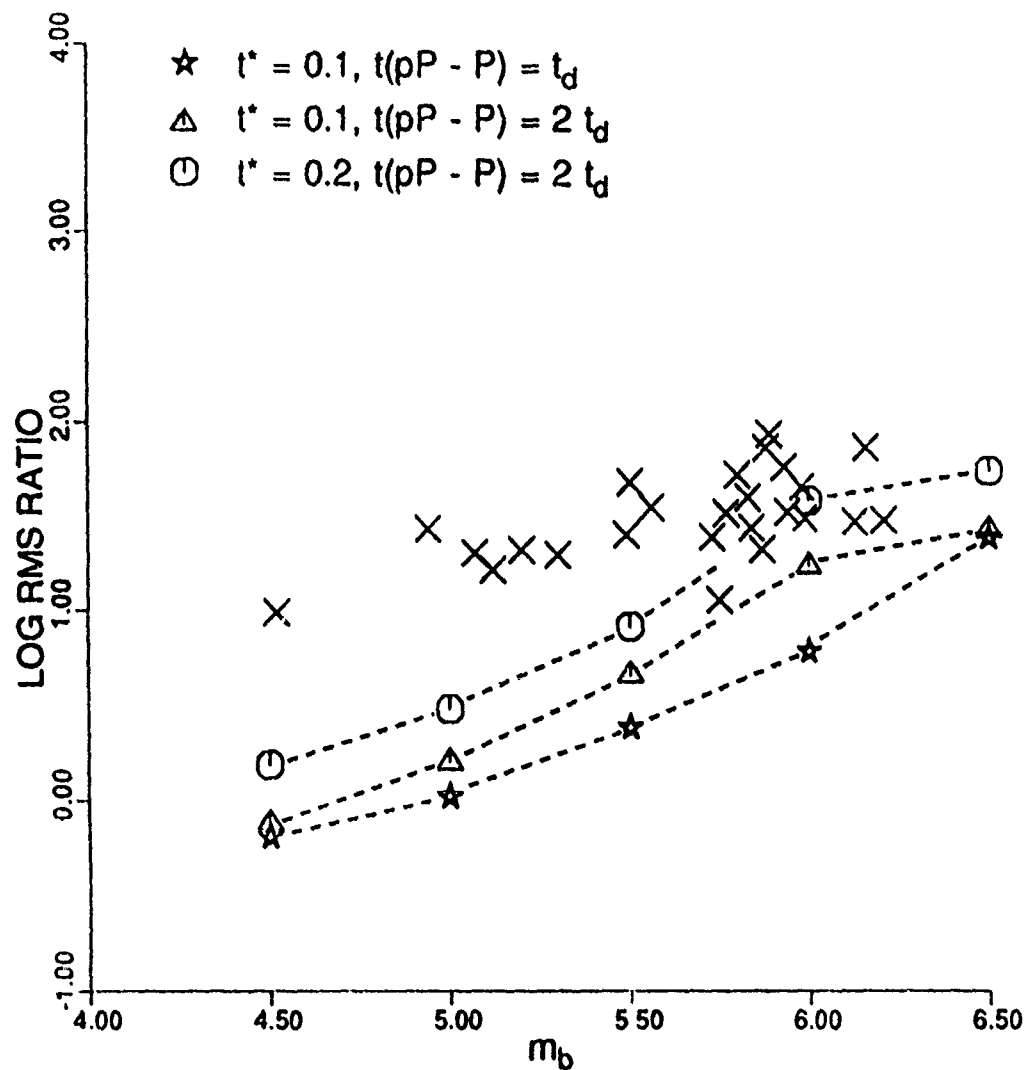


Figure 25. Log RMS ratio (0.5-2.0)/(3.0-5.0) versus m_b for observed data at NORSAR and three synthetics based on von Seggern and Blandford (1972) scaling and t^* and $t(pP-P)$ values as indicated.

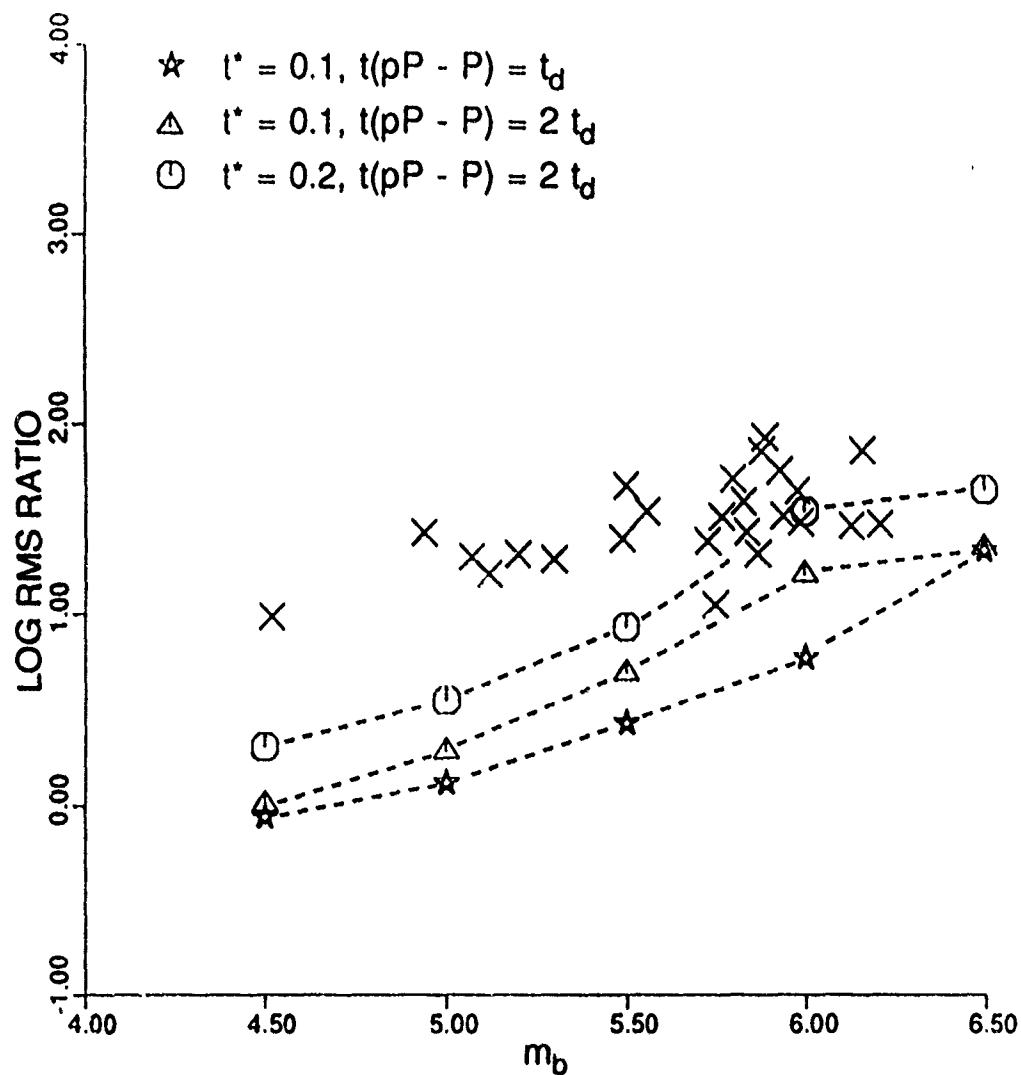


Figure 26. Log RMS ratio (0.5-2.0)/(3.0-5.0) versus m_b for observed data at NORSAR and three synthetics based on Mueller and Murphy (1971) scaling and t^* and $t(pP-P)$ values as indicated.

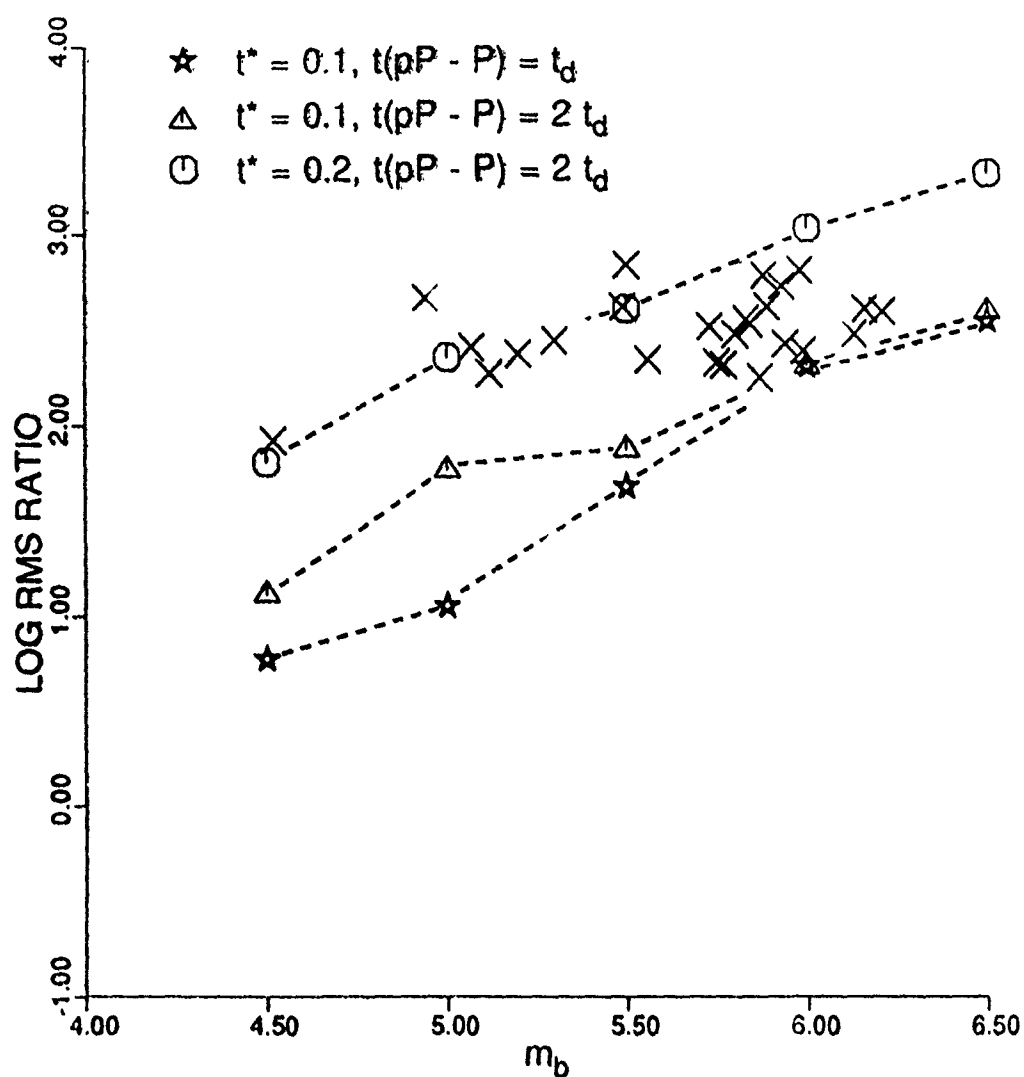


Figure 27. Log RMS ratio (0.5-2.0)/(7.0-9.0) versus m_b for observed data at NORSAR and three synthetics based on von Seggern and Blandford (1972) scaling and t^* and $t(pP-P)$ values as indicated.

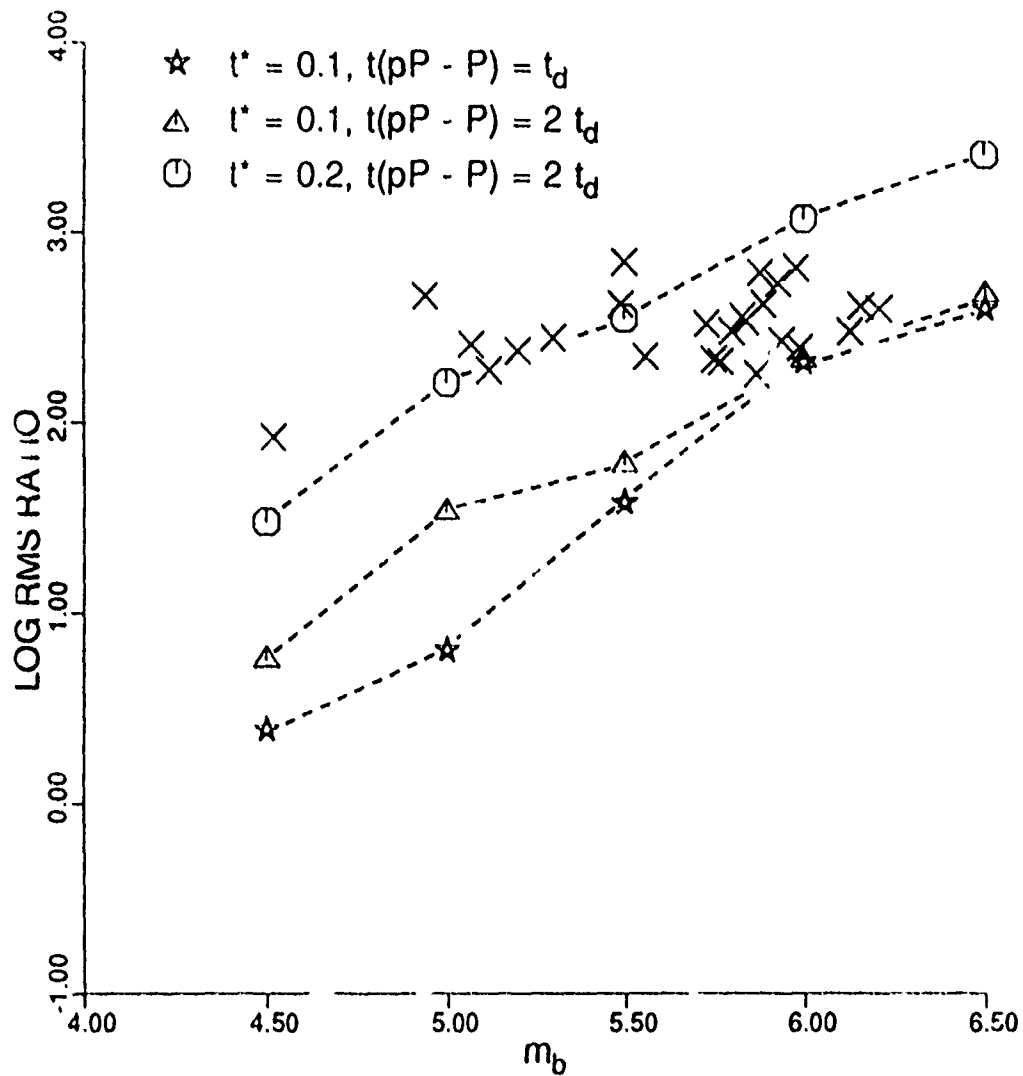


Figure 28. Log RMS ratio (0.5-2.0)/(7.0-9.0) versus m_b for observed data at WMQ and three synthetics based on Mueller and Murphy (1971) scaling and t^* and $t(pP-P)$ values as indicated.

teleseismic records of Yucca Flat explosions by Gupta *et al.* (1990b) suggested Rg-to-P arrivals within a few sec of the direct P. A finite difference study of scattering due to irregular low-velocity surface layers by Levander and Hill (1985) showed that when a planar pulse is incident upon the low-velocity layer, the roughness induces a strong resonant coupling to Rayleigh modes, a condition which cannot occur for a laterally invariant medium. The resonant coupling causes a long coda following the direct seismic arrival. Such a mechanism may be responsible for the scattering of explosion-generated Rg into teleseismic P coda.

4. STUDY OF NOVAYA ZEMLYA EXPLOSIONS

As for most other test sites, there is considerable controversy over the interpretation of pP parameter estimates of Novaya Zemlya explosions (*e. g.* Burdick, 1990; Lay, 1991). There is general agreement over the existence of strong pP reflections but considerable disagreement regarding the pP-P delay times as well as pP/P amplitudes. The most reliable delay times, consistent with the geology of the test site, have so far been those derived by the maximum likelihood multichannel deconvolution methods (Chan *et al.*, 1988; Der *et al.*, 1987b). We used inter-shot spectral ratios, averaged over all available sensors, to obtain significantly more precise delay times for several large shots. Burdick (1990) showed that the spectral estimation procedure used in the spectral averaging method of Murphy (1989) tends to underestimate the pP amplitudes due to spectral smoothing. We made a comparison of theoretical and observed source spectra in order to estimate pP/P amplitudes of several large explosions.

4.1. P-WAVE SOURCE SPECTRA FROM U.K. ARRAY DATA

The U. K. array data from the EKA ($\Delta \approx 29^\circ$, source azimuth, $\Phi \approx 264^\circ$), GBA ($\Delta \approx 61^\circ$, $\Phi \approx 155^\circ$), and YKA ($\Delta \approx 41^\circ$, $\Phi \approx 353^\circ$) were collected for as many as 19 Novaya Zemlya explosions (Table 3) out of which only one explosion (27 September 1973 or 73270) is from the southern Novaya Zemlya test site region. The number of usable (free from clipping or spike) sensors available at each array for each explosion is indicated in the table. For the largest explosion (66300), all channels of data, except one, were clipped. Most of the data in Table 3 is from Lilwall and Marshall (1986) who carried out a least squares joint epicenter estimate of origin time and epicenter together with a maximum-likelihood estimate of

magnitude. The surface topography in the northern Novaya Zemlya region is characterized by steep mountain slopes whereas topography at the southern site is less pronounced.

TABLE 3
NOVAYA ZEMLYA SHOTS RECORDED AT UK ARRAYS

No.	DATE	LAT	LON	ORIGIN TIME	m _b	NUMBER OF SENSORS			
						EKA	GBA	YKA	
1	25 Oct 1964	64299	73.386	54.997	07:59:58.1	4.82	18	0	0
2	27 Oct 1966	66300	73.388	54.845	05:57:58.1	6.47	1	0	0
3	07 Nov 1968	68312	73.388	54.873	10:02:05.5	6.11	1	1	2
4	14 Oct 1969	69287	73.389	54.796	07:00:06.6	6.18	2	1	0
5	27 Sep 1973	73270	70.756	53.746	06:59:58.5	5.83	16	0	17
6	29 Sep 1976	76273	73.360	54.880	02:59:57.7	5.77	1	2	17
7	20 Oct 1976	76294	73.399	54.835	07:59:58.1	4.89	20	17	0
8	01 Sep 1977	77244	73.339	54.626	02:59:58.0	5.71	8	0	17
9	09 Oct 1977	77282	73.414	54.935	10:59:58.1	4.51	15	9	0
10	10 Aug 1978	78222	73.293	54.885	07:59:58.0	6.04	0	0	10
11	27 Sep 1978	78270	73.350	54.677	02:04:58.6	5.68	15	1	18
12	24 Sep 1979	79267	73.346	54.679	03:29:58.8	5.80	19	0	17
13	18 Oct 1979	79291	73.318	54.821	07:09:58.8	5.85	20	1	17
14	11 Oct 1980	80285	73.335	54.938	07:09:57.5	5.80	0	10	14
15	01 Oct 1981	81274	73.308	54.817	12:14:57.3	5.91	0	11	11
16	11 Oct 1982	82284	73.348	54.601	07:14:58.7	5.52	15	16	17
17	18 Aug 1983	83230	73.358	54.974	16:09:58.9	5.84	0	19	16
18	25 Sep 1983	83268	73.326	54.564	13:09:58.2	5.71	12	0	17
19*	25 Oct 1984	84299	73.370	54.960	06:29:57.7	5.90	0	16	13

* from Sykes and Ruggi (1986)

Frequency-domain source terms were derived by a least squares analysis of all available data from each array for the Novaya Zemlya explosions listed in Table 3. Results from 14 explosions recorded at the EKA array, based on use of the P(6.4 sec) window, are shown in Figure 29 in which the source spectra are arranged in order of decreasing m_b . Note that source spectra for the three largest explosions are based on extremely limited data (see Table 3) so that the corresponding source spectra should be less reliable. Results of similar analysis carried out by using the P(12.8 sec) windows are shown in Figure 30. An examination of the source spectra in Figures 29 and 30 indicates rather distinct spectral nulls (indicated by arrows) for most of the larger shots at a frequency of about 2.5 to 3.0 Hz. The spectral nulls in Figure 30 are generally less distinct than in Figure 29, probably due to greater contamination by later arrivals in the longer P window. Seismic velocities in the shallow crust at the Novaya Zemlya test site are somewhat smaller than those at the Shagan River test site (V. Adushkin, oral communication). Since the spectral nulls due to pP for large Shagan River explosions occur at a frequency of about 4 Hz, the spectral nulls observed at frequency of 2.5 to 3.0 Hz for the larger Novaya Zemlya shots are also expected to be due to cancellation by pP.

The GBA data for 12 Novaya Zemlya explosions (Table 3) was analyzed in the same manner as the EKA data and the source spectra, based on use of the P(6.4 sec) window, are shown in Figure 31. The spectra are arranged in order of decreasing m_b . A few of the larger shots show prominent spectral nulls (indicated by arrows) at frequency that lies between 2.5 and 3.0 Hz. Results of similar analysis of the YKA data from 14 explosions are shown in Figure 32. Again, the source spectra of many larger shots suggest prominent spectral nulls at frequency of about 2.5 to 3.0 Hz. It should be noted that the spectral nulls for a given

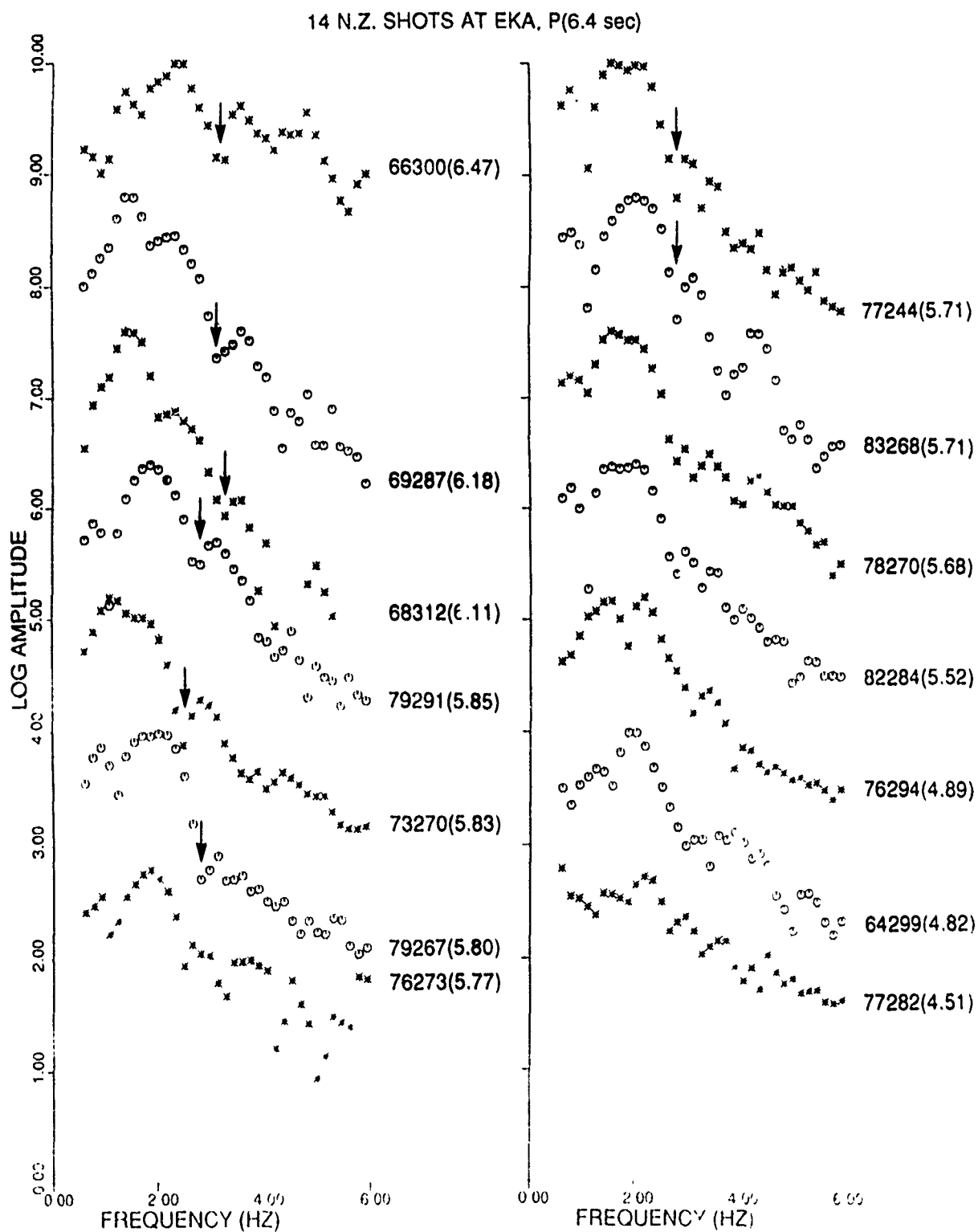


Figure 29. Source spectra (not corrected for instrument response) of 14 Novaya Zemlya explosions derived from P(6.4 sec) window of EKA array data. The shots are arranged in order of decreasing m_b . Prominent spectral nulls are indicated by arrows.

14 N.Z. SHOTS AT EKA, P(12.8 sec)

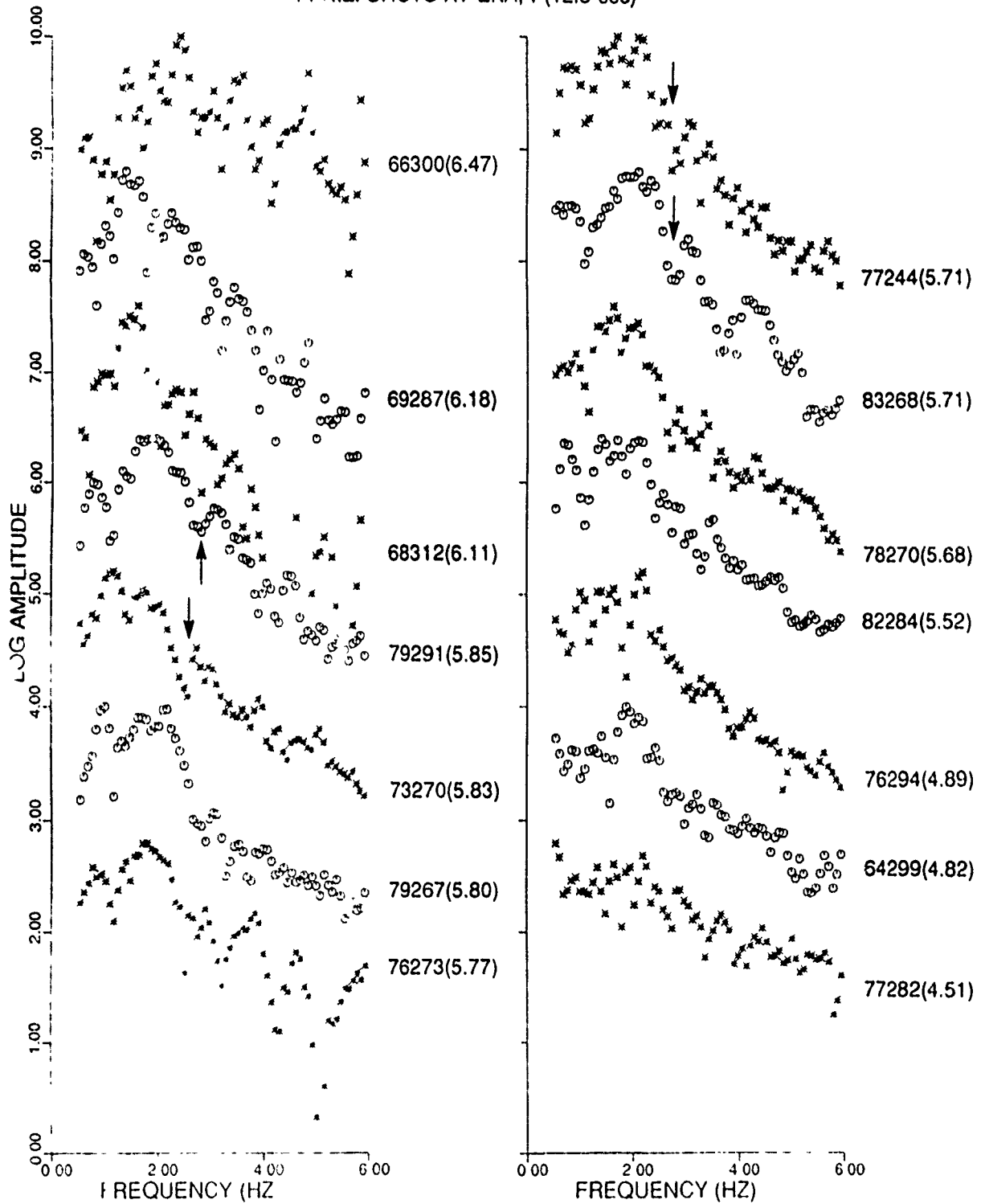


Figure 30. Similar to Figure 29 for the P(12.8 sec) window. The spectral nulls are generally less distinct than in Figure 29 due to contamination by later arrivals.

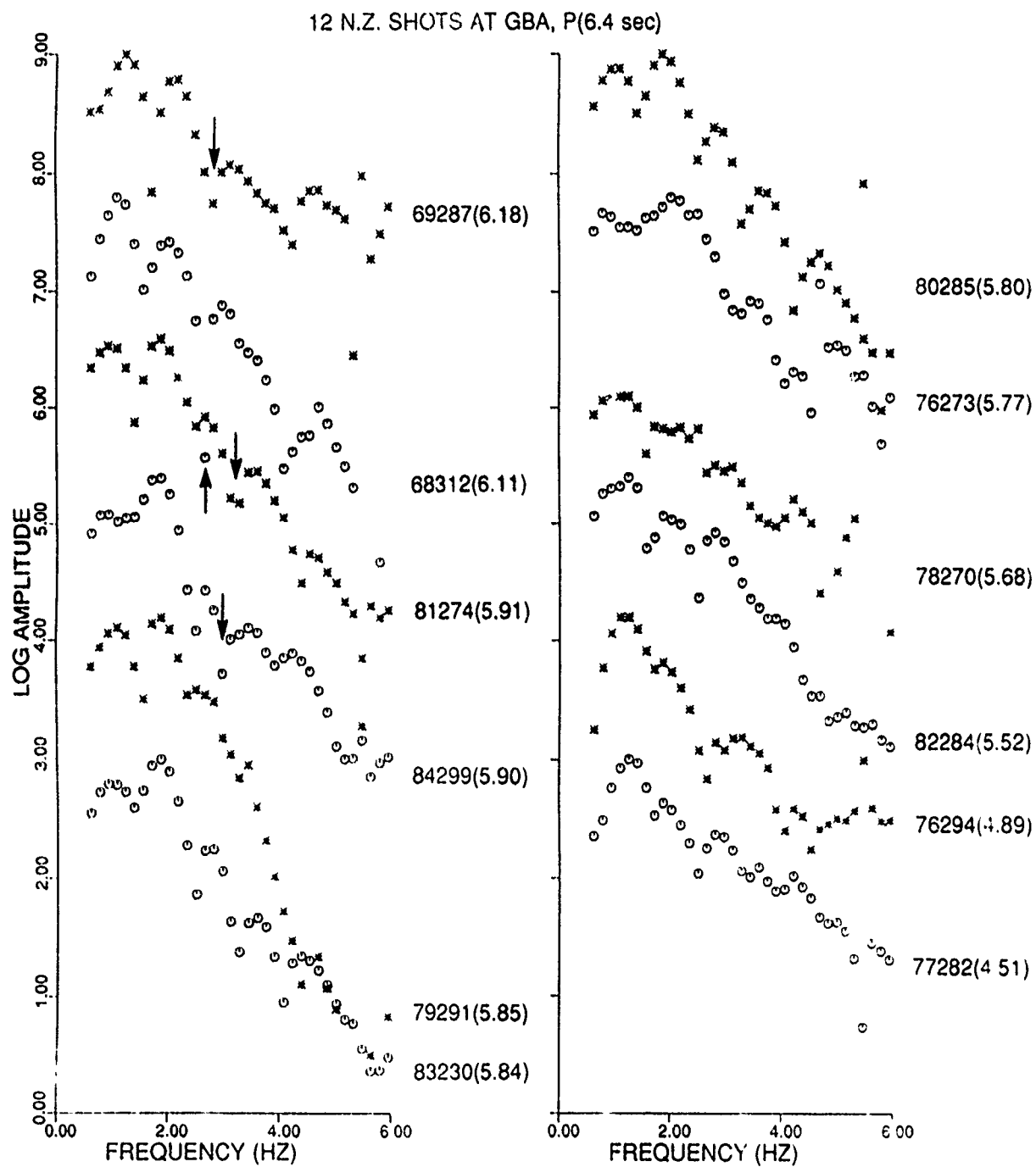


Figure 31. Similar to Figure 29 for 12 explosions recorded at the GBA array.

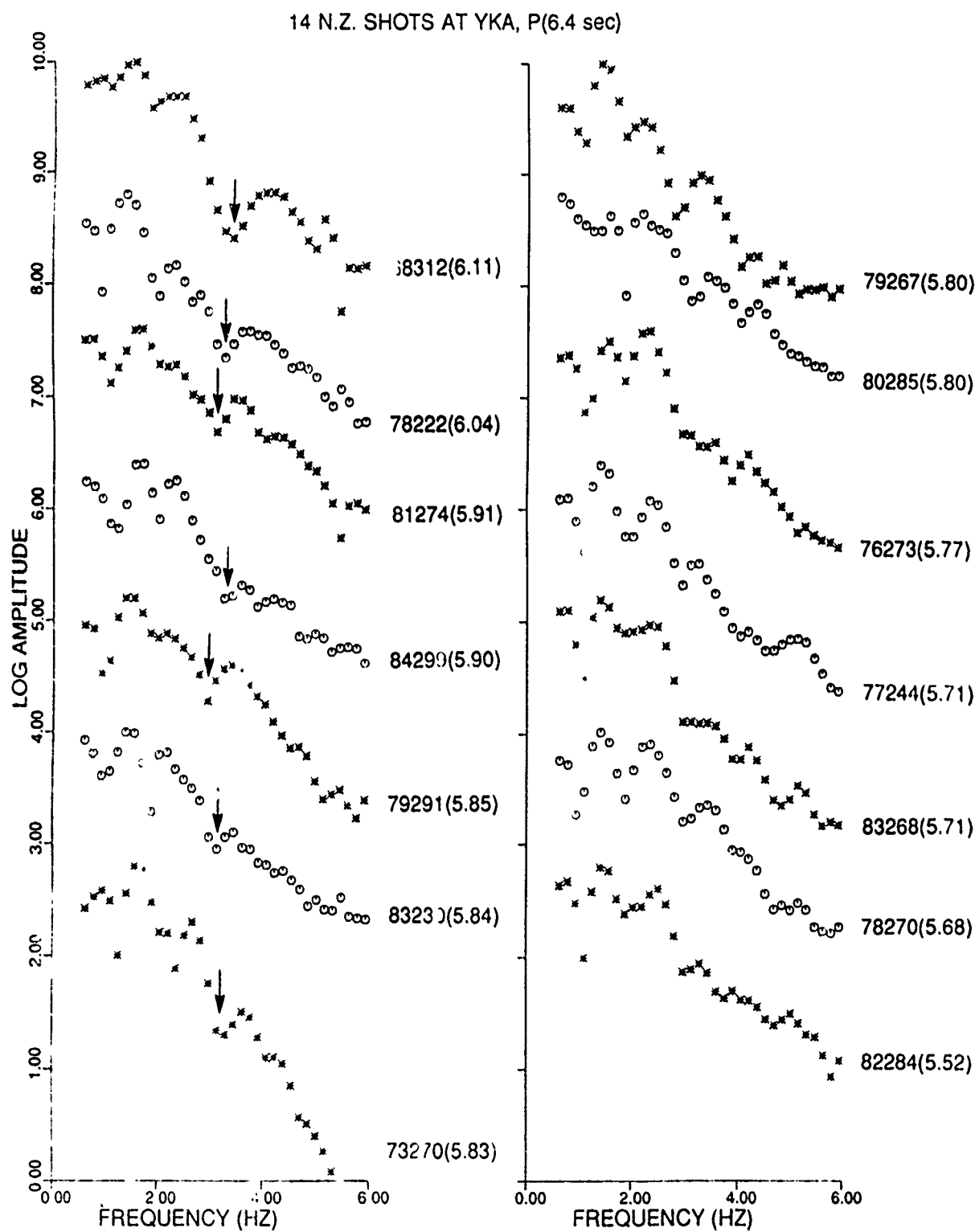


Figure 32. Similar to Figure 29 for 14 explosions recorded at the YKA array.

explosion observed at the three arrays (Figures 29, 31, and 32) are generally at somewhat different frequencies. Possible reasons are differences in source-receiver paths and take-off polar and azimuthal angles.

Spectral ratios $P/P\text{-coda}$, with a P window of 6.4 sec and the contiguous $P\text{-coda}$ window of 12.8 sec, were computed for all usable data from the three arrays (Table 1). As mentioned earlier, the pP nulls in spectra of $P\text{-coda}$ are expected to be significantly less distinct than in spectra of the initial P so that the spectral ratio $P/P\text{-coda}$ should be useful for determining the null frequencies. In order to emphasize the spectral nulls, power thresholds of $S/N > 1.0$ and 1.5 were applied to the P and $P\text{-coda}$ spectra, respectively. Using a least squares regression technique applied to each spectral amplitude, frequency-domain source terms were obtained for all explosions except shot 66300 for which data from only one sensor is available (Table 3). The source terms $P/P\text{-coda}$ for 18 explosions, shown in Figure 33, indicate distinct spectral nulls (indicated by arrows) for most shots of m_b larger than 5.5. Null frequencies for the large shots are at about 2.5 to 3.0 Hz and do not show a systematic variation with m_b .

4.2. INTER-SHOT RATIOS AND ESTIMATES OF NULL FREQUENCY

Spectral ratios of closely spaced explosions at a common recording station provide source information that is virtually free from propagation path effects, including attenuation and receiver function (King *et al.*, 1972). The procedure can be used to estimate spectral nulls or delay times if shot depths of the two explosions are significantly different. Numerous applications of this technique have indicated the pP delay time to be longer than expected from known overburden velocities and its amplitude significantly smaller than that expected for elastic free surface reflection.

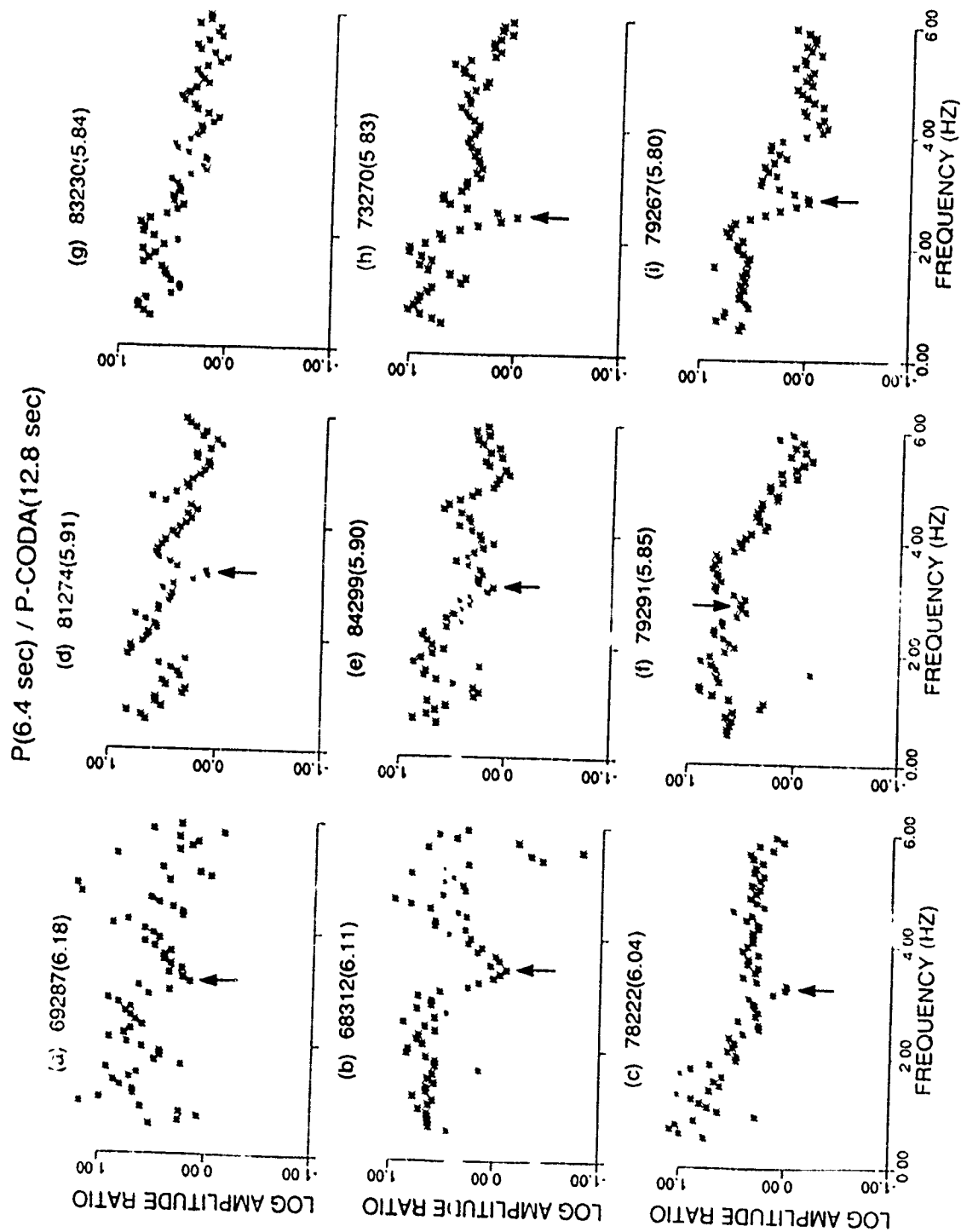


Figure 33. Frequency-domain source terms $P(6.4 \text{ sec})/P\text{-CODA}(12.8 \text{ sec})$ derived from all available array data for 18 Novaya Zenlya shots. The spectra are arranged in order of decreasing m_b and the suspected pP null frequencies are denoted by arrows.

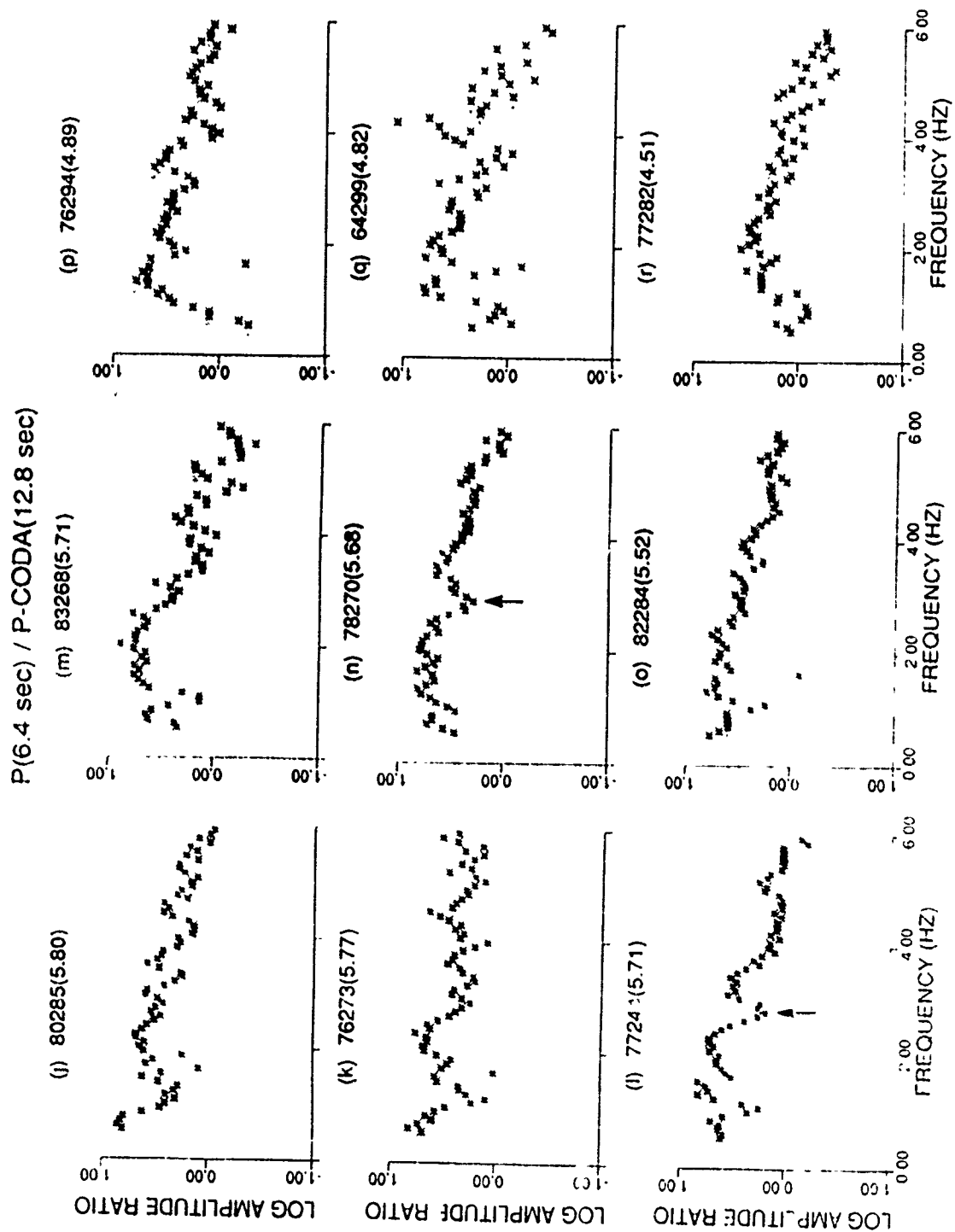


Figure 33. (Continued).

Inter-shot spectral ratios were obtained by combining a large shot with a small shot recorded at common stations. P(6.4 sec) long windows were used and, in order to emphasize nulls in spectra of the larger shot, a power ratio of $S/N > 1.0$ for the larger explosion and $S/N > 1.5$ for the smaller explosion were used. Results from the EKA data for the four largest shots (each with 3 or more usable sensors), combining each with three smallest available shots, are shown in Figures 34 and 35. These plots are based on the average of all common sensors and only those frequency values for which data from three or more sensors were available are shown. The vertical lines represent one standard deviation error bars derived from the values from 3 or more sensors. Distinct spectral nulls are observed on all plots in Figures 34 and 35 and the null frequency for each of the four large explosions stays remarkably constant when the large shot is combined with three *different* smaller shots. Results derived from similar analysis of data from two large explosions recorded at GBA and YKA are shown in Figures 36 and 37, respectively. In Figures 37a, b, c, error bars are not given since data from only two sensors were available for shot 68312. Distinct and consistent spectral nulls are again observed at frequencies of about 2.5 to 3.0 Hz in both Figures 36 and 37.

The spectral null frequencies for 8 relatively large explosions in Figures 34 through 37 agree well with those in Figure 33. This is especially true of explosions 79267 (Figures 34d, e, f and 33i), 81274 (Figures 36a, b, c and 33d), and 68312 (Figures 37a, b, c and 33b). It seems therefore that inter-shot spectral ratios provide a simple and effective method of estimating null frequencies and corresponding delay times.

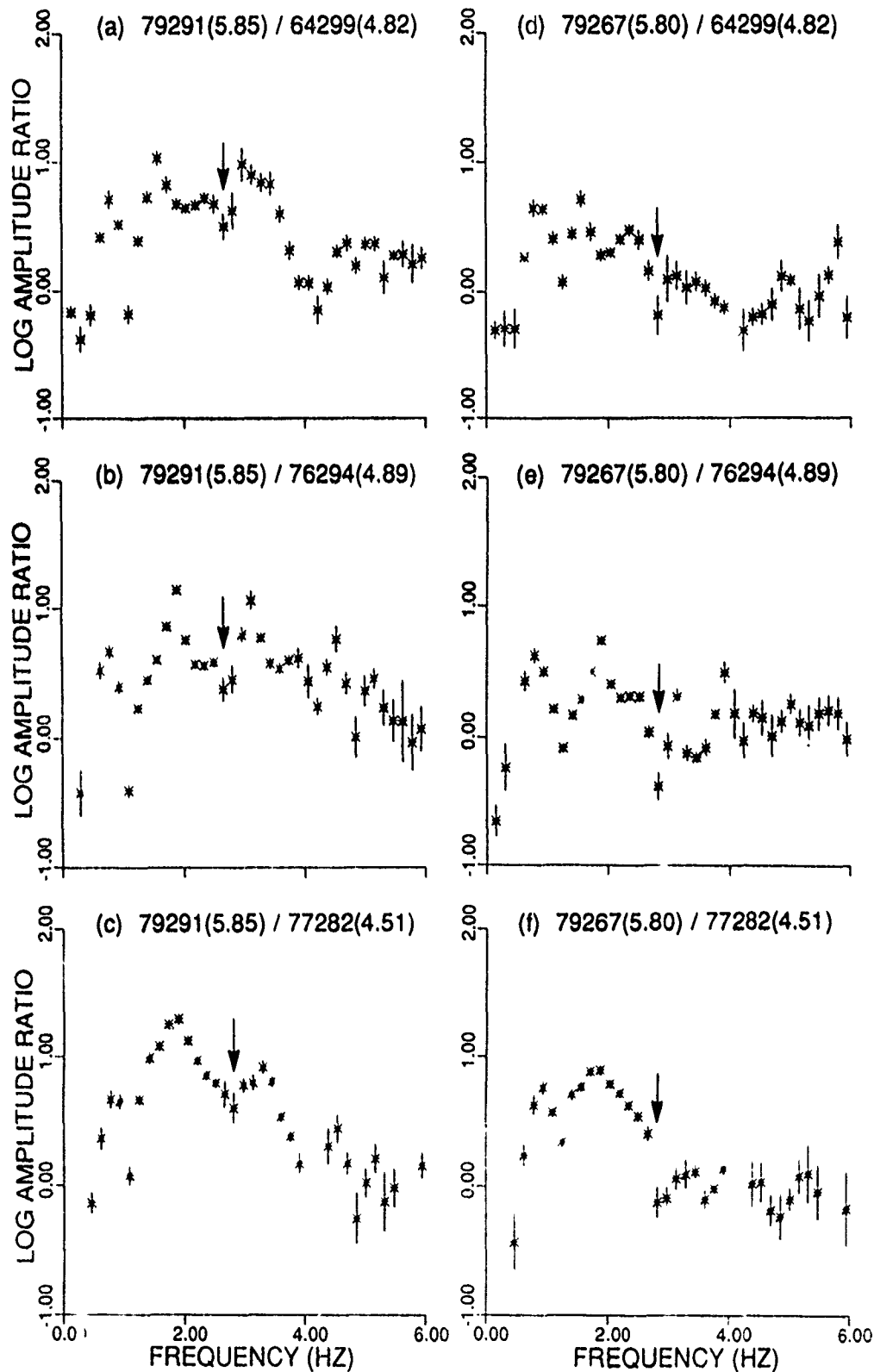


Figure 34. Inter-shot spectral ratios, averaged over all common sensors, for two large explosions recorded at EKA, each combined with three smaller shots. Prominent and consistent spectral nulls (indicated by arrows) are observed at about 3 Hz. The vertical lines represent error bars with one standard deviation.

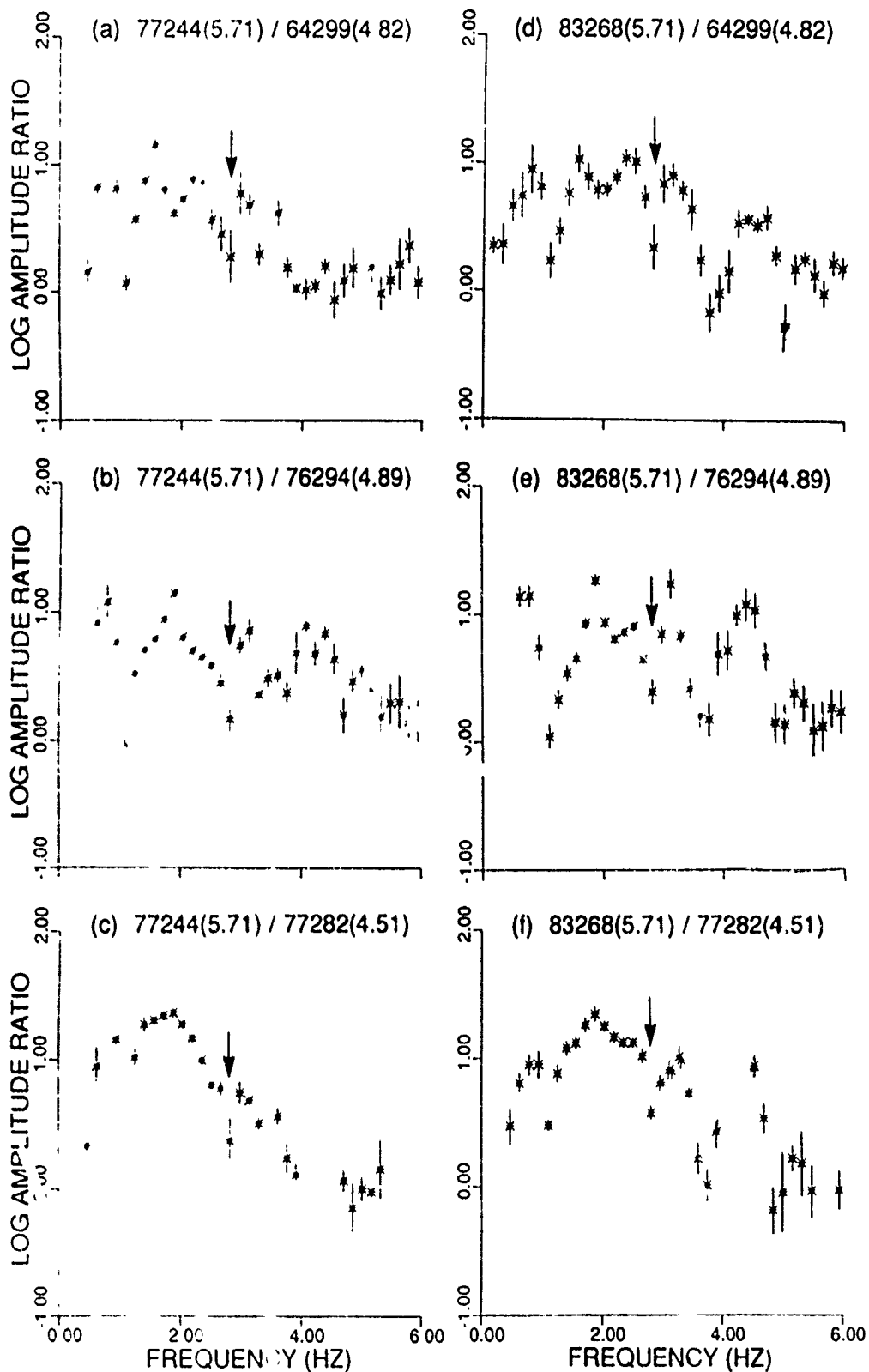


Figure 35. Similar to Figure 34 for two additional larger shots. Distinct and consistent spectral nulls are again observed.

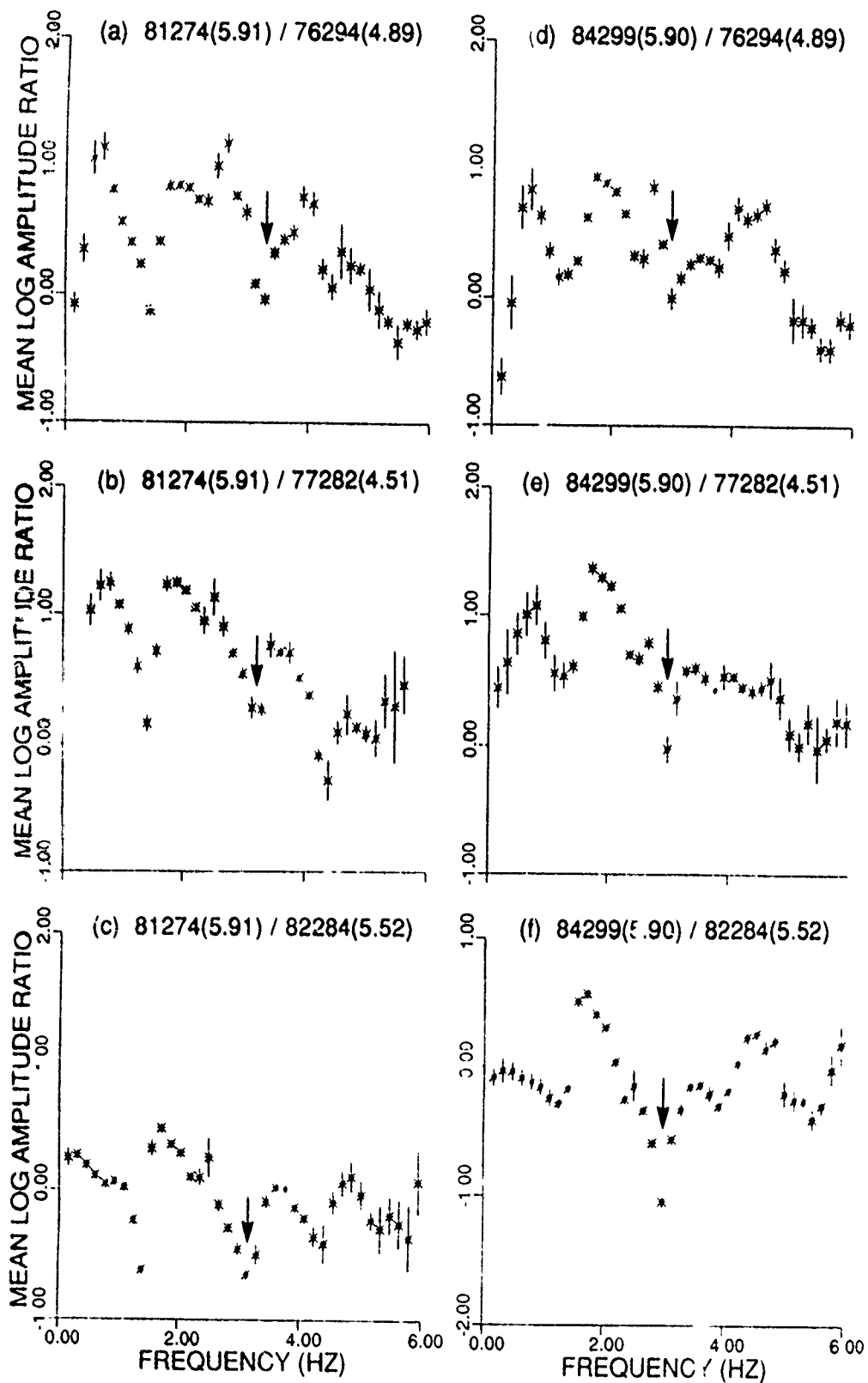


Figure 36. Similar to Figure 34 for two large explosions recorded at GBA showing distinct and consistent spectral nulls.

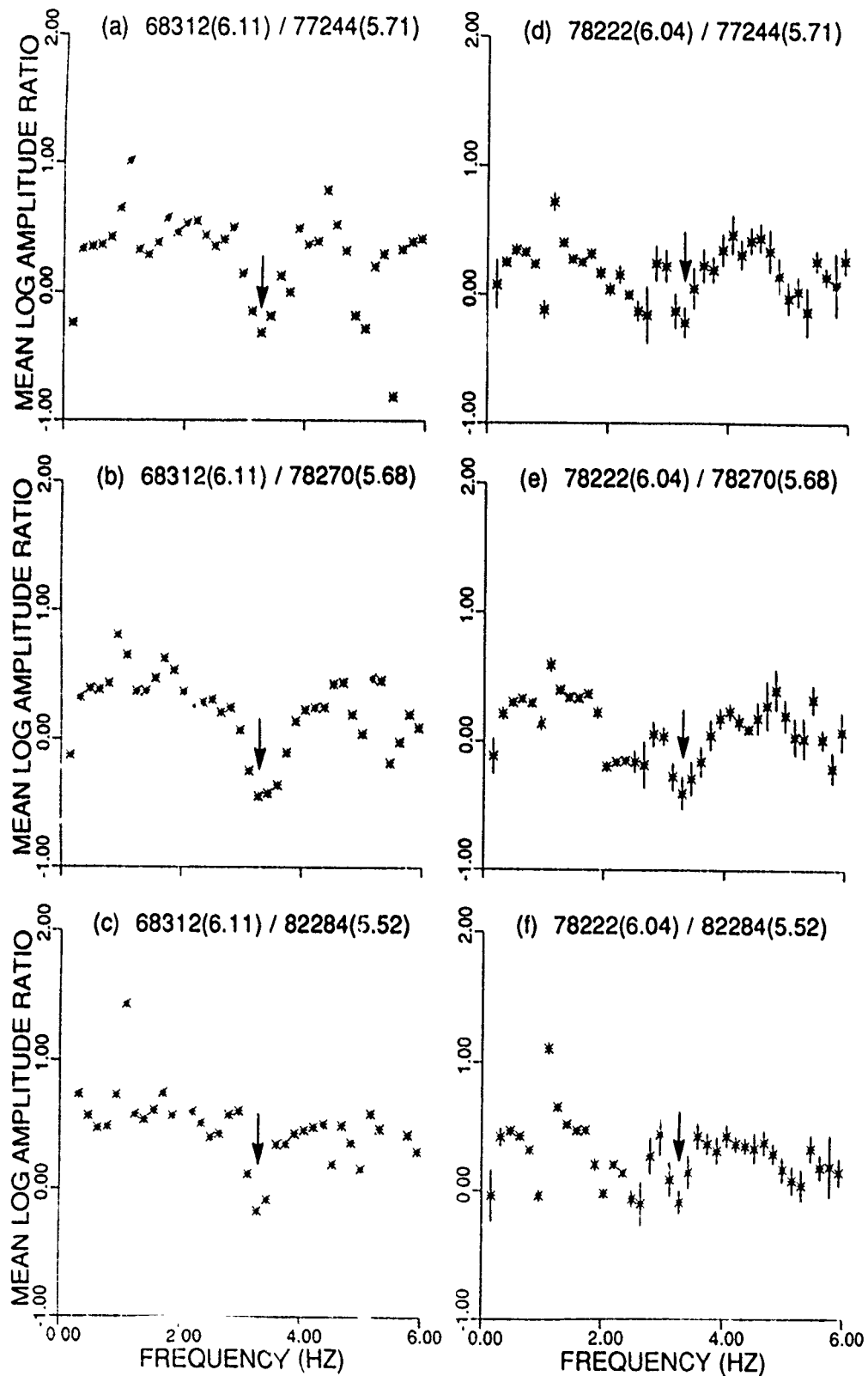


Figure 37. Similar to Figure 34 for two large explosions recorded at YKA showing consistent spectral nulls that are considerably more prominent for shot 68312 than for shot 78222.

4.3. ESTIMATES OF pP/P BY COMPARISON WITH SYNTHETICS

In order to resolve the large ambiguity associated with pP/P amplitudes as determined by various investigators, we selected a few events with distinct pP spectral nulls and compared their spectra with those of theoretical waveforms (synthetics). Three relatively large explosions selected for this purpose are 73270 from southern Novaya Zemlya and 79267 and 79291 from northern Novaya Zemlya. The reasons for their selection are: (1) data from a large number of sensors are available (Table 3), (2) the EKA source spectra of these explosions in Figure 29 appear to provide distinct spectral nulls at frequency of 2.5, 2.8, and 2.8 Hz, respectively, and (3) the three null frequencies agree remarkably well with those derived from P/P-coda (Figure 33) and from inter-shot spectral ratios (Figure 34). According to Sykes and Ruggi (1986), these 3 explosions had estimated yields of 100, 55, and 70 kt, respectively. Following Chan *et al.* (1988) for Novaya Zemlya explosions recorded at EKA, t^* was assumed to be 0.23 whereas the times were assumed to be those given by the observed null frequencies. Theoretical seismograms were obtained by using von Seggern and Blandford (1972) scaling relationship for several different assumed values of (frequency independent) pP/P amplitude. Spectra of theoretical seismograms were obtained by using signal windows of P(6.4 sec) and P(3.2 sec) with Parzen taper. These spectra were compared with the source spectra, derived by using the same window lengths, for the three explosions mentioned above. Some of the results are shown in Figures 38, 39, and 40 which suggest a pP/P value of about 0.4 to 0.6 in nearly all cases.

An examination of the spectra of synthetics in Figures 38, 39, and 40 suggests that the pP/P amplitude exerts strong influence on shape of the spectra at frequencies close to the pP null frequency (or "strength" of the pP null). Variations in yield have only a minor influence.

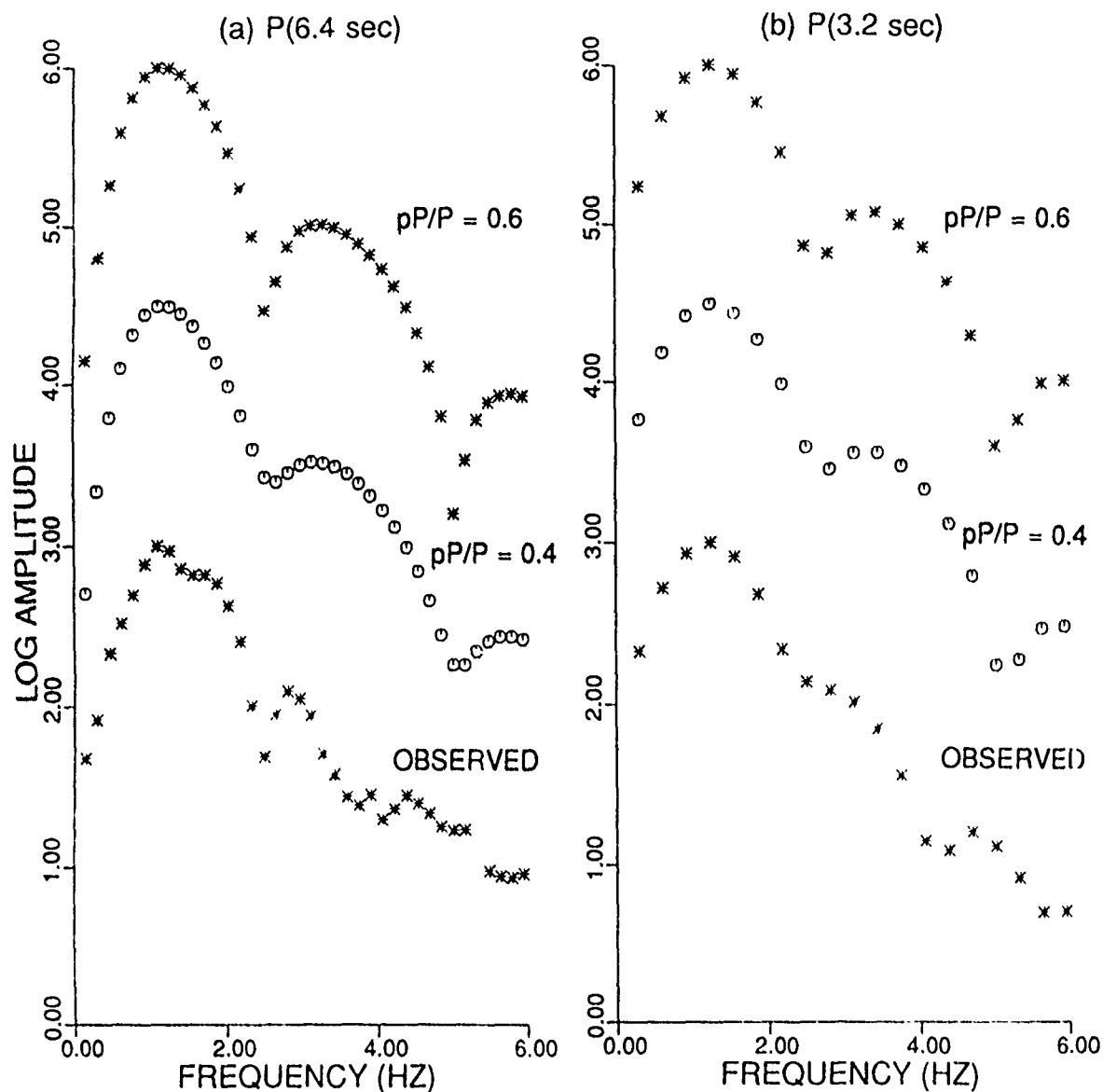


Figure 38. Theoretical and observed spectra for shot 73270 recorded at EKA array. Top two spectra are based on reflection coefficient values of 0.6 and 0.4, respectively and the use of (a) P(6.4 sec) and (b) P(3.2 sec) windows. Comparisons suggest pP/P of about 0.6 and 0.4 for the observed spectra in (a) and (b), respectively.

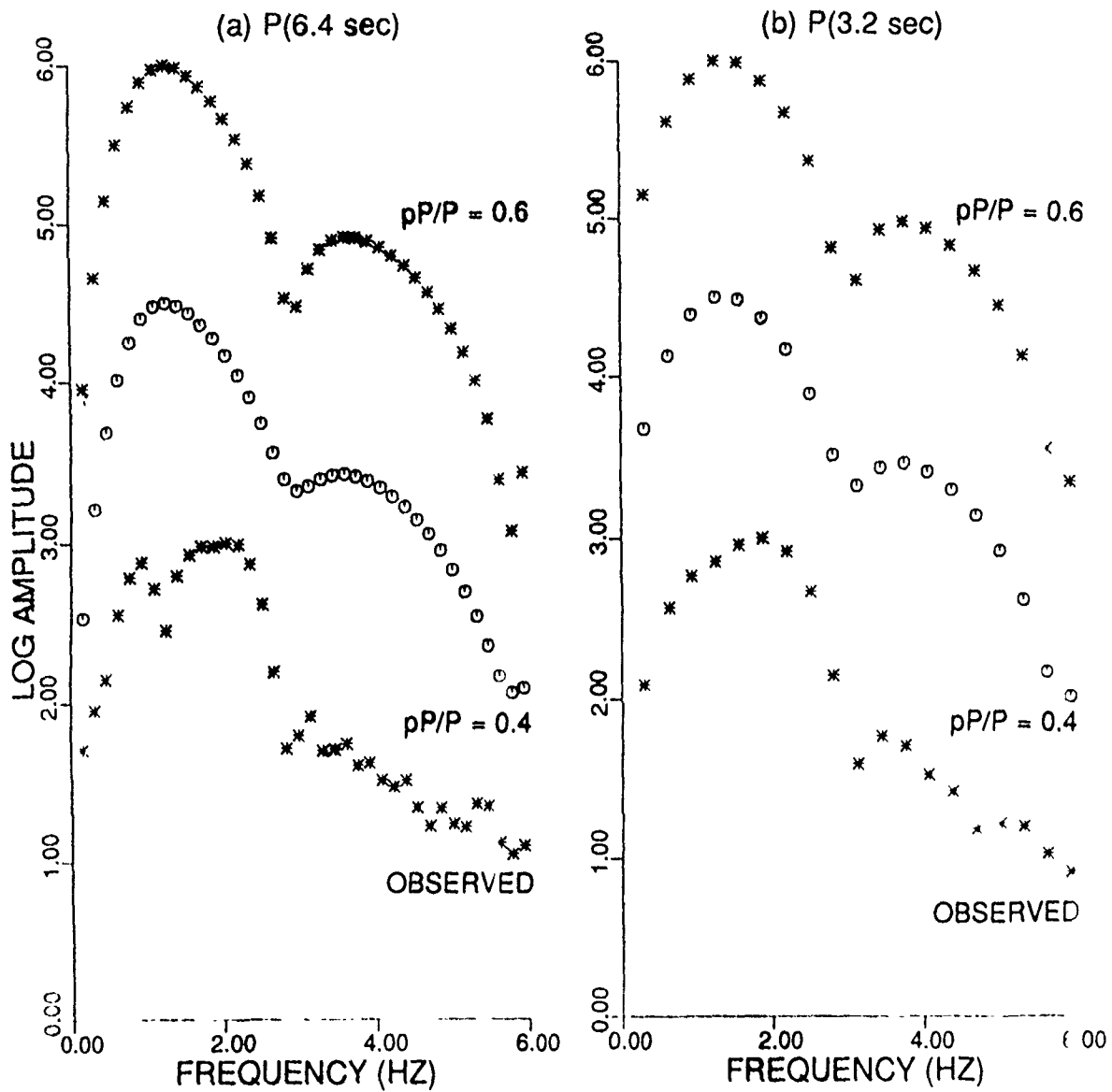


Figure 39. Similar to Figure 38 for shot 79270. Comparisons suggest pP/P of about 0.4 each for the observed spectra in both (a) and (b).

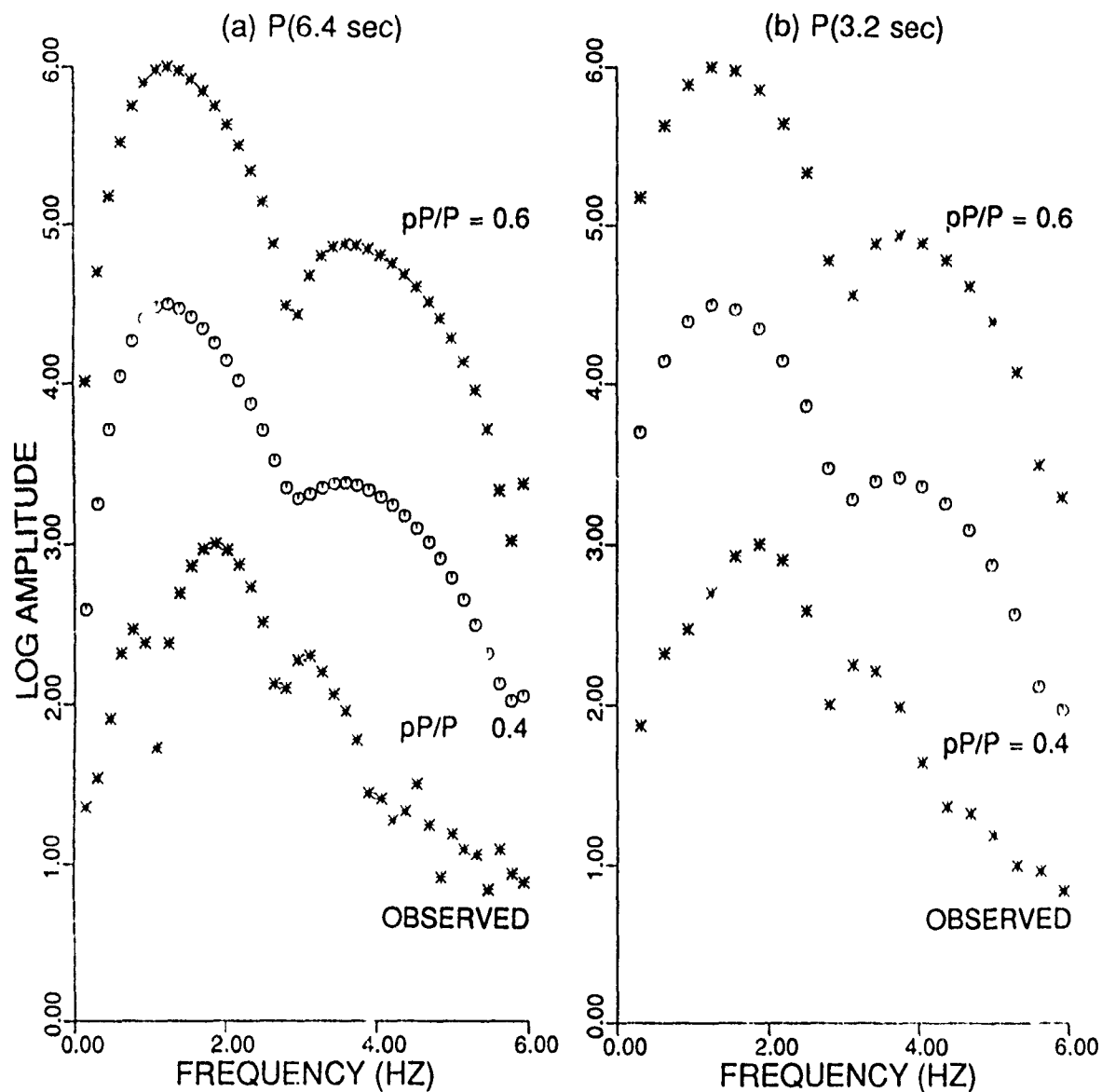


Figure 40. Similar to Figure 38 for shot 79291. Comparisons suggest pP/P of about 0.6 each for the observed spectra in both (a) and (b).

Construction of additional synthetics showed that reasonable variations in t^* also did not have much effect on the strength of the pP null. A comparison of the P(6.4 sec) spectra in Figures 29, 31, and 32 with the spectra of synthetics would therefore suggest pP/P amplitude to be about 0.4-0.6 for most large shots and considerably smaller than 0.4 for the smaller m_b shots.

5. CONCLUSIONS

A large amount of teleseismic and regional data from Shagan River explosions have been analyzed by using several methods of analysis such as frequency-domain isolation of source and receiver terms, multichannel deconvolution, use of spectral ratios P/P-coda and Pn/Lg for teleseismic and regional data, respectively, and inter-shot spectral ratios at common stations. The P-wave spectra appear to show three different types of spectral nulls: distinct nulls due to cancellation by pP at the expected frequency of about 4 Hz in both teleseismic and regional data for large shots ($m_b \approx 6$), low-frequency (less than about 2 Hz) nulls in teleseismic data, generally stronger for smaller explosions and for shots in the NE Shagan region, and nulls at about 3 Hz in teleseismic data for most shots. The low-frequency nulls are probably due to near-source scattering whereas the 3 Hz null appears to be due to teleseismic path effect such as a multiple arrival. An investigation of the scaling of P-wave spectra is carried out by comparison of observed data from WMQ and NORSAR with synthetics assuming several t^* and pP reflection coefficient values. The observed P spectra vary more slowly with m_b than predicted by either Mueller and Murphy (1971) or von Seggern and Blandford (1972) scaling relationships, in qualitative agreement with Stewart's (1988) analysis of Shagan River explosions recorded at the U.K. arrays. The differences between theoretical and observed spectra are greater at lower than at the higher frequencies.

Source terms derived from P-wave spectra of several larger Novaya Zemlya explosions show distinct nulls at frequencies close to those expected for nulls due to pP. The spectral null frequencies differ by small amounts from one array to another, presumably because of variation in path effect. Spectral ratio of P/P-coda, averaged over all available sensors at all arrays, provides another method for estimating spectral nulls. The simplest and most reliable

method for estimating null frequencies of larger explosions is found to be inter-shot spectral ratios at common receivers. The frequency of spectral nulls determined by this method stays remarkably constant when the larger shot is combined with various smaller shots and the results agree well with those determined by the spectral ratio P/P -coda averaged over all sensors. A knowledge of pP spectral nulls may be used to determine shot depths if the overburden velocities are known. Delay times of large Novaya Zemlya explosions determined in this study are in good agreement with those from source deconvolutions and appear to be consistent with the overburden velocities in the test site region. A comparison of the observed data with synthetics suggests the pP/P amplitudes for the larger events to be about 0.4 to 0.6. The null frequencies do not seem to vary significantly with m_b ; this will be consistent with Leith *et al.*'s (1990) suggestion that explosions at the northern test site are emplaced in near-horizontal tunnels so that the larger shots may be relatively underburied and therefore associated with somewhat larger than expected pP null frequencies.

6. ACKNOWLEDGMENTS

We thank Bob Blandford, Chris Lynnes, and Robert Cessaro for valuable advice and suggestions during the course of this study. Sincere thanks are also due to Rong-Song Jih for the use of his least squares inversion program. This research was funded by the Defense Advanced Research Projects Agency and monitored by the Phillips Laboratory under Contract F19628-89 C-0063. The views and conclusions contained in this paper are those of the authors and should not be interpreted as necessarily representing the official policies, either expressed or implied, of the Defense Advanced Research Projects Agency or the U. S. Government.

7. REFERENCES

- Bache, T. C., P. D. Marshall, and L. B. Bache (1985). Q for teleseismic P waves from Central Asia, *J. Geophys. Res.* 90, 3575-3587.
- Bache, T. C., P. D. Marshall, and J. B. Young (1984). Q and its effect on short-period P-waves from explosions in Central Asia, *AWRE O 17/84*, Atomic Weapons Research Establishment, H. M. Stationery Office, London.
- Blandford, R. R. (1981). Seismic discrimination problems at regional distances, in *Identification of Seismic Sources - Earthquake or Underground Explosions*, E. S. Husebye and S. Mykkeltveit, Editors, D. Reidel Publishing Co., Dordrecht, Holland, 695-740.
- Bocharov, V. S., S. A. Zelentsov, and V. N. Mikhailov (1989). Characteristics of 96 underground nuclear explosions at the Semipalatinsk test site, *Atomic Energy* 67(3).
- Bonham, S., W. J. Dempsey, and J. Rachlin (1980). Geologic environment of the Semipalatinsk area, U.S.S.R. (*Preliminary Report*), U. S. Geological Survey, Reston, Virginia.
- Burdick, L. J. (1990). Resolution of the pP paradox at Novaya Zemlya, *PL-TR-91-2042*, Phillips Laboratory, Hanscom Air Force Base, Massachusetts. ADA235959
- Chan, W. W., K. L. McLaughlin, R. K. Cessaro, M. E. Marshall, and A. C. Lees (1988). Yield estimation of Novaya Zemlya explosions from short-period body waves, *TGAL-88-03*, Teledyne Geotech, Alexandria, Virginia.
- Der, Z., T. McElfresh, R. Wagner, and J. Burnetti (1985). Spectral characteristics of P waves from nuclear explosions and yield estimation, *Bull. Seism. Soc. Am.* 75, 379-390 (also errata p. 1222-1223).
- Der, Z. A., R. H. Shumway, and A. C. Lees (1987a). Multi-channel deconvolution of P waves at seismic arrays, *Bull. Seism. Soc. Am.* 77, 195-211.
- Der, Z. A., A. C. Lees, W. W. Chan, R. H. Shumway, K. L. McLaughlin, E. Smart, T. W. McElfresh, and M. E. Marshall (1987b). Maximum-likelihood multichannel deconvolution of P waves at seismic arrays, *TGAL-87-3*, Teledyne Geotech, Alexandria, Virginia.
- Gupta, I. N., R. R. Blandford, R. A. Wagner, J. A. Burnetti, and T. W. McElfresh (1985). Use of P coda for determination of yield of nuclear explosions, *Geophys. J.* 83, 541-553.
- Gupta, I. N. and R. R. Blandford (1987). A study of P waves from Nevada Test Site explosions: near-source information from teleseismic observations?, *Bull. Seism. Soc. Am.* 77, 1041-1056.
- Gupta, I. N., W. W. Chan, and R. A. Wagner (1990a). A comparative study of regional phases from underground nuclear explosions at East Kazakh and Nevada Test Sites, *GL-TR-90-0170*, Geophysics Laboratory, Hanscom Air Force Base, Massachusetts. ADA230567

- Gupta, I. N., C. S. Lynnes, T. W. McElfresh, and R. A. Wagner (1990b). F-k analysis of NORESS array and single-station data to identify sources of near-receiver and near-source scattering, *Bull. Seism. Soc. Am.* 80, 2227-2241.
- Gupta, I. N., T. W. McElfresh, and R. A. Wagner (1991). Near-source scattering of Rayleigh to P in teleseismic arrivals from Pahute Mesa (NTS) shots, *Explosion Source Phenomenology*, Geophysical Monograph 65, American Geophysical Union, Washington, D.C.
- Hudson, J. A. and A. Douglas (1985). On the amplitudes of seismic waves, *Geophys. J.* 42, 1039-1044.
- Kafka, A. L. (1990). Rg as a depth discriminant for earthquakes and explosions: a case study in New England, *Bull. Seism. Soc. Am.* 80, 373-394.
- King, C. Y., W. H. Bakun, and J. N. Murdock (1972). Source parameters of nuclear explosions MILROW and LONGSHOT from teleseismic P waves, *Geophys. J.* 31, 27-44.
- Lay, T. (1991). Yield estimation, free-surface interactions, and tectonic release at Novaya Zemlya, *Proc. 13th Annual PL/DARPA Seismic Research Symposium*, DARPA, Arlington, Virginia. PL-TR-91-2208, ADA241325.
- Leith, W. and J. Unger (1989). Three-dimensional geological modelling of the Shagan River nuclear test site, *Paper presented at DARPA/AFTAC Annual Seismic Research Review*, Patrick Air Force Base, Florida.
- Leith, W., J. R. Matzko, and J. Unger (1990). Geology and image analysis of the Soviet Nuclear Test Site at Malochkiy Shar Novaya Zemlya, U.S.S.R., *Proc. 12th Annual DARPA/GL Seismic Research Symposium*, DARPA, Arlington, Virginia. GL-TR-90-0212, ADA226635.
- Levander, A. R. and N. R. Hill (1985). P-SV resonances in irregular low-velocity surface layers, *Bull. Seism. Soc. Am.* 75, 847-864.
- Lilwall, R. C. and P. D. Marshall (1986). Body wave magnitudes and locations of Soviet underground explosions at the Novaya Zemlya test site, *AWRE O 17/86*, Atomic Weapons Research Establishment, H. M. Stationery Office, London, U.K.
- Lyman, N. S., A. Douglas, P. D. Marshall, and J. B. Young (1986). P seismograms recorded at Eskdalemuir, Scotland from explosions in Nevada, USA, *AWRE O 10/86*, Atomic Weapons Research Establishment, H. M. Stationery Office, London, U.K.
- Marshall, P. D., T. C. Bache, and R. C. Lilwall (1985). Body wave magnitudes and locations of Soviet underground explosions at the Semipalatinsk Test Site, *AWRE O 16/84 (re-issue)*, Atomic Weapons Research Establishment, H. M. Stationery Office, London, U.K.
- McLaughlin, K. L., L. M. Anderson, and A. C. Lees (1987). Effects of local geologic structure on Yucca Flats, Nevada Test Site, explosion waveforms: two-dimensional linear finite-difference simulations, *Bull. Seism. Soc. Am.* 77, 1211-1222.
- Mueller, R. A. and J. R. Murphy (1971). Seismic characteristics of underground nuclear detonations, Part I, Seismic spectrum scaling, *Bull. Seism. Soc. Am.* 61, 1675-1692.

- Murphy, J. R., B. W. Barker, and A. O'Donnell (1989). Network-averaged teleseismic P-wave spectra for underground explosions. Part 1. Definitions and examples, *Bull. Seism. Soc. Am.* 79, 141-155.
- Murphy, J. R., J. L. Stevens, D. C. O'Neill, B. W. Barker, K. L. McLaughlin, and M. E. Marshall (1991). Development of a comprehensive seismic yield estimation system for underground nuclear explosions, *PL-TR-91-2161*, Phillips Laboratory, Hanscom Air Force Base, Massachusetts. ADA240814
- Ringdal, F. and P. D. Marshall (1989). Yield determination of Soviet underground nuclear explosions at the Shagan River test site, *NORSAR Scientific Rep. 2-88/8*, 36-67, Kjeller, Norway.
- Sereno, T. J. Jr. (1990). Frequency-dependent attenuation in Eastern Kazakhstan and implications for seismic detection thresholds in the Soviet Union, *Bull. Seism. Soc. Am.* 80, 2089-2105.
- Shumway, R. H. and R. R. Blandford (1978). On detecting and estimating multiple arrivals from underground nuclear explosions, *SDAC-TR-77-8*, Teledyne Geotech, Alexandria, Virginia.
- Stead, R. J. and D. V. Helmberger (1988). Numerical-analytical interfacing in two dimensions with applications to modeling NTS seismograms, *PAGEOPH* 128, Nos. 1/2, 157-193.
- Stewart, R. C. (1988). P-wave seismograms from underground explosions at the Shagan River test site recorded at four arrays, *AWE O 4/88*, Atomic Weapons Establishment, H. M. Stationery Office, London, U.K.
- Sykes, L. R. and S. Ruggi (1986). Soviet underground nuclear testing: Inferences from seismic observations and historical perspective, *NWD 86-4*, Natural Resources Defense Council, Washington, D.C.
- von Seggern, D. H. and R. R. Blandford (1972). Source time functions and spectra for underground nuclear explosions, *Geophys. J.* 31, 83-97.

Prof. Thomas Ahrens
Seismological Lab, 252-21
Division of Geological & Planetary Sciences
California Institute of Technology
Pasadena, CA 91125

Prof. Keiiti Aki
Center for Earth Sciences
University of Southern California
University Park
Los Angeles, CA 90089-0741

Prof. Shelton Alexander
Geosciences Department
403 Deike Building
The Pennsylvania State University
University Park, PA 16802

Dr. Ralph Alewine, III
DARPA/NMRO
3701 North Fairfax Drive
Arlington, VA 22203-1714

Prof. Charles B. Archambeau
CIRES
University of Colorado
Boulder, CO 80309

Dr. Thomas C. Lache, Jr.
Science Applications Int'l Corp.
10260 Campus Point Drive
San Diego, CA 92121 (2 copies)

Prof. Muawia Barazangi
Institute for the Study of the Continent
Cornell University
Ithaca, NY 14853

Dr. Jeff Barker
Department of Geological Sciences
State University of New York
at Binghamton
Vestal, NY 13901

Dr. Douglas R. Baumgardt
ENSCO, Inc
5400 Port Royal Road
Springfield, VA 22151-2388

Dr. Susan Beck
Department of Geosciences
Building #77
University of Arizona
Tucson, AZ 85721

Dr. T.J. Bennett
S-CUBED
A Division of Maxwell Laboratories
11800 Sunrise Valley Drive, Suite 1450
Reston, VA 22091

Dr. Robert Blandford
AFTAC/IT, Center for Seismic Studies
1330 North 17th Street
Suite 1450
Arlington, VA 22209-2308

Dr. G.A. Bollinger
Department of Geological Sciences
Virginia Polytechnical Institute
21044 Derring Hall
Blacksburg, VA 24061

Dr. Stephen Bratt
Center for Seismic Studies
1300 North 17th Street
Suite 1450
Arlington, VA 22209-2308

Dr. Lawrence Burdick
Woodward-Clyde Consultants
566 El Dorado Street
Pasadena, CA 91109-3245

Dr. Robert Burrige
Schlumberger-Doll Research Center
Old Quarry Road
Ridgefield, CT 06877

Dr. Jerry Carter
Center for Seismic Studies
1300 North 17th Street
Suite 1450
Arlington, VA 22209-2308

Eric Chael
Division 9241
Sandia Laboratory
Albuquerque, NM 87185

Prof. Vernon F. Cormier
Department of Geology & Geophysics
U-45, Room 207
University of Connecticut
Storrs, CT 06268

Prof. Anton Dainty
Earth Resources Laboratory
Massachusetts Institute of Technology
42 Carleton Street
Cambridge, MA 02142

Prof. Steven Day
Department of Geological Sciences
San Diego State University
San Diego, CA 92182

Art Frankel
U.S. Geological Survey
922 National Center
Reston, VA 22092

Marvin Denny
U.S. Department of Energy
Office of Arms Control
Washington, DC 20585

Dr. Cliff Frolich
Institute of Geophysics
8701 North Mopac
Austin, TX 78759

Dr. Zoltan Der
ENSCO, Inc.
5400 Port Royal Road
Springfield, VA 22151-2388

Dr. Holly Given
IGPP, A-025
Scripps Institute of Oceanography
University of California, San Diego
La Jolla, CA 92093

Prof. Adam Dziewonski
Hoffman Laboratory, Harvard University
Dept. of Earth Atmos. & Planetary Sciences
20 Oxford Street
Cambridge, MA 02138

Dr. Jeffrey W. Given
SAIC
10260 Campus Point Drive
San Diego, CA 92121

Prof. John Ebel
Department of Geology & Geophysics
Boston College
Chestnut Hill, MA 02167

Dr. Dale Glover
Defense Intelligence Agency
ATTN: ODT-1B
Washington, DC 20301

Eric Fielding
SNEE Hall
INSTOC
Cornell University
Ithaca, NY 14853

Dr. Indra Gupta
Teledyne Geotech
314 Montgomery Street
Alexandria, VA 22314

Dr. Mark D. Fick
Mission Research Corporation
735 State Street
P.O. Drawer 719
Santa Barbara, CA 93102

Dr. N. Hagedorn
Pacific Northwest Laboratories
Battelle Boulevard
Richland, WA 99352

Prof. Stanley Flatté
Applied Sciences Building
University of California, Santa Cruz
Santa Cruz, CA 95064

Dr. James Hannon
Lawrence Livermore National Laboratory
P.O. Box 808
L-205
Livermore, CA 94550

Dr. John Foley
NER-Geo Sciences
1100 Crown Colony Drive
Quincy, MA 02169

Dr. Roger Hansen
AFTAC/TTR
Patrick AFB, FL 32925

Prof. Donald Forsyth
Department of Geological Sciences
Brown University
Providence, RI 02912

Prof. David G. Harkrider
Seismological Laboratory
Division of Geological & Planetary Sciences
California Institute of Technology
Pasadena, CA 91125

Prof. Danny Harvey
CIRES
University of Colorado
Boulder, CO 80309

Prof. Donald V. Helmberger
Seismological Laboratory
Division of Geological & Planetary Sciences
California Institute of Technology
Pasadena, CA 91125

Prof. Eugene Herrin
Institute for the Study of Earth and Man
Geophysical Laboratory
Southern Methodist University
Dallas, TX 75275

Prof. Robert B. Herrmann
Department of Earth & Atmospheric Sciences
St. Louis University
St. Louis, MO 63156

Prof. Lane R. Johnson
Seismographic Station
University of California
Berkeley, CA 94720

Prof. Thomas H. Jordan
Department of Earth, Atmospheric &
Planetary Sciences
Massachusetts Institute of Technology
Cambridge, MA 02139

Prof. Alan Kafka
Department of Geology & Geophysics
Boston College
Chestnut Hill, MA 02167

Robert C. Kemerait
ENSCO, Inc.
445 Pineda Court
Melbourne, FL 32940

Dr. Max Koontz
U.S. Dept. of Energy/DP 5
Forrestal Building
1000 Independence Avenue
Washington, DC 20585

Dr. Richard LaCoss
MIT Lincoln Laboratory, M-200B
P.O. Box 73
Lexington, MA 02173-0073

Dr. Fred K. Lamb
University of Illinois at Urbana-Champaign
Department of Physics
1110 West Green Street
Urbana, IL 61801

Prof. Charles A. Langston
Geosciences Department
403 Deike Building
The Pennsylvania State University
University Park, PA 16802

Prof. Thorne Lay
Institute of Tectonics
Earth Science Board
University of California, Santa Cruz
Santa Cruz, CA 95064

Dr. William Leith
U.S. Geological Survey
Mail Stop 928
Reston, VA 22092

James F. Lewkowicz
Phillips Laboratory/GPEH
Hanscom AFB, MA 01731-5000

Mr. Alfred Lieberman
ACDA/VI-OA State Department Building
Room 5726
320-21st Street, NW
Washington, DC 20451

Prof. L. Timothy Long
School of Geophysical Sciences
Georgia Institute of Technology
Atlanta, GA 30332

Dr. Robert Masse
Denver Federal Building
Box 25046, Mail Stop 967
Denver, CO 80225

Dr. Randolph Martin, III
New England Research, Inc.
76 Olcott Drive
White River Junction, VT 05001

Dr. Gary McCartor
Department of Physics
Southern Methodist University
Dallas, TX 75275

Prof. Thomas V. McEvilly
Seismographic Station
University of California
Berkeley, CA 94720

Prof. Art McGarr
U.S. Geological Survey
Mail Stop 977
U.S. Geological Survey
Menlo Park, CA 94025

Dr. Keith L. McLaughlin
S-CUBED
A Division of Maxwell Laboratory
P.O. Box 1620
La Jolla, CA 92038-1620

Stephen Miller & Dr. Alexander Florence
SRI International
333 Ravenswood Avenue
Box AF 116
Menlo Park, CA 94025-3493

Prof. Bernard Minster
IGPP, A-025
Scripps Institute of Oceanography
University of California, San Diego
La Jolla, CA 92093

Prof. Brian J. Mitchell
Department of Earth & Atmospheric Sciences
St. Louis University
St. Louis, MO 63156

Mr. Jack Murphy
S-CUBED
A Division of Maxwell Laboratory
11800 Sunrise Valley Drive, Suite 1212
Reston, VA 22091 (2 Copies)

Dr. Keith K. Nakanishi
Lawrence Livermore National Laboratory
L-025
P.O. Box 808
Livermore, CA 94550

Dr. Carl Newton
Los Alamos National Laboratory
P.O. Box 1663
Mail Stop C335, Group ESS-3
Los Alamos, NM 87545

Dr. Bao Nguyen
AFTAC/TTR
Patrick AFB, FL 32925

Prof. John A. Orcutt
ICPP, A-025
Scripps Institute of Oceanography
University of California, San Diego
La Jolla, CA 92093

Prof. Jeffrey Park
Kane Geology Laboratory
P.O. Box 6666
New Haven, CT 06511-8130

Howard Patton
Lawrence Livermore National Laboratory
L-025
P.O. Box 808
Livermore, CA 94550

Dr. Frank Pilotte
HQ AFTAC/TTR
Patrick AFB, FL 32925-6001

Dr. Jay J. Pulli
Radix Systems, Inc.
2 Taft Court, Suite 203
Rockville, MD 20850

Dr. Robert Reinke
ATTN: FCTVTD
Field Command
Defense Nuclear Agency
Kirtland AFB, NM 87115

Prof. Paul G. Richards
Lamont-Doherty Geological Observatory
of Columbia University
Palisades, NY 10964

Mr. Wilmer Rivers
Teledyne Geotech
314 Montgomery Street
Alexandria, VA 22314

Dr. George Rothe
HQ AFTAC/TTR
Patrick AFB, FL 32925-6001

Dr. Alan S. Ryall, Jr.
DARPA/NMRO
3701 North Fairfax Drive
Arlington, VA 22209-1714

Dr. Richard Sailor
TASC, Inc.
55 Walkers Brook Drive
Reading, MA 01867

Prof. Charles G. Sammis
Center for Earth Sciences
University of Southern California
University Park
Los Angeles, CA 90089-0741

Prof. Christopher H. Scholz
Lamont-Doherty Geological Observatory
of Columbia University
Palisades, CA 10964

Dr. Susan Schwartz
Institute of Tectonics
1156 High Street
Santa Cruz, CA 95064

Secretary of the Air Force
(SAFRD)
Washington, DC 20330

Office of the Secretary of Defense
DDR&E
Washington, DC 20330

Thomas J. Sereno, Jr.
Science Application Int'l Corp.
10260 Campus Point Drive
San Diego, CA 92121

Dr. Michael Shore
Defense Nuclear Agency/SPSS
6801 Telegraph Road
Alexandria, VA 223 0

Dr. Matthew Sibol
Virginia Tech
Seismological Observatory
4044 Derring Hall
Blacksburg, VA 24061-0420

Prof. David G. Simpson
IRIS, Inc.
1616 North Fort Myer Drive
Suite 1400
Arlington, VA 22209

Donald L. Springer
Lawrence Livermore National Laboratory
L-025
P.O. Box 808
Livermore, CA 94550

Dr. Jeffrey Stevens
S-CUBED
A Division of Maxwell Laboratory
P.O. Box 1620
La Jolla, CA 92038-1620

Lt. Col. Jim Stobie
ATTN: AFOSR/NL
Bolling AFB
Washington, DC 20332-6448

Prof. Brian Stump
Institute for the Study of Earth & Man
Geophysical Laboratory
Southern Methodist University
Dallas, TX 75275

Prof. Jeremiah Sullivan
University of Illinois at Urbana-Champaign
Department of Physics
1110 West Green Street
Urbana, IL 61801

Prof. L. Sykes
Lamont-Doherty Geological Observatory
of Columbia University
Palisades, NY 10964

Dr. David Taylor
ENSCO, Inc.
445 Pineda Court
Melbourne, FL 32940

Dr. Steven R. Taylor
Los Alamos National Laboratory
P.O. Box 1663
Mail Stop C335
Los Alamos, NM 87545

Prof. Clifford Thurber
University of Wisconsin-Madison
Department of Geology & Geophysics
1215 West Dayton Street
Madison, WS 53706

Prof. M. Nafi Toksoz
Earth Resources Lab
Massachusetts Institute of Technology
42 Carleton Street
Cambridge, MA 02142

Dr. Larry Turnbull
CIA-OSWR/NED
Washington, DC 20505

DARPA/RMO/SECURITY OFFICE
3701 North Fairfax Drive
Arlington, VA 2203-1714

Dr. Gregory van der Vink
IRIS, Inc.
16116 North Fort Myer Drive
Suite 1440
Arlington, VA 22209

HQ DNA
ATTN: Technical Library
Washington, DC 20305

Dr. Karl Veith
EG&G
5211 Auth Road
Suite 240
Suitland, MD 20746

Defense Intelligence Agency
Directorate for Scientific & Technical Intelligence
ATTN: DTIB
Washington, DC 20340-6158

Prof. Terry C. Wallace
Department of Geosciences
Building #77
University of Arizona
Tucson, AZ 85721

Defense Technical Information Center
Cameron Station
Alexandria, VA 22314 (5 Copies)

Dr. Thomas Weaver
Los Alamos National Laboratory
P.O. Box 1663
Mail Stop C335
Los Alamos, NM 87545

TACTEC
Battelle Memorial Institute
505 King Avenue
Columbus, OH 43201 (Final Report)

Dr. William Wortman
Mission Research Corporation
8560 Cinderbed Road
Suite 700
Newington, VA 22122

Phillips Laboratory
ATTN: XPG
Hanscom AFB, MA 01731-5000

Prof. Francis T. Wu
Department of Geological Sciences
State University of New York
at Binghamton
Vestal, NY 13901

Phillips Laboratory
ATTN: GPE
Hanscom AFB, MA 01731-5000

AFTAC/CA
(STINFO)
Patrick AFB, FL 32925-6001

Dr. Michel Bouchon
I.R.I.G.M.-B.P. 68
38402 St. Martin D'Herès
Cedex, FRANCE

DAARPA/PM
3701 North Fairfax Drive
Arlington, VA 22203-1714

Dr. Michel Campillo
Observatoire de Grenoble
I.R.I.G.M.-B.P. 53
38041 Grenoble, FRANCE

DARPA/RMO/RETRIEVAL
3701 North Fairfax Drive
Arlington, VA 22203-1714

Dr. Kin Yip Chun
Geophysics Division
Physics Department
University of Toronto
Ontario, CANADA

Prof. Hans-Peter Harjes
Institute for Geophysics
Ruhr University/Bochum
P.O. Box 102148
4630 Bochum 1, GERMANY

Prof. Eystein Husebye
NTNF/NORSAR
P.O. Box 51
N-2007 Kjeller, NORWAY

David Jepsen
Acting Head, Nuclear Monitoring Section
Bureau of Mineral Resources
Geology and Geophysics
G.P.O. Box 378, Canberra, AUSTRALIA

Ms. Eva Johannisson
Senior Research Officer
National Defense Research Inst.
P.O. Box 27322
S-102 54 Stockholm, SWEDEN

Dr. Peter Marshall
Procurement Executive
Ministry of Defense
Blacknest, Brimpton
Reading FG7-FRS, UNITED KINGDOM

Dr. Bernard Massinon, Dr. Pierre Mechler
Societe Radiomana
27 rue Claude Bernard
75005 Paris, FRANCE (2 Copies)

Dr. Svein Mykkeltveit
NTNT/NORSAR
P.O. Box 51
N-2007 Kjeller, NORWAY (3 Copies)

Prof. Keith Priestley
University of Cambridge
Bullard Labs, Dept. of Earth Sciences
Madingley Rise, Madingley Road
Cambridge CB3 0EZ, ENGLAND

Dr. Jorg Schlittenhaardt
Federal Institute for Geosciences & Nat'l Res.
Postfach 510153
D-3000 Hannover 51, GERMANY

Dr. Johannes Schweitzer
Institute of Geophysics
Ruhr University/Bochum
P.O. Box 1102148
4360 Bochum 1, GERMANY